# Grasping for the Task — Human Principles for Robot Hands

THÈSE N$^{O}$ 6702 (2016)

PRÉSENTÉE LE 30 MARS 2016

À L'ÉCOLE POLYTECHNIQUE FÉDÉRALE DE LAUSANNE
À LA FACULTÉ DES SCIENCES ET TECHNIQUES DE L'INGÉNIEUR
LABORATOIRE D'ALGORITHMES ET SYSTÈMES D'APPRENTISSAGE

ET

À L'INSTITUTO SUPERIOR TÉCNICO (IST) DA UNIVERSIDADE DE LISBOA

PROGRAMME DOCTORAL EN ROBOTIQUE, CONTRÔLE ET SYSTÈMES INTELLIGENTS
ET
DOUTORAMENTO EM ENGENHARIA ELECTROTÉCNICA E DE COMPUTADORES

POUR L'OBTENTION DU GRADE DE DOCTEUR ÈS SCIENCES (PhD)

PAR

Ravin Luis DE SOUZA

acceptée sur proposition du jury:

Prof. H. Bleuler, président du jury
Prof. A. Billard, Prof. J. Santos-Victor, directeurs de thèse
Prof. T. Asfour, rapporteur
Prof. O. Brock, rapporteur
Prof. S. Micera, rapporteur


Suisse
2016

# Abstract

The significant advances made in the design and construction of anthropomorphic robot hands, endow them with prehensile abilities reaching that of humans. However, using these powerful hands with the same level of expertise that humans display is a big challenge for robots. The vast configuration space of hand, object and task makes the problem complex to tackle. Traditional approaches to grasping with dexterous hands focus on generating the best grasps from a force-closure sense, using the hand in a finger-tip (precision) or an enveloping (power) fashion. In the context of anthropomorphic hand-arm systems, reasoning in this way ignores the variety of prehensile postures available to the hand and also the larger context of arm action with which the task has to be performed. A different perspective is therefore required.

This thesis explores a paradigm for grasp formation based on generating oppositional pressure within the hand, which has been proposed as a functional basis for grasping in humans (MacKenzie and Iberall, 1994). A set of *opposition primitives* encapsulates the hand's ability to generate oppositional forces. The regions of the hand that will be in opposition, together with distribution of grasping force, constitutes the oppositional intention. For precision and power grasps, their dexterity and overall robustness properties are a consequence of engaging finger-tips only or maximizing contact with hand surface. With opposition primitives, varying the oppositional intention purposefully engages different parts of the hand, leading to different qualities for force and motion generation on a grasped object. Matching contact regions of primitives with opposing surfaces on the object decides how a primitive may be applied. This also constrains the wrist-pose, thus exposing the primitive's functionality to the arm and higher levels of the system. In this thesis we leverage these properties of opposition primitives to both interpret grasps formed by humans and to construct grasps for a robot considering also the larger context of arm action.

In the first part of the thesis we examine the hypothesis that hand representation schemes based on opposition are correlated with hand function. We propose hand-parameters describing oppositional intention and compare these with commonly used methods such as joint angles, joint synergies and shape features. We expect that opposition-based parameterizations, which take an interaction based perspective of a grasp, are able to discriminate between grasps

that are similar in shape but different in functional intent. We test this hypothesis using qualitative assessment of precision and power capabilities found in existing grasp taxonomies.

The next part of the thesis presents a general method to recognize oppositional intention manifested in human grasp demonstrations. A data glove instrumented with tactile sensors is used to provide the raw information regarding hand configuration and interaction force. A 21-DOF human hand model, comprising 4 fingers, palm and thumb, able to achieve most human postures and which can be customized to different hand sizes, is constructed. Special attention is given to the issue of thumb opposition - against finger tips, finger surfaces, finger sides, and palm - which plays an important role in many commonly encountered grasps. For a grasp combining several cooperating oppositional intentions, hand surfaces can be simultaneously involved in multiple oppositional roles. We characterize the low-level interactions between different surfaces of the hand based on captured interaction force and reconstructed hand surface geometry. This is subsequently used to separate out and prioritize multiple and possibly overlapping oppositional intentions present in the demonstrated grasp. We evaluate our method on several human subjects across a wide range of hand functions.

The last part of the thesis applies the properties encoded in opposition primitives to optimize task performance of the arm, for tasks where the arm assumes the dominant role. An example is cutting, where the downward force and forward-backward motion at the cutting blade is primarily generated in the arm. For these tasks, choosing the strongest power grasp available (from a force-closure sense) may constrain the arm to a sub-optimal configuration. Weaker grasp components impose fewer constraints on the hand, and can therefore explore a wider region of the object relative pose space. We take advantage of this to find the good arm configurations from a task perspective. The final hand-arm configuration is obtained by trading off overall robustness in the grasp with ability of the arm to perform the task. We validate our approach, using the tasks of cutting, hammering, screw-driving and opening a bottle-cap, for both human and robotic hand-arm systems.

**Keywords:** Grasping with dexterous hands, Grasp recognition, Task-oriented hand-arm configuration, Opposition primitives, Tactile sensing

# Résumé

Les avancées significatives de la conception et de la construction des mains anthropomorphe des robots, dotent eux avec capacités presque humains. Cependant, l'utilisation de ces mains puissantes, avec le même niveau d'expertise que les humains, est un grand défi pour les robots. Compte tenu de la grande espace de configuration de la main, de l'objet et de la tâche, le problème devient complexe à aborder. Les approches traditionnelles pour saisir des objets avec une main dextre se focalisent sur la génération de configurations de préhension du point de vue de 'force-closure', utilisant la main pour attraper des objets du bout des doigts (saisie de précision) ou bien par enveloppement (saisie de puissance). Dans le contexte des systèmes main-bras anthropomorphes, ce raisonnement ne tient compte ni de la diversité des postures préhensiles disponibles avec une main, ni du contexte plus large des mouvements du bras avec lequel la tâche doit être effectuée. On a donc besoin d'une perspective differente.

Cette thèse explore un modèle de formation de préhension fondée sur l'opposition entre les parties de la main, ce qui a été proposé comme une base fonctionnelle pour la préhension chez les humains (Mackenzie et Iberall, 1994). Un ensemble de primitives formalisent la capacité de la main à créer des forces opposées. Les parties de la main qui seront dans l'opposition, ainsi que la distribution de la force de préhension, constitue l'intention d'opposition. Les propriétés fonctionnelles de la préhension de précision et de force sont dérivées de l'utilisation du bout des doigts ou d'une grande surface de la main dans chaque cas. Avec les primitives d'opposition, l'utilisation de surfaces de la main peut être modulée. Chaque primitive conduit les contacts avec un objet à un endroit particulier de la main, conduisant à différentes qualités de force et de mouvement pour un objet saisi. Les régions de contact de primitives correspondant à des surfaces opposées sur l'objet décide comment une primitive peut être appliquée. Cela limite également la pose du poignet, exposant ainsi la fonctionnalité de la primitive au bras et aux niveaux supérieur du système. Dans cette thèse nous profitons les propriétés des primitives de l'opposition pour interpréter la préhension créée par les humains et pour construire des nouvelles configurations de saisie pour une robot en considérant le système bras-main en entier.

Dans la première partie de la thèse, nous examinons l'hypothèse que les systèmes de représentation de la main sur la base de l'opposition sont en cor-

rélation avec la fonction de la main. Nous proposons un paramétrage de la main décrivant l'intention d'opposition et les comparons avec des méthodes couramment utilisées telles que les angles des articulations, des synergies communes et des caractéristiques basées sur la forme. Nous nous attendons à ce que des paramétrages en fonction de l'opposition, qui ont un point de vue sur la base de l'interaction d'une préhension, sont capables de discriminer entre saisies qui sont semblables dans la forme mais différentes dans l'intention fonctionnelle. Nous testons cette hypothèse par évaluation qualitative des capacités de précision et de puissance trouvés dans taxonomies existantes de préhension.

La partie suivante de la thèse présente une méthode générale pour reconnaître l'intention d'opposition manifestée lors de démonstrations de préhension humaines. Un gant de données instrumenté avec des capteurs tactiles est utilisé pour fournir l'information brute sur la configuration de la main et la force de l'interaction. Un modèle de la main humaine à 21 degrés de liberté, comprenant 4 doigts, la paume et le pouce, en mesure d'atteindre la plupart des postures humaines et qui peuvent être personnalisé pour différentes tailles de main, est construit. Une attention particulière est accordée à la question de l'opposition du pouce - contre le bout des doigts, les surfaces de doigts, sur les côtés des doigts et la paume - qui joue un rôle important dans de nombreuses configurations de saisie couramment rencontrées. Pour une préhension combinant plusieurs intentions d'opposition coopérantes, les surfaces des mains peuvent être impliquées simultanément dans plusieurs rôles d'opposition. Nous caractérisons les interactions de bas niveau entre les différentes surfaces de la main sur la base de la force de l'interaction capturée et la géométrie de la surface de la main reconstruite. Ceci est ensuite utilisé pour séparer et prioriser de multiples intentions d'opposition présentes dans les préhensions présentées, qui éventuellement se chevauchent. Nous évaluons notre méthode avec plusieurs sujets humains avec un large éventail de fonctionnalités de la main.

La dernière partie de la thèse applique les propriétés de primitives de l'opposition pour optimiser les performances de la tâche du bras, pour les tâches où le bras assume un rôle dominant. Un exemple est la découpe, pour laquelle la force vers le bas et le mouvement d'avant en arrière de lame sont principalement générés par le bras. Pour ces tâches, choisir la saisie la plus puissante possible (au sens de 'force closure') peut limiter le bras à une configuration sous-optimale. Des composantes plus faibles de la saisie imposent moins de contraintes sur la main, et laissent donc à explorer une région plus large de positions possibles relatives à l'objet. Nous profitons de ceci pour trouver les bonnes configurations du bras à partir d'une perspective basée sur la tâche à accomplir. La configuration finale main-bras est obtenue en compensant la robustesse globale de la saisie avec la capacité du bras à effectuer la tâche. Nous validons notre approche, en utilisant les tâches de découpe, d'utilisation d'un marteau, et d'ouverture d'un bouchon de bouteille à la fois chez l'humain et avec un système robotique main-bras.

**Mots Clé:** Préhension avec les mains dextres, reconnaissance de préhension, configuration main-bras orientée pour la tâche, les primitives d'opposition, sensation tactile.

*To my wonderful and ever caring parents.*
*To my beloved Cristina and our lovely children Mrinali and Mark.*

*From you I have received*
*endless love, support and encouragement.*

# Acknowledgments

I would like to extend my thanks to the IST-EPFL joint doctoral initiative for accepting me into the program and FCT for the doctoral scholarship. In a special way, I would like to deeply thank my advisors, Prof. José Santos-Victor from Vislab at IST and Prof. Aude Billard from LASA at EPFL, for giving me the unique opportunity to pursue Ph.D research under their supervision at two world-class research labs. I feel especially privileged to have not one but two highly competent and accomplished researchers and scientists to guide me. I am thankful to José for introducing me to the problem of robot grasping and for allowing me to look at the problem from a non-traditional *opposition-based* perspective. Thanks for his patience and encouragement during the initial years exploring this vast and already well researched topic. Thanks for his generous concern and support in negotiating the transition to Lausanne with family. I am thankful to Aude for accepting me in her lab at the mid-way point and for providing such an excellent and stimulating environment with state-of-art multimodal sensory equipment and robotic hand-arm platforms for research. More than that, I especially thank Aude for her availability, incredible patience, constant support and guidance through the many discussions which helped shape, focus and develop my thinking and scientific approach. I much appreciate her also for the help and experience so generously extended on several occasions for negotiating, the sometimes tricky, life situations with a family here in Switzerland. Both my supervisors have invested precious time and considerable energy in reading and correcting my articles and thesis through many iterations always providing insightful and fruitful guidelines. For this I am very grateful. Without their continued support, patience, availability and advice, this thesis would not have been possible.

I would like to thank Prof. Silvestro Micera (EPFL), Prof. Oliver Brock (TUB) and Prof. Tamim Asfour (KIT) for accepting to read and evaluate my thesis. I am grateful for all the time and effort they invested and their valuable insights and comments on the earlier version of the manuscript. I also thank Prof. Hannes Bleuler (EPFL) for his service as the president of the jury.

I have been fortunate to experience a diversity of scientific research in two world-class labs and have benefited greatly from the insights, experience and friendship of so many wonderful colleagues. I would like to thank Prof. Alexan-

dre Bernardino to whom I went to with all questions, ideas and problems in the initial days of the Ph.D. Thanks for keeping your door always open and many thanks for the enthusiastic and engaging discussions which helped me to focus my ideas. Thanks for involving me in several technical activities of the HANDLE project and for the immensely constructive advice on my articles and thesis proposal.

My thanks to Bruno Damas, Ricardo Ferreira and Manuel Marques, my office mates at IST, with whom I shared many pleasant personal and technical conversations. I am forever grateful to Manuel for showing me each day a living example of indomitable spirit, quite courage and perpetual cheerfulness under severe physical handicap. Thanks to Prof. José Gaspar, Plinio Moreno, Dario Figueira, Giovanni Saponaro, Nuno Moutinho, Rui Figueiredo, Matteo Taiana, Jonas Hörnstein, Jonas Ruesch, Duarte Aragão, Filipe Veiga and all the Vislab members for making a lively and stimulating atmosphere for working and relaxing. Thanks for all the fun times we had at Espadachim. My special thanks to Luka Lukic and Sebastian Gay, and later on Hang Yin, fellow students in the IST-EPFL program, for exchanging experiences, tips and procedures which made transition between two countries, universities and labs manageable. I thank also Ana Santos, the lab secretary, who handled all administrative issues with characteristic efficiency.

I am immensely grateful to Dr. Sahar El-Khoury, with whom I was fortunate to work with when I first came to EPFL. Thanks for your dedication and patience as we worked through the various iterations of the data-glove, its calibration, the many issues integrating information from different sensory channels and the tedious process of gathering human data. I learned much from your experience and professionalism. The entire lab benefited from your bubbly enthusiasm and cheerfulness. My especial thanks for reading all my articles and contributing your vast experience to providing detailed and constructive feedback. Thanks also for the french translations of housing applications which enabled me to find a house!

I would like to thank Miao Li and Hang Yin, my office-mates. My thanks to Miao for his great drive for research which always inspires me, the many interesting discussions we had on robotic grasping and for sharing his experience on the Allegro Hand and OpenRave simulator. My thanks to Hang Yin for showing me quietness and confidence. Thanks for being ever ready as sounding board for ideas and to help in trouble shooting any hardware problem. I am grateful to Nicolas Sommer for sharing his experience and insights in controlling the robot hand. I am especially grateful for the many hours we spent in realizing opposition-based grasp plans on the Kuka-Allegro robotic platform. Thanks for solving all the computing needs (and also french translation needs) for everyone in the lab. My thanks to Bidan Huang and her advisor Prof. Joanna J. Bryson for the many interesting discussions on the use of the data-glove. Thanks to Ashwini Shukla, Suengsu Kim, Mohammad Khansari Zadeh, Klas Kronander,

Guillaume de Chambrier and Nadia Figueroa for sharing their technical expertise and code and coding skills on several occasions. I am grateful to Sina Mirazzavi for his help with images, photos and videos and for being the goto person to resolve any technical problem with the robot. We have interesting discussions on a range of topics in the LASA lab and share many laughs together, during break-times, lunch-breaks, ski-outings, dinners. My thanks go to all members of the LASA lab for making such a vibrant work atmosphere and a memorable experience.

I would like to thank our lab secretary Joanna Erfani and the EDPR secretary Corinne Lebet and Sandra Roux from the doctoral school for taking care of all the administrative aspects during the Ph.D.

We have had the pleasure of knowing several people outside of the university who have made our stay in Portugal and Switzerland both possible and pleasurable for me and my family. In Lisbon we are especially grateful to Alfredo and Vera Bruto da Costa, for accepting us in their home till we found a place. Even after, yours was our home away from home always open with much warmth and love for us during the years in Portugal. Thanks to Edgar and Manuela Sousa for all the love and affection showered on us and our children. Thanks to Nuno, Margarida, Bernardo, Ana Catarina, André, Ana Berta for all the joyful moments we shared together. In Switzerland we are grateful to our neighbours Mme. Bretton, Alexia and Christophe de Buttet and their children for their warm welcoming and friendship, help in living, schooling, and many other things. Thanks to Mme. Bretton for being a grand-mother to our children. Special thanks go to our friends Shushila and Mathias, Hannah and Rico, Shiny and George for many joyful moments spent together.

I deeply thank my dear wife Cristina for her endless love, support and encouragement by which I was sustained throughout the Ph.D. Thank you for bringing so much joy into my life and for being the strong pillar of our home, keeping the home-fires burning so that I could complete my research. I thank my children, Mrinali and Mark, who bring joy and happiness into our lives. I am deeply grateful to my parents who have believed in me and given me all that is worth having in this life. It is to their steadfast love and support also that I owe this thesis. I am grateful to my brother and sister, my parents-in-law, and so many other family back home in India whose prayers and well-wishes I could always count on and have benefited greatly from.

Finally, I say Deo Gratias! Thanks be to Almighty God who makes all things possible and from whom my family and I have received love, blessing upon blessing, the grace to endure, kindness and mercy beyond measure.

*Thy steadfast love is great*
*is great to the heavens*
*and thy faithfulness*
*thy faithfulness to the clouds*

# Table of Contents


**1 Introduction . . . . . 1**
- 1.1 Motivation . . . . . 1
  - 1.1.1 Contributions of this thesis . . . . . 4
- 1.2 Opposition-based representation of the hand . . . . . 5
  - 1.2.1 The role of oppositions in the temporal dimension of reaching and grasping . . . . . 7
  - 1.2.2 Assumptions in this thesis . . . . . 7
- 1.3 Grasping with robot hands: comparing precision and power to hand oppositions . . . . . 9
  - 1.3.1 Precision grasps . . . . . 9
  - 1.3.2 Power grasps . . . . . 9
  - 1.3.3 Compliant grasps . . . . . 10
  - 1.3.4 Task-oriented grasps . . . . . 10
  - 1.3.5 Key limitation . . . . . 11
  - 1.3.6 Comparison with opposition-based representation . . . . . 11
- 1.4 Thesis Outline . . . . . 13

**2 Hand-Representation: Shape v/s Opposition . . . . . 15**
- 2.1 Foreword . . . . . 15
- 2.2 Hand Representation . . . . . 16
  - 2.2.1 Shape based . . . . . 16
  - 2.2.2 Opposition based . . . . . 17
- 2.3 Hand Function Space . . . . . 19
  - 2.3.1 Functional ordering . . . . . 20
- 2.4 Obtaining hand parameters from a grasp demonstration . . . . . 22
  - 2.4.1 Shape-based Parameters . . . . . 22
  - 2.4.2 Opposition-based Parameters . . . . . 23
- 2.5 Grasp Data . . . . . 26
- 2.6 Results . . . . . 28
- 2.7 Conclusion . . . . . 31
  - 2.7.1 From continuous to discrete opposition-based representation 32

**3 Opposition primitives to interpret human grasp behaviour . 33**
- 3.1 Foreword . . . . . 33
- 3.2 Introduction . . . . . 33
- 3.3 Literature Review . . . . . 36
- 3.4 Human grasp data . . . . . 38
  - 3.4.1 'Sensorized' data glove . . . . . 38
  - 3.4.2 Kinematic Model . . . . . 40
  - 3.4.3 Calibration . . . . . 42
- 3.5 Component model for human grasp behaviour . . . . . 43
  - 3.5.1 Opposition concepts in a sensing framework . . . . . 43

3.5.2 Extending the Opposition Space definition . . . 44
3.5.3 Primitive set for recognizing grasp intention . . . 46
3.5.4 Grasp Signature . . . 47
3.6 Inferring a grasp signature . . . 50
3.6.1 A metric for patch level opposition (PLO) . . . 50
3.6.2 Feasible patch level oppositions (the PLO-space) . . . 51
3.6.3 Computing a grasp signature . . . 54
3.7 Experimental Validation . . . 56
3.7.1 Single expert demonstrator . . . 56
3.7.2 Different grasps on the same object . . . 58
3.7.3 Multiple naïve demonstrators . . . 60
3.8 Discussion: limitations, applications and future directions . . . 67
3.9 Conclusions . . . 68

**4 Opposition primitives for task-oriented hand-arm configuration 69**
4.1 Foreword . . . 69
4.2 Introduction . . . 69
4.3 Literature Review . . . 71
4.3.1 Stable grasp generation . . . 71
4.3.2 Task-oriented grasp generation . . . 73
4.3.3 Combining hand configuration with arm configuration . . . 74
4.4 Primitives as bridge between hand-function and arm-function . . . 76
4.4.1 Basis for grasp construction . . . 76
4.4.2 Functionally relevant wrist-pose space . . . 79
4.5 Task-Oriented configuration of hand-arm system . . . 84
4.5.1 Task Model . . . 84
4.5.2 Task Suitability metric . . . 87
4.5.3 Algorithm . . . 88
4.6 Characterization of directional quality for hand and arm . . . 91
4.6.1 Hand Quality . . . 91
4.6.2 Arm Quality . . . 97
4.7 Application to human hand-arm system . . . 99
4.7.1 Simulation setup . . . 99
4.7.2 Simulation Results: Cutting task . . . 100
4.7.3 Simulation Results: Hammering, Screw-driving, Open-cap Tasks . . . 103
4.7.4 Discussion . . . 107
4.8 Application to robotic hand-arm system . . . 112
4.8.1 Experimental setup . . . 112
4.8.2 Open Cap Task . . . 115
4.8.3 Hammering Task . . . 119
4.8.4 Discussion . . . 123
4.9 Conclusion . . . 124

**5 Conclusion . . . 125**
5.1 Main Contributions . . . 125
5.2 Perspectives on opposition-based grasping . . . 127

**References . . . 129**

Chapter 1

# Introduction

## 1.1 Motivation

Grasping plays a central role in our daily life. The human hand is a very versatile grasping device endowed with large flexibility in grasp formation. Daily interaction with the real world requires humans to use this flexibility in a variety of ways. Though the musculo-skeletal system presents formidable complexity in terms of sensory information to be processed and parameters to be controlled, we are extremely adept at using all hand flexibility available to command the right mix of qualities, when and where they are required, according to the demands of a task and respecting the larger context of arm action.

Consider that we are doing the task of calligraphy writing. For beautiful well-shaped strokes we grasp the pencil between the thumb, the tip of the index finger and the side of the middle finger. This grasp provides sufficient stability to withstand the writing forces without overwhelming dexterity of motion required to shape the different letters. If we should commit an error and need to use the eraser on the opposite end of the pencil, we change the grasp. Greater forces and coarser motions are involved. These are provided by the wrist. We angle the pencil differently in the hand, adding more finger-tips along the pencil length perhaps pressing also against the index-side. We might try to use the pencil to pry out something that is wedged in-between the cracks of the bench on which we are sitting. Even greater forces are required. These are provided by the arm. Now we fix the pencil in the palm and the thumb clamps the pencil against the extended index finger to keep the tip directed appropriately. The new grasp also positions the pencil as an extension of the arm which makes it easier to generate and control the prying motion. We exploit flexibility in grasp formation to hold the same object in functionally different ways. We also use flexibility in grasp formation to optimize higher-level objectives in the hand-arm system. However, it is not our experience to reason in terms of muscle signals, finger joint angles and precise object contacts. Rather, we seem to know even before the grasp is formed what functionality will be brought to the grasp and what constraints will result on the arm by engaging different parts of the hand.

Robotic systems, modelled on the human, aim at realizing similar kinds of interaction with the real world (Asfour et al., 2006; Borst et al., 2007; Kaneko et al., 2008). These systems, equipped with anthropomorphic hand-arm de-

signs, display capabilities in reaching and grasp formation approaching that of humans. While several decades of research (Bicchi, 2000) has seen much progress in robotic grasping and manipulation, harnessing the capabilities of these complex systems autonomously and in a task context still remains a significant challenge. The object, task, hand, the larger hand-arm embodiment and the environment form a high dimensional space. Grasp planning must therefore ignore some parts of the problem and adopt simplifications for others in order to make the computation tractable.

The vast majority of methods in the grasping literature see the problem in terms of object contacts and/or hand configuration[1]. This represents the final outcome of a realized grasp. Commonly followed approaches in planning for this outcome adhere to the broad dichotomy of hand-functionality presented by Napier (1956). In his paper, Napier proposed two kinds of grasps. Precision grasps, using only the finger-tips, leverage the capabilities of the dexterous hand for manipulability and fine control. Power grasps, using all finger surfaces and the palm, look to maximize the surface area of the hand in contact with the object allowing for large forces to be resisted. Accordingly, grasps are found satisfying some overall robustness or dexterity criteria. However, from the earlier examples, the hand is capable of finer variation of function where both precision and power can be combined in a single grasp, pressure can be emphasized selectively in response to task requirements and flexibility in grasp formation can exploited to optimize higher objectives of the hand-arm system. A different perspective on grasp generation is therefore required which can model and harness such capabilities essential to the execution of tasks in the real-world.

The problem lies in that too much focus is given to the outwardly visible final outcome of grasp planning which are contacts and configuration. Lesser importance is given to characterizing the known functional abilities of the agent, in this case the hand, and how these can be harnessed towards the task for a given object. The abilities for generating force, motion, stiffness/compliance, tactile sense vary over the grasping surface of the hand. Questions like: Which hand surfaces will be used and how hand surfaces will interact with each other, determine to large extent the functional capabilities of the hand brought to the grasp and how they can be controlled. Methods which focus only on configuration and contact neglect to represent what happens inside the hand, how this relates to task goals and why some hand surfaces are better than others from a task perspective. Consequently this information is not available at planning, when the choice of hand surfaces have to be made, nor during task execution, when the functional reason for choosing particular hand surfaces must be exercised and/or modulated. Figure 1.1 takes the example of egg-beating and examines the common grasp employed for this purpose to illustrate these points further.

[1] Prevailing techniques are discussed in Section 1.3

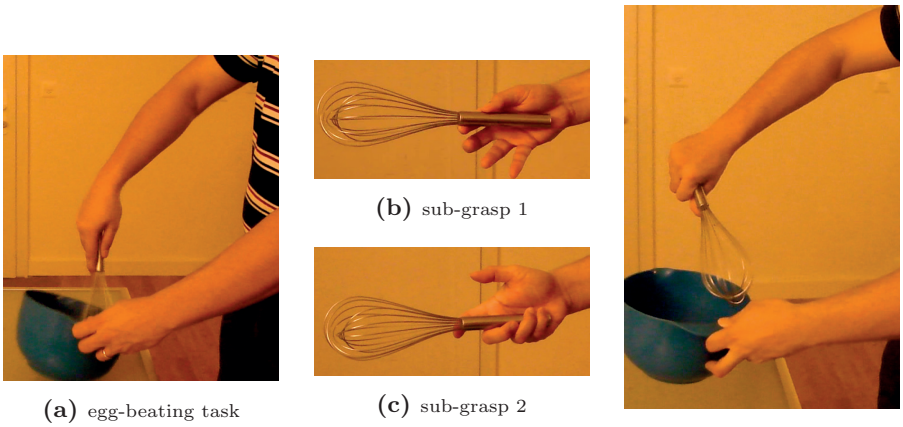

**(a)** egg-beating task

**(b)** sub-grasp 1

**(c)** sub-grasp 2

**(d)** egg-beating task with strong grasp

**Figure 1.1:** Figure 1.1a shows the functional use of hand surfaces in the context of a commonly employed hand-arm configuration for egg-beating. The grasp is composed of two sub-grasps; the thumb and index finger makes one part ( 1.1b) and rest of the fingers and palm make up the other part ( 1.1c). These sub-grasps are not in any grasp taxonomy. Neither can we plan for them using overall stability as a criteria because they are not stable by themselves. Yet this flexibility is allowed by the hand and is used here in a task context.
The particular hand surfaces chosen and the manner in which they are engaged have vital task relevance. Force distribution among the contacts and stiffness in the fingers contribute to creating two axes of oppositional pressure which cooperate to hold the tool stably. This is maintained and modulated in step with higher level arm action to ensure adequate grip properties during egg-beating. The thumb-index finger combination contribute to small reorientations of the tool. Also, having greater tactile sensitivity than the other stronger sub-grasp, it senses state of the grasp and provides input to grasp modulation. Finally, the particular combination of sub-grasps positions the tool as an extension of the forearm which makes the wrist flexibility directly relevant to task motions. Holding the tool in an overall more robust fashion ( 1.1d) requires the arm to solely generate the beating motion or constrains the arm to a poor configuration for egg-beating forces if the wrist has to be involved.

To sum up, the anthropomorphic hand displays lot of flexibility in grasp formation. In order to leverage this in a task-oriented manner this flexibility must be represented. Furthermore, the functional consequences of engaging particular hand surfaces and the impact on higher levels of the system cannot be ignored.

This thesis explores a human inspired paradigm for representing grasps that is based on generating oppositional pressure within the hand. The task relevance of this representation stems from the fact that it directly represents the way hand surfaces are intended to be used. In particular, it models *interaction between hand surfaces* and *the functional role of fingers* in a grasp. With this model, the functional qualities of any group of interacting surfaces may be represented at the planning stage. The problem of finding precise configuration and contact is treated as secondary and addressed only after the functional abilities available to the hand have been appropriately selected, customized and setup for use in a task context. It therefore presents a promising, and till now largely unexplored, way to computationally reason with flexibility for grasp formation available to the anthropomorphic hand in a task-oriented fashion.

### 1.1.1 Contributions of this thesis

In this thesis we develop the concept of opposition-based representation into a computational framework. This is applied in the context of modelling task relevant information from a human grasp demonstration and also planning grasps for a robotic system considering the task performance of both hand and arm together.

Data-driven approaches aim at understanding strategies of human grasping, their representation and transfer to robotic hand-arm systems. Approaches thus far aim to capture and classify the demonstrated configuration. In this thesis, we consider the demonstrated hand surface usage to be task relevant. This is captured in the raw sense from the pose and force vectors ($\mathbf{D} = [\mathbf{p}, \mathbf{f}]_{i=1}^{n}$) associated with a grasping patch decomposition imposed on the surface of the hand. Task-relevance is first represented by modelling interactions between hand surfaces at the patch level. The resulting 144 dimensional continuous feature is a step forward from seeing tactile and configuration data as disconnected information. However, to be able to recreate $\mathbf{D}$, we present a general method to separate the grasp into a set of cooperating high level oppositional intentions, allowing overlap in the underlying hand surfaces used to form them. This *grasp signature*, while not suited to accurately recreate the demonstrated configuration or shape, is better positioned to recreate, maintain and adapt the task relevant information, i.e the $\mathbf{D}$, that was demonstrated.

Representing a grasp demonstration in a task relevant manner implies the ability to first capture appropriate sensory information. For this purpose, we construct a sensor setup consisting of a data-glove covered with tactile sensors to simultaneously record the hand configuration along with tactile force. Close attention is paid to the kinematic model and its calibration in order to capture the intended use of hand surfaces against each other in the demonstrated grasp.

This thesis also applies the concepts of opposition-based representation to planning task-oriented configurations for high DOF hand-arm systems. Due to the high dimensional configuration space, current approaches treat hand and arm configuration separately, preferring to use the strongest grasp reachable by the arm or the quickest reachable grasp satisfying some stability criteria. This is liable to constrain the arm poorly for task goals (e.g. Figure 1.1d). We use weaker grasp components to discover regions of the arm configuration space better suited for the task. Methods are proposed to quantify the task-relevance of different oppositions possible for the anthropomorphic hand at the sub-grasp level and relate this to higher levels of the hand-arm system within a task context. By this we are able to optimize the quality of the arm configuration for generating task related forces and motions before the grasp has been completed configured. The task relevance of the grasp, being closely tied to the properties of the selected opposition, is retained for use during execution. The computational framework developed provides a means for dimensionality reduction in

task-oriented planning for anthropomorphic hand-arm systems with high DOF.

## 1.2 Opposition-based representation of the hand

The idea of using hand-oppositions to explain prehensile posturing from a functional perspective is not new. It was introduced earlier by Iberall (Iberall et al., 1986; Iberall, 1987; Iberall et al., 1990; Iberall, 1997; Arbib et al., 1985). However, it has been largely unexplored with regards to representing human grasp demonstrations and in computational frameworks for task-oriented planning. Here we introduce a set of key concepts from these works that form the foundation of reasoning about grasp formation in terms of oppositions and which we build upon in this thesis.

**Definition 1.1** *An **opposition** is the setting up of the ability to generate a pair of opposing forces within a hand-centric coordinate frame using a subset of the hand surface.*

**Definition 1.2** *A **virtual finger (VF)** is an abstract representation, a functional unit, for a collection of individual hand surfaces that work together for the purpose of applying an oppositional force.*

**Definition 1.3** *The hand surfaces working together in a virtual finger are known as the **virtual finger grasping surface** and may include frontal finger surfaces, finger sides, thumb surface and also the palm.*

**Definition 1.4** *The **focus of pressure** within the VF grasping surface represents a region that takes a primary role in the generation of oppositional pressure.*

**Definition 1.5** *The starting configuration of the hand from which 2 virtual fingers are be brought together against the object surface to complete the opposition is termed the **opposition pre-shape**.*

**Definition 1.6** *Specifying the opposition preshape and properties of the virtual finger grasping surface for a VF pair instantiates an **oppositional intention** which is also termed as an **opposition primitive**.*

**Definition 1.7** *The **axis of opposition** or the **opposition vector** is the line joining the foci of pressure of the VF pair that make up an opposition primitive*

The virtual finger and opposition (as a pair of virtual fingers) serves as an abstraction that can encode several task relevant functional properties of the underlying hand surfaces they represent and their intended manner of use. The most obvious one is the force generated by the united action of all surfaces

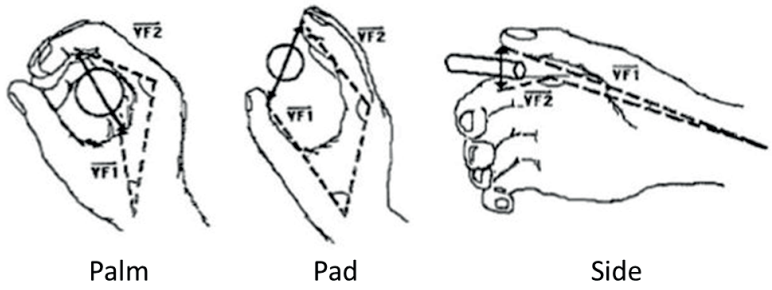


**Figure 1.2:** Opposition primitives as proposed by Iberall et al. (1986)

associated with a VF. But the representation is open to several other task relevant properties provided a suitable method for their quantification is available. Properties like tactile sensitivity, range of force, resolution of force, amount of compliance possible, force distribution, motion generation and so on. The power of this abstraction can be seen from the fact that it separates the mechanical degrees of freedom from the functional properties of a VF pair which are more relevant for the task. From a planning perspective, we can reason with functionally correlated state variables. At the same time, enough information remains (pre-shape, surface - {size, location, orientation}, opposing constraints) to constrain the prehensile posture.

Using these concepts, 3 types of opposition primitives have been proposed (Figure 1.2), each bringing different abilities for force and motion on the grasped object.

1. **Pad opposition**. Occurs between hand surfaces along a direction closely parallel to the palm. Occurs between thumb pads and finger pads. Commands lighter forces but opens up degrees of freedom for manipulability in the hand.

2. **Palm opposition**. Occurs between hand surfaces along a direction closely perpendicular to the palm. Occurs between fingers surfaces and the palm. Can generate strong forces at the cost of dexterity and tactile sensitivity.

3. **Side opposition**. Occurs between hand surfaces along a direction closely transverse to the palm. Occurs between thumb surface and the radial sides of the fingers. Provides intermediate forces while leaving some room for dexterous ability.

Finally, different oppositions may occur together bringing different capabilities of the hand to the grasp. A combination of oppositions, or an opposition space, can be defined as follows.

**Definition 1.8** *A collection of virtual fingers formed by a kinematically feasible combination of oppositions acting together sets up an* ***opposition space*** *where a cooperating set of opposing forces between the virtual fingers can be generated on a grasped object*

Note that there is no exact notion of prehensile posture in the opposition space paradigm. Contact and configuration proceed from the oppositional intention. The outwardly visible posture is an outcome of closing the fingers according to the oppositional intention. Each combination of opposition primitives corresponds to the setting up of a different opposition space within the hand. These spaces are not isolated from each other but can be seen as a continuum. By changing the underlying hand surfaces used and how pressure is distributed it is possible to transition between neighbouring opposition spaces.

### 1.2.1 The role of oppositions in the temporal dimension of reaching and grasping

Prehension in humans has a temporal dimension. The arm reaches for the object while simultaneously pre-shaping the hand in preparation for grasping. A closure phase then completes the grasp leading to the object being held stably. Task execution follows stable grasping. Task execution may require the object to be manipulated in-hand. Even without in-hand manipulation, changes in compliance and force distribution may be required depending on the task forces and the action of the arm. These changes do not affect the underlying grasp structure. However responding to unexpected perturbations may require adaptations to the grasp structure as well. As mentioned in (Iberall et al., 1986), and described briefly below, opposition-based grasped formation represents a theory of prehension that can guide the task relevant planning and control of the hand-arm system over all these phases.

In the planning stage, an opposition space is decided for the hand along with the location of opposition axes inside the object. Pre-shaping with the hand does not target a point in joint configuration space, rather it is concerned with setting up the chosen opposition space in the hand. Reaching and pre-shaping are coordinated so as to align the virtual finger grasping surfaces with the planned opposition axes inside the object. During hand closure, virtual finger grasping surfaces are driven towards each other to manifest the oppositional intention. Here the arm is used to adapt the wrist pose as the fingers close so that oppositional pressure within the object can be established as planned. During task execution the grasp maintains the planned opposing force, but other properties related to sensing, motion and compliance, expressed relative to an opposition, can also be exercised. Finally, since the opposition space was decided for a particular task context, task relevant adaptation of the grasp is achieved by modulating properties of the constituent oppositions and/or transitioning to a neighbouring opposition space.

### 1.2.2 Assumptions in this thesis

This thesis uses an opposition-based model to represent grasps in a task-oriented manner. This model considers interaction between hand surfaces as the means

to simplify the complexity encountered in reality. The following key assumptions are made:

- Only static grasps are considered. These are the phases involving pre-shape and closure leading to a stable grasp. Other phases in the reach and grasp temporal continuum mentioned in section 1.2.1, including in-hand manipulation, are not considered.

- A discrete set of opposition primitives is considered sufficient to represent all the ways opposing force can be generated in a task relevant manner.

- An opposition primitive is modelled with one region where pressure is assumed to be focused (the centre of pressure) and surrounding contiguous cooperating hand surfaces. Chapter 4 discusses this in more detail.

- Only oppositions between hand surfaces are considered. Opposition can also occur against task forces, such as pressing a button, or against gravity, but these are not considered for the purposes of this thesis.

These assumptions may not allow to explain all variations of human grasp behaviour or grasping with dexterous robot hands. Nevertheless, the model retains several useful properties for task-oriented grasp formation which we leverage in this thesis. These are summarized below:

- Opposing surface constraints on the hand matched to opposing surfaces on the object identifies the ways a primitive may be applied.

- In the context of a single primitive, knowing regions on the hand where contacts will likely be generated and where pressure will be focused allows to quantify force and motion generation abilities and represent them in a hand-centric manner even before a grasp is formed. Primitives may therefore be differentiated from each other from a functional perspective and may be assessed against task requirements. This incorporates task relevance into grasp planning while simultaneously constraining the hand configuration.

- A grasp controller focuses on driving the opposing hand parts together. By maintaining oppositional and co-operational constraints on the grasping surfaces of the hand, a grasp controller preserves the functional role of the fingers through hand-closure and during task execution. The final contacts and configuration found become related to the task through the higher level oppositional intention.

- Positioning oppositional intention in the object constrains the wrist-pose and thereby the arm. By this, functional roles of the hand can be propagated upward in the hand-arm system and used to optimize global objectives in task-oriented configuration even before a grasp is formed.

## 1.3 Grasping with robot hands: comparing precision and power to hand oppositions

Common strategies employed when reasoning about grasp formation with robot hands adopt a precision or a power approach. Whereas precision grasps seek to optimize finger-tip placement, power grasps maximize contact of the hand with the object involving also the palm. Here we discuss these approaches and compare them with an opposition-based approach.

### 1.3.1 Precision grasps

Optimal contacts on the object can be found by maximizing a force-closure metric (Nguyen, 1987; Mirtich and Canny, 1994; Ding et al., 2001; Zhu and Wang, 2003). This ensures that any external perturbation can be resisted through force applied at the contacts. However, these contacts should also be feasible for the hand. Hence the object relative hand pose and finger kinematics must also be considered (Borst et al., 2002; Zhixing and Dillmann, 2011; Saut and Sidobre, 2012; El-Khoury et al., 2013; Hang et al., 2014b). For real-world application, the timely generation of grasp plans is important. Thus, heuristics may be introduced to bypass lengthy optimization, trading-off optimality of contacts for speed (Borst et al., 1999; El-Khoury and Sahbani, 2009). Also, to cope with real-world uncertainties, regions of contact may be found such that the grasp has similar quality as long as the contact falls within it (Zheng and Qian, 2005; Roa and Suárez, 2009; Krug et al., 2010). Notwithstanding these advances, global optimization of finger-tips do not exhibit a variety of grasps that leverage hand capabilities from contacts made on other parts of the hand.

### 1.3.2 Power grasps

Here contacts are no longer planned, rather they emerge from hand-closure following an enveloping strategy. Structural decompositions of the object (Michel et al., 2004; Huebner and Kragic, 2008; Przybylski et al., 2011; Roa et al., 2012) or shape approximations (Miller et al., 2003; Goldfeder et al., 2007) can be examined to answer how the hand should be applied such that a stable grasp will be the result. It has been shown also that searching the hand-object configuration space for the best approaches is computationally feasible with an eigengrasp representation (Ciocarlie and Allen, 2009), which projects hand joints into a lower dimensional subspace of hand synergies (Santello et al., 1998). Human demonstrations present another way by which information about successful grasps can be obtained (Li et al., 2007; Ekvall and Kragic, 2007; Herzog et al., 2014). Grasp experience built up in this way is generalizable to other objects as long as similarity to known models can be quantified (Saxena et al., 2008; Curtis and Xiao, 2008; Stark et al., 2008; Goldfeder and Allen, 2011). The methods discussed here do not consider task requirements. Force-closure is once again

the metric of choice by which grasp candidates are ranked for selection. This maximizes the chances to end up with a stable grasp. However, the downside of planning in simulation is that conditions in the real-world cannot be fully modelled Due to uncertainties in pose, object properties and robot control, grasps that are strong in simulation often turn out poor in practice (Balasubramanian et al., 2012; Weisz and Allen, 2012; Kim et al., 2013). This suggests the need to choose configuration, object-relative pose and closure techniques such that the grasp is automatically funnelled towards a stable configuration.

### 1.3.3 Compliant grasps

Strategies incorporating compliant shaping of the hand to the object have been proposed as means to counter uncertainties in model, sensing and actuation (Dollar and Howe, 2007). Here contact forces are harnessed to adapt the hand so as to maximize contact with the object and balance forces to achieve robust grasping. This can be done actively using traditional hands (Cutkosky and Kao, 1989). Several hands based on passive compliance have been designed which embeds this intelligence in the mechanical structure of the links and joints (Brown et al., 2010; Dollar and Howe, 2010; Odhner et al., 2014; Catalano et al., 2014; Deimel and Brock, 2015). Strategies for grasp planning with compliance choose a compliance funnel for the hand and match this with the object shape (Eppner et al., 2012; Eppner and Brock, 2013; Bonilla et al., 2015). Pre-grasp interactions with the object have been proposed as a means to guide the object into the compliance funnel (Dogar and Srinivasa, 2010; Kappler et al., 2010). In contrast to traditional planning approaches, contacts with the environment are encouraged as they facilitate compliance. For this, human strategies to naturally exploit environment constraints, such as contact with supporting surface, push against a wall, sliding along/off a surface, etc, can be characterized and applied to robot hands (Kazemi et al., 2012; Eppner et al., 2015; Heinemann et al., 2015).

These strategies however tend to use the whole hand as a compliance funnel whereas the prehensile capability of these hands is more comprehensive, spanning a variety of precision and power. Also, the problem of giving task relevance to a particular compliance is largely unaddressed in the planning. The variety of grasps realized by compliant hands delegate task relevance to the human, activating the closure only once the hand has been positioned appropriately (Catalano et al., 2014). Optimizing the ability for compliance while engaging the appropriate prehensile capability for the task is therefore a relevant question.

### 1.3.4 Task-oriented grasps

Considering that the object grasped is meant to be used in a task context, quality metrics can be adapted to measure robustness in task directions (Li and Sastry, 1988; Borst et al., 2005; Haschke et al., 2005; Li et al., 2007; Aleotti and Caselli, 2010; El-Khoury et al., 2015). These strategies discover grasps that

have a lower force-closure measure but are suited for task goals. In many cases the object should be grasped in a specific way since particular hand-object contacts have a task-related meaning (Cutkosky and Wright, 1986; Kamakura et al., 1980). These task specific contacts may be pre-identified (Rosales et al., 2011) or recognized from human demonstration (Lin and Sun, 2014) and matched to object regions to obtain grasps with the desired task-related properties. Alternatively, knowledge-based approaches make use of pre-defined prehensile postures or pre-shapes as defined in grasp taxonomies. Heuristic rules are constructed which use characteristics of the task and properties of the object to select an appropriate category for grasping. The selected category ensures that desired regions of the hand will impact with the object (Bekey et al., 1993; Hillenbrand et al., 2004; Morales et al., 2006; Prats et al., 2010). Information on where the object should be grasped for the task is manually specified for each object-task scenario. However this can also be encoded as wrist-pose constraints for an object (Berenson et al., 2009, 2011) or learned from human demonstration (Steil et al., 2004; Rothling et al., 2007; El-Khoury et al., 2007; Song et al., 2010).

### 1.3.5 Key limitation

The main limitation of these approaches is that they lack a general way to encode the task-relevant meaning of specific hand-parts and the contacts they can generate. Where this information does get considered, it is discarded once the hand-configuration is selected. This information, such as force-distribution, stiffness, intended motion, tactile sensitivity, may be seen as the functional role of the fingers. Recent works propose to augment existing grasp taxonomies using such information (Liu et al., 2014). This information is required for constructing grasps so that different capabilities of the anthropomorphic hand can be considered towards task goals. It is also important when maintaining or adapting the grasp during task execution. For example, maintaining force distribution that is relevant for resisting task-specific forces, selectively emphasizing pressure (to keep a hammer head from twisting out of alignment) or selectively relaxing pressure (so as to increase tactile sensitivity or to increase compliance) while maintaining the task relevant meaning of the grasp.

### 1.3.6 Comparison with opposition-based representation

Current methods of for grasp formation with robot hands may be visualized as shown in Figure 1.3 in terms of how hand surfaces are engaged. At one end we have precision grasp strategies. These only use the finger tips and leave out other parts of the hand from consideration. At the other end we have the encaging strategies for power grasps. These position the hand with respect to the object so that closing the fingers results in maximal usage of hand surface

including the palm. In between we have the knowledge-based strategies which rely on existing taxonomies of human grasp behaviour. Here, different surfaces of the hand are engaged in a task relevant manner but the taxonomy categories are represented by their joint configuration. No instructions exist in the representation to indicate which surfaces are more important than others for exerting pressure. To resist task forces and perturbations we are essentially limited to increasing torques on all joints. The alternative would be to build a customized set of controllers for each taxonomy category. Hand synergies present an attractive low dimensional space to represent human-like hand configurations. Synergy based representations are sufficient to model the shape but do not represent which hand surfaces are involved and what they are expected to do during the task. Hand surfaces in contact cannot be decided before hand and arise from synergy-based closure till contact with the object is detected. Underactuated hands leverage hand synergies for closure and mechanical compliance in the construction to achieve a variety of prehensile postures. The common strategy in this case is to use the entire hand as a compliance funnel. Hand surfaces engaged depend on how the had has been positioned with respect to the object.

An opposition-based representation models the way hand surfaces interact with each other to generate opposing force. It therefore adopts the middle ground between the contact-level (precision) and encaging (power) based approaches. Both precision and power capabilities may be combined in a single grasp. Contacts are neither planned nor are they entirely ignored. Rather contacts are the outcome of a higher level oppositional intention which is decided in a task-relevant manner. Opposition primitives go beyond synergies in joint space to synergies in interaction space. These synergies encompass all the pose and force possibilities of each grasping surface on the hand. Since we must pre-identify a set of ways oppositional pressure can be created in the hand, an opposition-based approach can be termed as knowledge-based. However, it operates at a level below existing taxonomy based approaches, since it provides

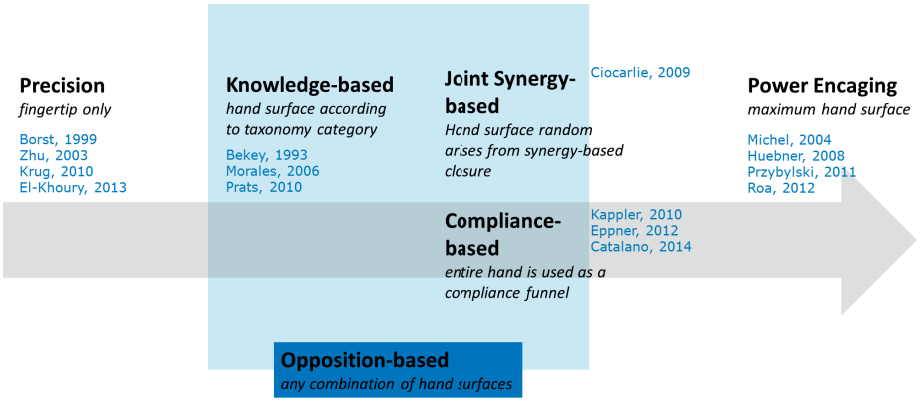


**Figure 1.3:** Methods for grasp formation with robot hands. A few representative works in each case have been listed alongside.

a basis from which a large set of prehensile postures can be constructed. An opposition-based approach relies heavily on compliance, but identifies several different types of compliance funnels which can be matched with the object and whose task relevance can be quantified during the planning stage.

## 1.4 Thesis Outline

The contributions of this thesis are organized chapter-wise as follows:

Chapter 2
**Hand representation: Shape v/s Opposition.**

Methods that attempt to capture the relationship between the grasp and the task, benefit from grasp features that have functional correlation. We contrast opposition-based and shape-based hand representation schemes on their ability to discriminate between grasps of different function. Modulating properties of opposing virtual fingers changes functionality brought to the grasp. This is used to develop an opposition based parameterization scheme. The number of parameters required are then significantly reduced by imposing the pre-shape conditions associated with primitives. Evaluation conducted with grasps taken from a functional taxonomy shows that representations based on shape (joint angles, joint synergies, shape features), while easy to extract from demonstration, bear little correlation with hand-function. Representations based on opposition require knowledge of which primitives are being employed. However, they show clear and consistent separation between precision, intermediate and power grasps.

Chapter 3
**Opposition primitives to interpret human grasp behaviour.**

Humans grasp for the task i.e. choices made on the use of hand surfaces stem from a perception of task demands even before a grasp is formed. In this chapter oppositional intention is seen as the essential meaning of a grasp, which drives grasp formation and which needs to be preserved/modulated during task execution in order to counter expected perturbations. We present a general method for interpreting demonstrated grasps, in terms of opposition primitives, from tactile force and joint angle information obtained using a sensorized data glove. A primitive model consisting of 41 oppositions for the hand is developed considering that thumb opposition against finger-tips, finger-surface, finger-side and palm should be recognized as separate grasp components. The more the human emphasizes an oppositional intention, stronger are the low level interactions between the virtual fingers of the primitive model for it. We present a metric for opposition strength based on tactile force and sensory geometry. This is used to

obtain a measure for likelihood of single primitive existence in a grasp demonstration and an importance distribution over the entire primitive set. Results from human grasp demonstrations show that, with a single expert demonstrator, the same grasp expressed on different objects, and different grasps on the same object can be recognized successfully. A recognition rate of 87% is achieved with multiple naïve demonstrators over a wide range of categories taken from a grasp taxonomy.

Chapter 4

**Opposition primitives for task-oriented hand-arm configuration**

In many real-world tasks, such as hammering, cutting, screw-driving or opening a tight bottle-cap, the wrist-arm combination is responsible for generating force and motion requirements while the hand transfers these to the object. For accomplishing such tasks with a robotic manipulator connected to a dexterous hand, the dual problems of stable grasp generation and optimizing arm function must be solved. These problems when addressed independently of each other may lead to arm configurations from where the object cannot be stably grasped or overly stable grasps which constrain the arm to configurations that are inefficient or impossible for task execution. Opposition primitives offer two advantages here. Firstly, they offer a principled way to expose a variety of grasps that are specialized for robustness in different task directions. Secondly, a larger wrist-pose space can be discovered than if we are limited to the strongest force-closure grasps. We leverage these properties to trade-off overall grasp robustness with the ability of the arm to deliver force and motion required for achieving task goals. The task is modelled by essential directions in which force and motion are required for task execution, such as downward force and forward/backward motion at the knife edge for cutting on a horizontal plane. Metrics are devised for the hand and arm based on their ability to provide force and motion in these directions. The approach is validated in the context of both human and robotic hand-arm systems. Results show that the configurations discovered, have better task-oriented quality from a hand-arm perspective, as compared with traditional methods for generating configurations for arms with dexterous hands.

Chapter 5

**Conclusion**

We summarize the thesis, outline the key contributions, discuss limitations and avenues for future work.

Chapter 2

# Hand-Representation: Shape v/s Opposition

## 2.1 Foreword

For a robotic gripper, an object relative grasping point and approach vector is sufficient to describe the way in which the gripper must be applied. Anthropomorphic hands, however, can organize in different shapes and forms to grip an object and impart force and motion (Cutkosky and Howe, 1990). Researchers have need to represent this flexibility for various purposes, such as identifying a grasp taxonomy category (Friedrich et al., 1999; Ekvall and Kragic, 2005), establishing correlation with object properties (Bernardino et al., 2013) and the task (Song et al., 2010), using pre-shapes in grasp planning (Morales et al., 2006; Harada et al., 2008; Prats et al., 2010), reproducing human-like reach and grasp motions (Ben Amor et al., 2012). These approaches rely on joint angles to capture hand configuration. However, we argue that this representation is associated with hand shape and is not well correlated with functional properties of the grasp. Approaches for task-oriented decision making benefit from hand representations that are correlated with hand function. We expect that oppositional intention, which represents the grasp from an interaction perspective, displays this property.

This chapter proposes 2 hand parametrization schemes based on opposition. Our goal is to evaluate these schemes against those based on shape from a functional correlation perspective. We use the notions of precision and power to describe hand functions qualitatively. A function space in terms of grasps with different capabilities of precision and power is constructed and ranked to obtain a functional ordering. The strategy adopted compares distance between grasps in parameter space to distance in functional space, where functional distance is seen as ordinal separation in an ordered grasp set. This work led to the following publication:

- R. de Souza, A. Bernardino, J. Santos-Victor, and A. Billard. On the representation of anthropomorphic robot hands: shape versus function. *Proceedings of* $12^{th}$ *IEEE-RAS International Conference on Humanoid Robots (Humanoids)*, pages 791-798. 2012.

## 2.2 Hand Representation

We distinguish between two kinds of representations for the hand: those based on shape and those based on opposition. This section will introduce these representation schemes.

### 2.2.1 Shape based

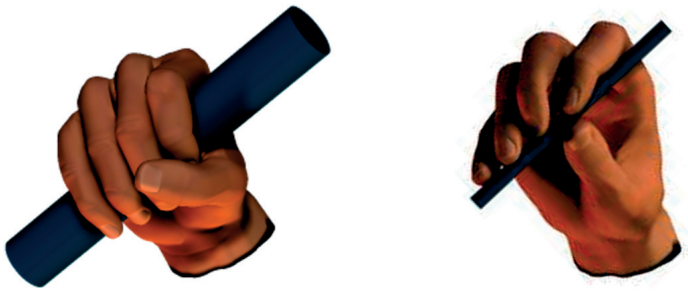

**(a)** Coal hammer **(b)** Sculpting or Engraving

**Figure 2.1:** While these grasps have similar shapes the function performed are very different. Figures taken from Feix et al. (2009)

Shape based representations focus on the outward appearance of the hand. Joint angles are a common way of representing complex hand shapes encountered in human grasp demonstration. Joint angles for the anthropomorphic hand form a high dimensional space. Exploiting the correlation that exists among finger joints, grasps may be represented by a lower dimensional subspace of hand synergies. Joint angles and hand synergies are convenient ways to represent a grasp. They are directly perceived from joint sensors and construction of complex hand shapes is easily achieved. However, these representations are not well correlated with hand-function. In many cases, the overall shape of the hand doesn't vary too much and similar shapes can be responsible for widely different functions. To illustrate this, Figure2.1a shows a grasp oriented towards delivering and resisting strong forces but this has a very similar shape to the grasp in Figure2.1b which is designed for more precise motions and moderate forces as would be encountered in a sculpting or engraving task.

Noting that the hand assumes similar shapes across different objects, Li et al. (2007) propose shape features and shape matching to generalize a demonstrated grasp to different objects. The shape feature descriptor is derived from a set of oriented points sampled from hand surfaces as they occur in a grasp demonstration. With this they can discriminate well between different hand shapes. Matching grasp shape to object shape however yields several grasps which must be pruned by assessing grasp quality against task criteria.

In this work we use joint angles, hand synergies and the shape feature described in Li et al. (2007) as shape based representations of a demonstrated grasp.

### 2.2.2 Opposition based

With an opposition based approach to hand representation, hand function is seen as the principal motive that drives all prehensile posturing, and the hand's ability to engage oppositional forces are seen as a functional basis. Engaging the different kinds of oppositions, namely pad, palm and side, brings different abilities to the grasp. Contrasting with the shape based representations, an opposition based representation takes an interaction view of the grasp, where particular hand surfaces impacting the object are given task relevant meaning and the outward shape becomes a consequence of this. Using the concept of virtual fingers to characterize cooperating hand surfaces (Arbib et al., 1985), each opposition can be seen as a virtual finger pair. Properties of these virtual fingers influence different functional abilities such as the degree to which force and motion can be generated, directions in which these capabilities are strong or weak, tactile sensitivity, etc.

Iberall et al. (1990) discuss different kinds of parameters for describing virtual fingers. The discussion lacks a practical implementation. However, the basic idea proposed is powerful. We develop it in this chapter to derive 2 parameterizations of virtual fingers which can be instantiated from a grasp demonstration. In essence, each virtual finger can be associated with a grasping surface (Section 1.2). This surface comes into purposeful contact with the object and allows the virtual finger to exercise its functions of applying pressure, imparting motion or gathering sensory information about hand-object interaction. A point on the grasping surface models the area where pressure is focused. An opposition vector is formed by joining the pressure foci of two virtual fingers in opposition. Properties of each grasping surface – its pose, surface area, curvature, location – can be varied, changing the properties of the opposition formed in the hand. Figure 2.2 shows different configurations of virtual finger pairs. Furthermore, as seen in Figure 2.2d, several pairs of virtual finger pairs can be defined corresponding to oppositions that can coexist.

An opposition based parameterization presents some challenges not encountered with shape representations. Firstly, extracting these parameters from a human demonstration is not as straightforward since we need to know what oppositions are involved and how pressure is distributed on the surface of the hand. Secondly, from the perspective of realizing a grasp, opposition information does not directly prescribe a hand-shape but encodes instructions from which the final prehensile posture can be achieved. However, as these parameterizations are based on interaction we expect them to be better correlated with the functional

abilities attributed to different hand shapes.

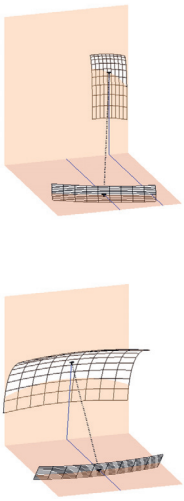

**(a)** VF configurations for palm opposition

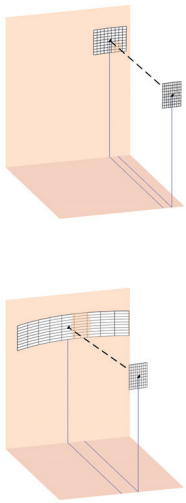

**(b)** VF configurations for pad opposition

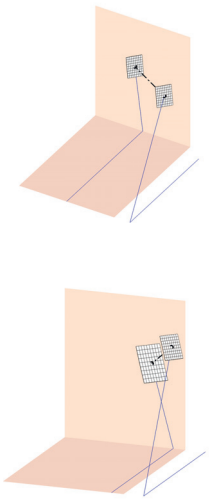

**(c)** VF configurations for side opposition

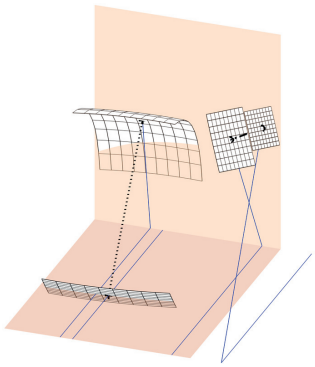

**(d)** Combining opposition types

**Figure 2.2:** The grasping surface associated with a virtual finger is modelled by a surface whose pose, area and curvature can be varied. Changing these properties also changes properties of the opposition that is formed in the hand. Coloured planes are used to put the virtual fingers in a hand-context. Horizontal coloured plane indicates dimensions of the palm. Vertical coloured plane indicates maximum reach of fingers about the palm.

## 2.3 Hand Function Space

The problem of task-relevant grasping revolves around hand-function, representing it and matching it to task requirements given a particular environment scenario. In this work, we are interested in hand parametrizations that have a strong and consistent correlation across the hand functional space. We must therefore define a suitable space of hand-function.

Key functions of the grasping hand are mainly understood along the lines of ability to exert force/torque and the ability to impart motion/change in orientation to a grasped object. Iberall et al. (1990); Cutkosky (1989) also mention ability to sense the state of the hand-object interaction. Some of these functions can be measured analytically from a kinematic model of the hand and a description of the contacts involved (Suárez et al., 2006). However, each metric typically focuses on a single aspect of hand function and one would need to compute an array of metrics to get a realistic picture. Moreover these metrics assume simplified contact models and rely on precise contact information, both of which do not hold when one considers real-life demonstrations.

Another approach is to look at hand function in a more qualitative manner. Precision and power have long been accepted as basic functional qualities by a line of researchers motivated to functionally categorize hand shape for varied reasons like prosthetics, anthropology, rehabilitation, realistic animation and also robotic grasping and manipulation. Considering that grasp taxonomies record various combinations of precision and power in the human prehensile repertoire, we choose a grasp data set based on Feix et al. (2009)[1], to provide a basis for evaluating various hand parametrization schemes on their ability to disambiguate hand function. We identify a representative set of grasps that spans the space of hand function, by varying precision and power abilities in big and in small steps. This set is depicted in Figure2.3a and is denoted by $\mathcal{GS}$. Functionality in the grasps chosen to vary as mentioned below. In the following, *power* should be seen as the ability to resist external wrenches from arbitrary directions. *dexterity/precision* should be seen as the ability to impart fine motion using the fingers.

- Strong power. Strong ability to resist external wrenches.
- Decreasing power. Increased ability to impart motions.
- Power with directional ability. Able to keep a tool stable against particular task wrenches. No dexterous ability.
- Power with dexterous ability.
- Strong precision. Poor resistance to external wrenches.
- Precision with Power. Dexterity with increased stability.

[1] This taxonomy represents a summary of a large number of grasp taxonomies proposed in the literature

### 2.3.1 Functional ordering

We base our strategy for evaluating how closely each hand parametrization scheme reflects hand function by relating distances measured in parameter space to distance in functional space. For this we first establish a functional ordering of the grasp data set.

We propose a metric for inter-grasp distance that converts the assessment of a human expert on functional abilities of grasps, to a computational measure of the distance between them. The metric is constructed by ranking all the grasps in the data set in descending order of their ability to exert power. The ranking is a qualitative assessment by a human expert. This is repeated once again for descending order of precision ability. Now, the distance between any two grasps is computed as an average of their separation in power and in precision according to their place in the respective expert sorted lists. It is possible to extend this scheme by defining other qualitative functional abilities (such as tactile sensitivity or amount of compliance allowed) and taking a weighted average of separation between grasps according to each function.

$$
\begin{aligned}
O_{power} &= \text{Grasp set ordered by decreasing power} \\
O_{precision} &= \text{Grasp set ordered by decreasing precision} \\
sep(O, g_1, g_2) &= \text{Ordinal distance between } g_1, g_2 \text{ in } O \\
fdist(g_1, g_2) &= \frac{sep(O_{power}, g_1, g_2) + sep(O_{precision}, g_1, g_2)}{2}
\end{aligned}
$$

The distance metric above can be used as a guide to find a functional ordering of the grasp set combining the different orderings produced by the human expert. One way of doing this is illustrated by Algorithm 1. Figure 2.3b, shows the result of applying this algorithm to the grasp data set, starting from grasp no. 13 (strong precision grasp). The grasp data set is therefore ordered in decreasing ability for precision. This ordering forms a baseline which will be used to evaluate functional correlation of the parameter spaces.

**Algorithm 1** Combine functional orderings of human expert

**Input:** unordered set $\Phi = \mathcal{GS}$, $g_{st} \in \Phi$, $fdist(g_1, g_2)$
**Output:** ordered set $\Psi$
1: $\Psi \leftarrow \Psi + g_{st},\ \Phi \leftarrow \Phi - g_{st}$
2: **while** $\Phi \neq \varnothing$ **do**
3: $N_{g_{st}} \leftarrow \{\Psi(1), \Psi(2), \Psi(3)\}$ $\{\Psi(1 \ldots 3)$ form a neighbourhood of $g_{st}\}$
4: $g_i = \underset{g \in \Phi}{\operatorname{argmin}}\ \overline{fdist}(N_{g_{st}}, g)$ $\{\overline{fdist}$ computes avg. distance over all $N_{g_{st}}\}$
5: $\Psi \leftarrow \Psi + g_i,\ \Phi \leftarrow \Psi - g_i$
6: **end while**

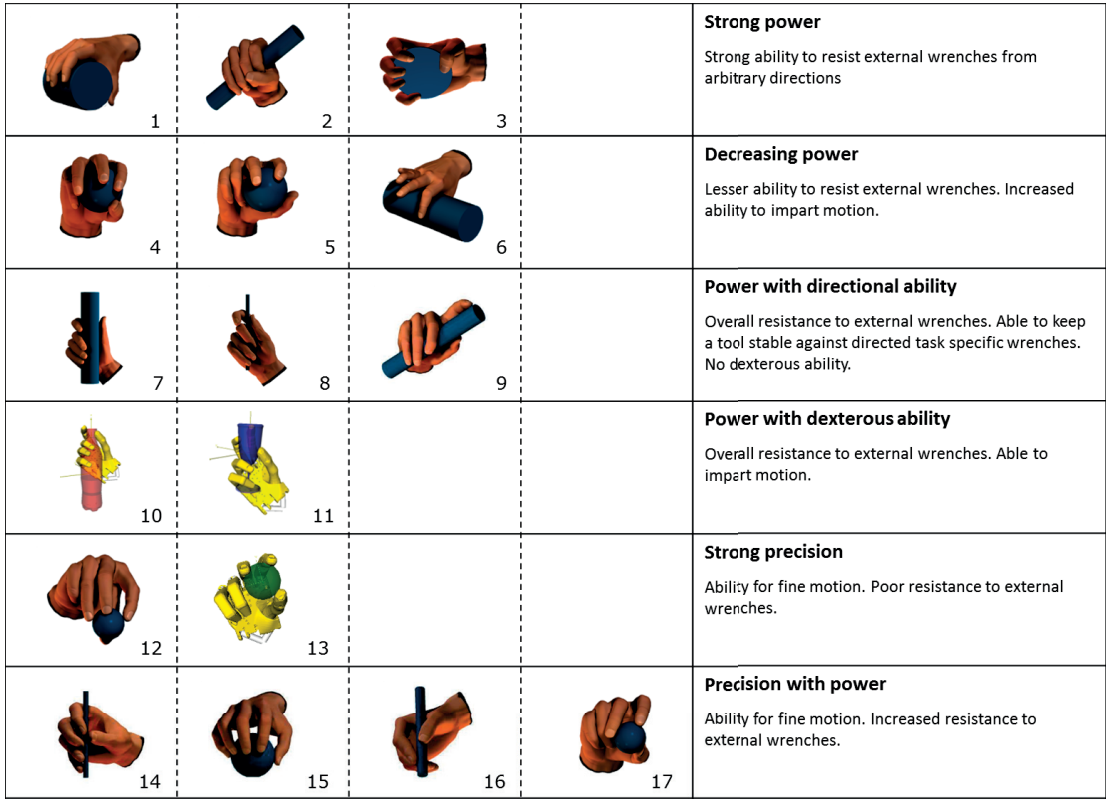


**(a)** Grasp data set $\mathcal{GS}$. Images are taken from Feix et al. (2009), except for 10,11 and 13

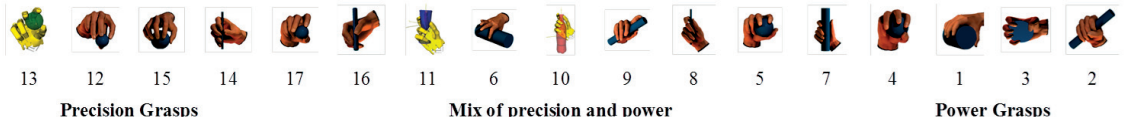


**(b)** Ordering of the grasp data set obtained using Algorithm 1 with $g_{st} = 13$

**Figure 2.3:** Grasp data set spanning functional space of precision and power.

## 2.4 Obtaining hand parameters from a grasp demonstration

This section describes in more detail the various shape and opposition based parameter spaces we compare, and how their parameter values can be obtained from a demonstrated grasp.

### 2.4.1 Shape-based Parameters

a) ***Joint Angles (jnt)***: Joint angle parameters are made up of the actuated degrees of freedom of the robot hand specified in radians. For the Shadow Robot hand used to demonstrate grasps (described in Section 2.5), this is an 18 dimensional vector $p_{jnt} \in \mathbb{R}^{18}$. Distance between two points in this parameter space is given by

$$d_{jnt}(p_x, p_y) = \|p_x - p_y\|_2 \qquad p_x, p_y \in \mathbb{R}^{18}$$

b) ***Hand Synergies (syn)***: Principal component analysis is performed on joint angles from the set of 57 commonly used grasps in Santello et al. (1998). A sub-subspace accounting for 90% of the variance in the joint angle data identified. 6 principal components are required for this. A synergy parameterization of a demonstrated grasp is the 6 dimensional vector $p_{syn} \in \mathbb{R}^6$ obtained by projecting the joint angles onto a lower dimensional subspace formed by hand synergies. Distance in this parameter space is given by

$$d_{syn}(p_x, p_y) = \|p_x - p_y\|_2 \qquad p_x, p_y \in \mathbb{R}^6$$

c) ***Shape Features (shp)***: We use the compound feature proposed in Li et al. (2007). A set of 3 dimensional features for all pairs of points on the hand surface of a demonstrated grasp are collected to form a compound feature. Each 3D feature for a pair of points consists of distance between the points and the angle that surface normals at the points make with the line joining the points. The grasp is represented by the compound feature $p_{shp}$ which captures its shape characteristics. Points are sampled from hand surfaces engaged in applying pressure against the object. Distance between two demonstrated grasps, $d_{shp}(p_x, p_y)$, in the feature space, is a weighted average of the distance between features in $p_x$, to their nearest neighbours in $p_y$. The weight of a feature is computed as the ratio of its occurrence in a grasp with respect to its occurrence in all other grasps of the data set. It represents importance of the feature to the overall shape of the grasp. An outcome of this definition is that the weights of features in $p_x$ and $p_y$ will be different (as they come from grasps of different shapes) and hence the distance measure is not symmetric, i.e. $d_{shp}(p_x, p_y) \neq d_{shp}(p_y, p_x)$. To

overcome this, we take the distance between two grasps as the average of the distances computed in both directions.

### 2.4.2 Opposition-based Parameters

We propose 2 parametrization schemes which are based on describing the virtual fingers present in a demonstrated grasp. All opposition based parameters are derived from point clouds obtained by sampling hand surfaces of a demonstrated grasp. Point clouds are expressed with respect to a hand-centric co-ordinate frame located at the wrist, as shown in Figure 2.4a.

a) ***VirtualFinger 1 (vf1)***: A demonstrated grasp is manually interpreted in terms of pad, palm and side oppositions. Each opposition is a virtual finger pair. As seen from Figure 2.4a, the set of 3D point clouds corresponding to the grasping surface for each virtual finger pair and the opposition vectors associated with them is available. The method for obtaining this is discussed in Section 2.5. From this information 8 scalar parameters per virtual finger can be defined as below and shown in Figure 2.4b. Parameters $p_{1...3}$ relate to the focus of opposition pressure while parameters $p_{4...8}$ relate to properties of the grasping surface engaged with the object. These parameters allow to describe a grasping surface patch of any pose and size in the hand-centric space.

| | |
|---|---|
| $p_1, p_2, p_3$ | Coordinates (x,y,z) of the focus of opposition. |
| $p_4, p_5$ | Each grasping surface can be associated with a plane defined by the focus of pressure (end-point of the opposition vector) and the directions of maximum and minimum variance of grasping surface point cloud. $p_4$ and $p_5$ constitute bounds of the point cloud projected onto this plane. |
| $p_6, p_7, p_8$ | A right-hand system is established at the focus of pressure with the opposition vector as the y-axis. $p_6, p_7$, and $p_8$ are the roll, pitch and yaw of the plane normal with respect to this coordinate frame. |

This set of 8 parameters describes 1 virtual finger. To complete the hand-parametrization, it is necessary to describe 2 virtual fingers for each opposition. This makes for a total of 48 parameters. Thus, a grasp is represented by a point $p_{vf1} \in \mathbb{R}^{48}$. If an opposition is not present in the demonstrated grasp, its virtual fingers are described by the zero vector. Furthermore, orientation parameters ($p_{6...8}$) are multiplied by a factor of 1 cm/rad to bring them on par with distance parameters ($p_{1...5}$). Distance between two points in this parameter space is given by

$$d_{vf1}(p_x, p_y) = \|p_x - p_y\|_2 \qquad p_x, p_y \in \mathbb{R}^{48}$$

b) ***VirtualFinger 2 (vf2)***: This parametrization scheme is based on the assumption that there exists a set of basic oppositional intentions underlying

grasp formation. These may be decided in response to various factors such as task demands, object properties, environment, personal preference, comfort, and so on. The important point is that they are decided before hand-closure and they guide the realization of a stable grasp. As hand-closure progresses, it becomes subject to other influences more concerned with satisfying hand kinematic constraints and ensuring compliance of the hand with the object surface.

For this parametrization scheme, we propose to ignore the final configuration observed and describe virtual fingers in their pre-shape pose. Each basic opposition type: pad, palm, side can be associated with a pre-shape. This is a known fixed configuration of the hand which captures the intention of a particular opposition type and serves as a starting point for hand closure. The grasping surface point clouds are projected to the pre-shape pose before parameter values are extracted. The set of parameters follows that of *VirtualFinger 1* exactly. However, the opposing surfaces being bound to pre-shape configurations allows several parameters to become fixed and hence can be ignored, as displayed in Figure 2.4c. Rationale and assumptions made for identifying the free parameters are listed below.

| **Opposition Type** | **Virtual Fingers** | **Assumptions/Rationale** |
|---|---|---|
| Palm | VF1 (Finger Surface) | We assume that pressure focus lies half-way up the finger surface (as measured from palm to tip of the middle-finger). Location along the fingers and size of the grasping patch can vary. |
| | VF2 (Palm) | Grasping patch is fixed on palm. Location and size can vary. |
| Pad | VF1 (Thumb pad) | No variable parameters, the grasping patch is always in the same position and has the same size. |
| | VF2 (Finger pad) | Grasping patch can span several finger-tips with focus located on any one finger. |
| Side | VF1 (Thumb pad) | No variable parameters, the grasping patch is always in the same position and has the same size. |
| | VF2 (Finger side) | Grasping patch is of fixed size. However, it can be located on any finger side and move along the finger length. |

Note that the free parameters indicate the general location of oppositional pressure within the hand and size of the opposing grasping surfaces without particular attention to accurate description as was the case with the earlier parameterization.

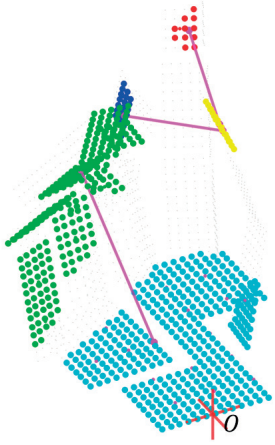


**(a)** Data for grasp no. 9 expressed with respect to a hand-centric coordinate frame located at the wrist. For each virtual finger grasping surface point clouds are indicated in with different colors. Opposition vectors are indicated by lines in magenta.

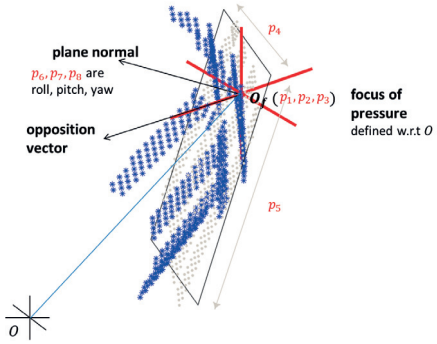


**(b)** *VirtualFinger1* parameter definition. Plane approximation for the grasping surface point cloud of a virtual finger. Parameters correspond to properties of this plane.

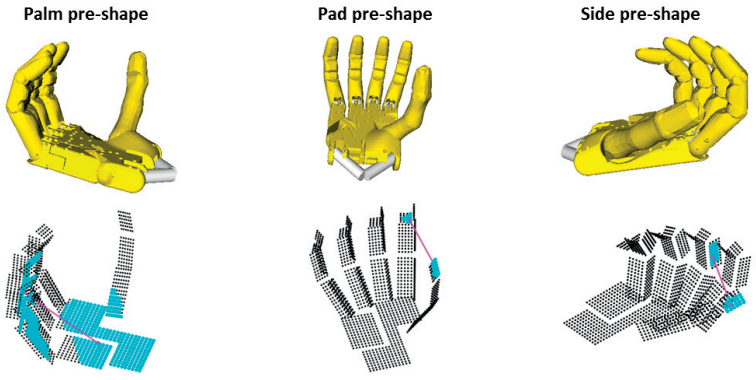


| | | | |
|---|---|---|---|
| VF1 | [$\boldsymbol{p_1}$ $p_2$ $p_3$ $\boldsymbol{p_4}$ $\boldsymbol{p_5}$ $p_6$ $p_7$ $p_8$] | [$p_1$ $p_2$ $p_3$ $p_4$ $p_5$ $p_6$ $p_7$ $p_8$] | [$p_1$ $p_2$ $p_3$ $p_4$ $p_5$ $p_6$ $p_7$ $p_8$] |
| VF2 | [$\boldsymbol{p_1}$ $\boldsymbol{p_2}$ $p_3$ $\boldsymbol{p_4}$ $\boldsymbol{p_5}$ $p_6$ $p_7$ $p_8$] | [$\boldsymbol{p_1}$ $p_2$ $p_3$ $\boldsymbol{p_4}$ $p_5$ $p_6$ $p_7$ $p_8$] | [$\boldsymbol{p_1}$ $\boldsymbol{p_2}$ $p_3$ $p_4$ $p_5$ $p_6$ $p_7$ $p_8$] |

**(c)** *VirtualFinger2* parameter definition. Opposition pre-shape conditions are imposed on the grasping surface point clouds. Several parameters can be fixed to their pre-shape configuration values (greyed out)

**Figure 2.4:** Opposition based representations for the grasp.

## 2.5 Grasp Data

Grasp data is collected in the context of a Shadow Robot hand model. A human experimenter demonstrates grasps using the Cyberglove to control an 18-DOF Shadow Robot hand model in the GraspIt! Simulator (Miller and Allen, 2004). The experimenter first demonstrates a sequence of postures, for which joint angles are known, for the purpose of calibration. Sensors values of the Cyberglove are mapped to the joint angles of the robot hand model using linear regression. The experimenter then demonstrates each of the grasps listed in Figure 2.3a using the same objects.

For each grasp that is demonstrated, we collect the following information required to extract hand parameter values, Figure 2.5.

1) ***Joint Angles***. These are obtained directly from the robot hand model.

2) ***Oppositions and opposing surfaces***. These are obtained through manual annotation. The experimenter is presented with a flat (2D) view of the hand surfaces. For all oppositions present in the grasp, the experimenter proceeds to delimit opposing surfaces impacting the object using a polygon approximation as shown in Figure 2.5b. A point within each polygon indicates where pressure is likely to be focused. This information is then transformed to a hand-centric frame using joint angles and known forward kinematics. Thus for each opposition present, point clouds corresponding to the opposing surfaces and the opposition vector is available.

This method allows us to gather data in a robot context. However, the presence of the simulator somewhat impedes the sense of naturalness in the demonstrations. Further, the process of delimiting opposing surfaces is based on estimation in the mind of the human annotator. In another part of the thesis, grasp data is gathered directly in a human context. We employ an array of tactile sensors to cover hand surfaces and participating oppositions are automatically discovered.

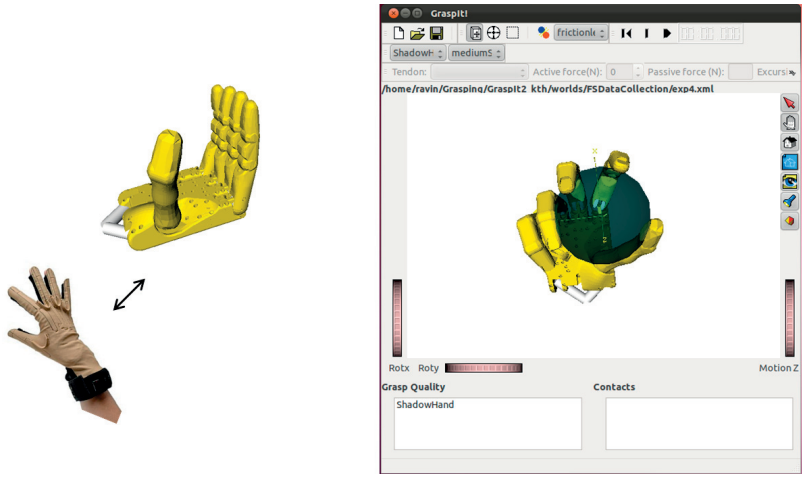


**(a)** Calibration is established between Cyberglove and the Shadow Robot hand model. The model is controlled in the GraspIt! simulator to form the grasp.

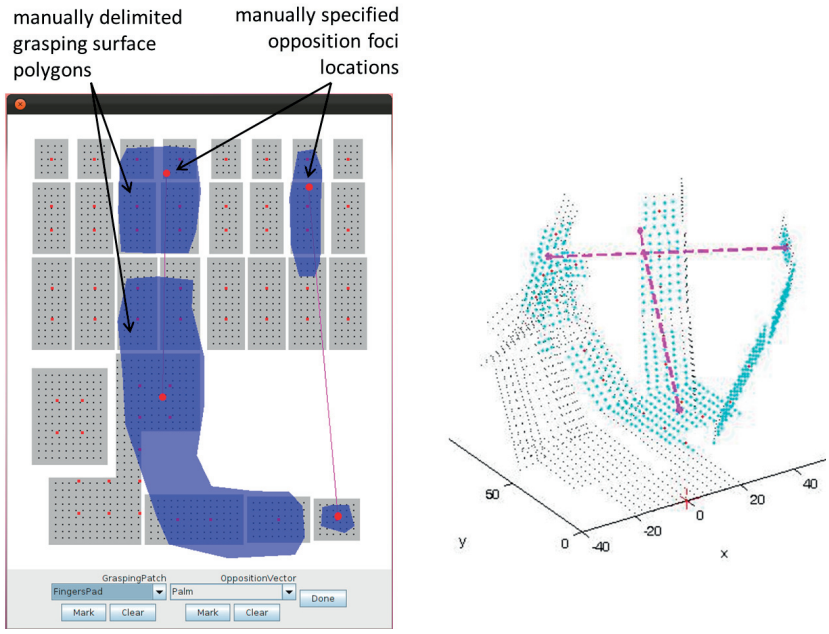


**(b)** Annotation mechanism to provide tactile information. Oppositions that are present and grasping surfaces associated with them are manually indicated using a 2D view of hand surfaces. Using the kinematic model annotations are transformed to a hand-centric reference frame.

**Figure 2.5:** Framework for grasp data collection.

## 2.6 Results

In this section we compare inter-grasp distances in parameter space against separations derived from human expert ordering of functional ability. Using the algorithm in 1 on the grasp data set an ordering of decreasing precision ability was obtained and was presented in Figure 2.3b. This ordering induces a separation among grasps in the data set that must also be respected by hand-parametrization schemes that are correlated with function.

Figures 2.6-2.9 report distances obtained from the various parametrization schemes. In each case, the x-axis corresponds to the human expert derived baseline ordering. The y-axis plots the average distance of each grasp to a small neighbourhood, $N_{13} = \{13, 12, 15\}$, of the strongest precision grasp. As we have taken care to choose our data set to adequately span the space of precision and power, we expect to see an increasing trend (not necessarily linear), where distance from $N_{13}$ increases for grasps further away from $N_{13}$ in the baseline ordering.

The distances reported by the shape based parametrizations ($jnt$, $syn$, $shp$) display no clear separation between precision and power. With $jnt$ and $syn$, a slight increasing trend can indeed be noticed, however, for the majority of the data set, distance to $N_{13}$ varies in a narrow band (0.6-1.6). The data for $shp$ is erratic and doesn't show any discernible trend at all. We notice that $syn$ data closely follows $jnt$ although the parameter spaces differ widely in dimensionality ($\mathbb{R}^6$ v/s $\mathbb{R}^{18}$). This is not surprising however as synergy parameters are obtained by projecting joint angles on a low dimensional subspace. We also notice that the shape based parametrizations schemes show anomalies wherein grasps clearly strong in power are reported closer to the high-precision neighbourhood than other more precision oriented grasps. These are more pronounced in the case of $shp$ (consider for example grasps 7,14 in Figure2.7).

In contrast to this, opposition based parametrization schemes ($vf1$, $vf2$) are clearly able to distinguish power from precision. Interestingly, we see emerge from the distance data, 3 categories of grasps that agree closely with the inter-grasp separations mandated by the human experience baseline. These categories correspond to strong power grasps, strong precision grasps and intermediate grasps with some combination of both. For instance, grasp 14 is a strong precision grasp, close to $N_{13}$ in the baseline ordering and also in parameter space. Similarly grasps 4,7 which are power oriented, and which are positioned at the far end of the baseline ordering, are also widely separated from $N_{13}$ in parameter space. Finally, grasps 10,11 close to the middle of the baseline ordering, also end up positioned between the strong precision and strong power grasps in parameter space.

Table 2.1 presents the Pearson correlation coefficient computed for each parametrization scheme against the human experience baseline. This is done by dividing, in each case, the covariance of two distance sets, one from param-

eter space and the other from the baseline metric, by the standard deviations of each set. The high correlation coefficients associated with the opposition based parametrizations suggest that these schemes are better than others to discriminate grasps close and far in precision and power.

Two further observations can be made. First, the range of distance data for the opposition based parameters (0-350 and 0-250), is much larger than that of the shape based ones (0-3 and 0-20). This indicates that opposition based parameters are more sensitive to variance in function. Second, parameters extracted from pre-shape ($vf2$) show very similar properties to those extracted from final posture of the hand ($vf1$). This indicates that representing the final configuration of opposing surfaces (accompanied by significant increase in number of parameters) doesn't add much more in discriminating hand-function. And that it is the underlying oppositional intention, encoded by the general location of oppositional pressure within the hand and the size of the opposing grasping surfaces, and not the final configuration of hand surfaces, which is important to discriminate hand-function.

These results imply that hand representations based on opposition would be better suited for data driven approaches which seek to relate the grasp to aspects of the task such as predicting stability of the grasp in a task context (Bekiroglu et al., 2013) or modelling the relationships between grasp, object and the task (Song et al., 2010, 2015).

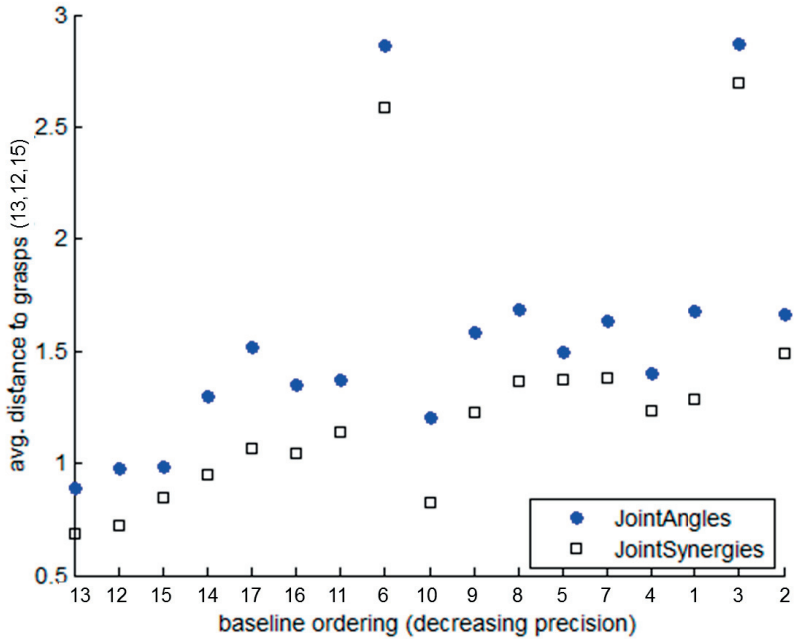


**Figure 2.6:** *Joint Angles and Synergies.* x-axis shows the baseline ordering on the grasp set obtained by Algorithm 1. For each grasp, distance in parameter space to a high precision neighbourhood $(13, 12, 15)$ is plotted.

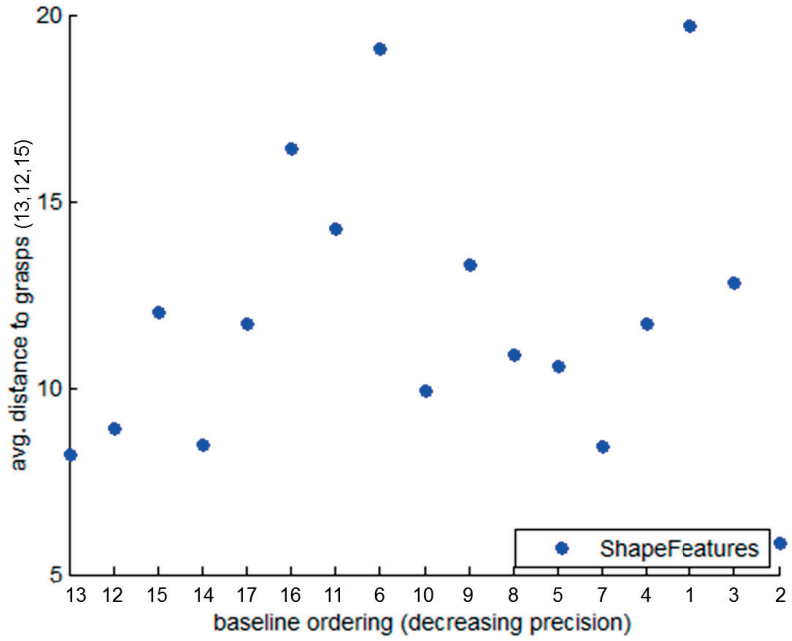


**Figure 2.7:** *Shape Features.* x-axis shows the baseline ordering on the grasp set obtained by Algorithm 1. For each grasp, distance in parameter space to a high precision neighbourhood $(13, 12, 15)$ is plotted.

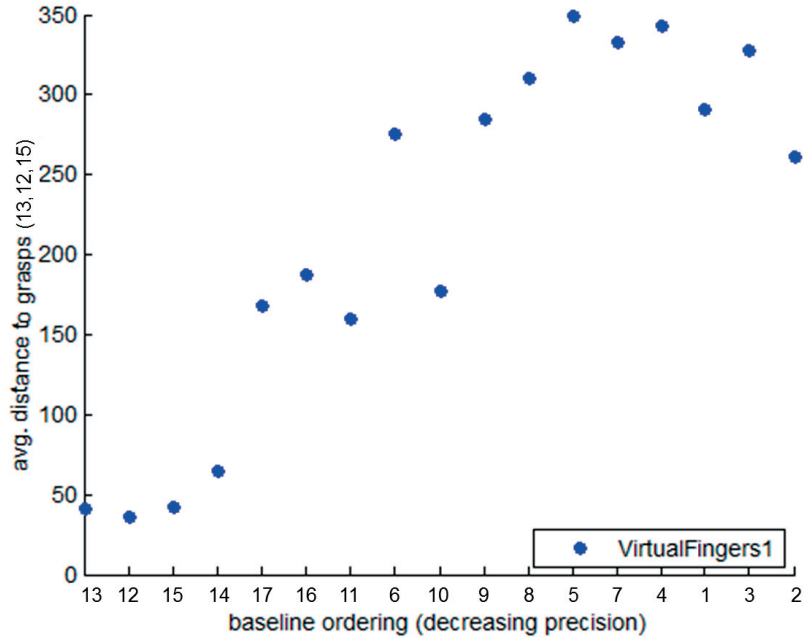


**Figure 2.8:** *Virtual Finger 1.* x-axis shows the baseline ordering on the grasp set obtained by Algorithm 1. For each grasp, distance in parameter space to a high precision neighbourhood $(13, 12, 15)$ is plotted.

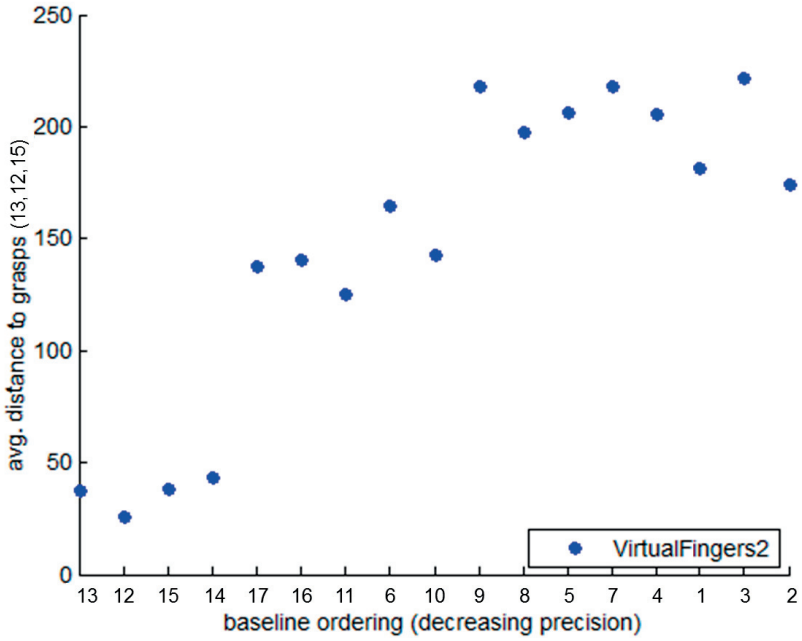


**Figure 2.9:** *Virtual Finger 2.* x-axis shows the baseline ordering on the grasp set obtained by Algorithm 1. For each grasp, distance in parameter space to a high precision neighbourhood $(13, 12, 15)$ is plotted.

| | *Joint Angles* | *Joint Synergies* | *Shape Features* | *Virtual Finger 1* | *Virtual Finger 2* |
|---|---|---|---|---|---|
| Pearson Coeff. | 0.5642 | 0.5885 | 0.0803 | 0.8629 | 0.8376 |
| p-Value | 0.0183 | 0.0129 | 0.7592 | 0 | 0 |

**Table 2.1:** Correlation of distances in parameter space to distances in functional space for the baseline ordering. p-values indicate the probability that a particular correlation occurs by chance.

## 2.7 Conclusion

In this chapter we have compared shape based representations of the hand to those based on hand opposition on their ability to discriminate between grasps in a functional space spanning precision and power. We proposed 2 parameterizations focused on describing qualities of the virtual fingers associated with the pad, palm and side opposition types. By examining grasping surfaces projected to their pre-shape configurations we could significantly reduce the number of parameters required. We obtained a functional ordering in a grasp set by combining human expert assessment of different functional abilities in grasps. Correlation of hand representation schemes with hand function was examined by comparing distance in parameter space to ordinal distance in the functional ordering.

We found that parameterizations based on opposition primitives exhibit a strong correlation with hand function as interpreted by human experience. These properties are not observed in the several shape based parameterizations considered. Moreover, we find that imposing opposition pre-shape constraints on hand surfaces engaged in applying pressure to the object, reduces dimensionality of the representation, but does not affect correlation with hand-function.

In the current work the experience of a single human subject was considered. The demonstrations also lacked a sense of naturalness due to the use of the GraspIt! simulator. In the next chapter we propose a sensing infrastructure for tactile and joint data which reintroduces the sense of naturalness and also facilitates data collection from multiple human demonstrators. The current work used manual annotation to indicate the types of opposition present in the grasp and the opposing surfaces associated with the virtual fingers. This proved to be the key information necessary for extracting opposition based parameters. Recognizing this information automatically from the raw data present in a completed grasp would be essential to any approach which seeks to combine and modulate different oppositional intentions on a grasped object. In the next chapter we propose a general method whereby the number, type and properties of several cooperating oppositional intentions can be detected automatically from tactile and joint data in a grasp demonstration.

### 2.7.1 From continuous to discrete opposition-based representation

For the purpose of automatically recognizing oppositional intention from grasp demonstration, the next chapter introduces certain changes in assumptions and notation listed below.

- We switch the opposition-based representation of a grasp from the continuous parameter space (used in this chapter), to a discrete opposition primitive set representation. We will determine the existence and importance of cooperating elements of this set in a demonstrated grasp. Once the particular cooperating oppositions are identified, the continuous representations developed in this chapter can be extracted.

- Extensions to the 3 basic opposition categories of Iberall et al. (1986) - pad, palm, side - are proposed. This is so that opposition capabilities of the thumb can be properly represented and recognized.

- To better reason with data collected from the sensing infrastructure, we impose a patch decomposition on the grasping surfaces of the hand corresponding to the tactile sensors utilized. The concepts of virtual finger grasping surface and opposition primitives are now defined in terms of grasping patches.

Chapter 3

# Opposition primitives to interpret human grasp behaviour

## 3.1 Foreword

In the previous chapter we have examined the functional correlation associated with opposition-based parameterization of the hand. We saw that this can be observed from the way hand surfaces are used either from a final grasp or from a pre-shape viewpoint. We assumed knowledge of the oppositions present and hand surfaces engaged, in order to extract the hand parameters. In this chapter we will discover the particular set of oppositional intentions underlying grasp formation from sensory information (tactile and configuration) available in a grasp demonstration. We base our approach on the assumption that information about oppositional intention is preserved across pre-shape and hand closure. Accordingly, an information template for opposition primitives is proposed and a method is devised by which this can be instantiated in a grasp context so as to obtain a measure of primitive likelihood. Prior knowledge on primitive coexistence guides the selection of cooperating primitives. Grasping experiments with humans show that the proposed method is robust over a wide range of human grasp behaviour. This work led to the following publications:

- R. de Souza, S. El-Khoury, J. Santos-Victor, and A. Billard. Towards comprehensive capture of human grasping and manipulation skills. In *Proceedings of* $13^{th}$ *International Symposium on the 3D Analysis of Human Movement (3D-AHM)*, pages 84-87. 2014. ISBN 978-2-880-74856-2
- R. de Souza, S. El-Khoury, J. Santos-Victor, and A. Billard. Recognizing the grasp intention from human demonstration. *Robotics and Autonomous Systems*, 2015. doi: 10.1016/j.robot.2015.07.006

## 3.2 Introduction

Robot hands are endowed with flexibility sufficient to mimic human grasp formation but harnessing this flexibility in a task-oriented fashion remains a significant challenge. Considering that humans are extremely adept at controlling the high degree of freedom hand-wrist-arm musculo-skeletal system to grasp

and manipulate objects according to task requirements, it is of interest to study human grasping behaviour in order to extract underlying principles which may be transferred to robotic or prosthetic devices.

In any human grasping endeavour, surfaces of the hand engaged and the manner they are applied to the object does not happen randomly, rather choices have been made even before a grasp is formed. These choices stem from a perception of task demands and are related to the functionality brought to grasp. For example, tasks requiring dexterity (turning a dial, writing, Figure3.1a), make use of the finger tips which open up degrees of freedom and bring into play required manipulability for in-hand motion. Also, greater sensitivity associated with finger tips is essential for controlling the manipulation (Johansson and Flanagan, 2009). In contrast, tasks requiring power (opening a tight bottle cap, screw-driving) make use of finger surfaces and the palm. Use of these hand-parts is directly related to transmission of torque and motion generated by the wrist-arm system.

Grasp taxonomies such as proposed by Cutkosky (1989); Kamakura et al. (1980) derive from studies of human grasp behaviour in various task contexts and attempt to categorize the various ways hands can be used from a functional viewpoint. Several works recognize a taxonomy category from human demonstration using cues such as visual features of the grasp or joint angles from a data glove (Kjellstrom et al., 2008; Friedrich et al., 1999; Ekvall and Kragic, 2005) also incorporating tactile information (Aleotti and Caselli, 2006; Bernardin et al., 2005). Identifying a taxonomy category is a useful starting point for transfer of task-oriented hand configuration to a robotic device. However, key information is lacking on how to recreate the grasp or adapt it to a different objects while preserving underlying functional roles of the fingers involved. For example, if the object is perturbed or used in a task context, are all hand surfaces equally important for applying pressure or are some more important than others. Similarly, if the properties of the object change how can we purposefully change the hand configuration and object contacts made while remaining confident that the essential meaning of the grasp is preserved. Heuristics have to be designed on a case by case basis to encode the meaning of each grasp. A more general approach defines a set of grasp components from which a wide range of grasps may be constructed. The problem is then identifying and prioritizing the appropriate set of components present in a grasp demonstration.

We adopt the hypothesis that opposition primitives, while engaging the hand in a well-defined manner, are also correlated with the end-function to be delivered on a grasped object (Iberall, 1987). Accordingly, a grasp can be interpreted as a cooperating set of oppositions between hand-parts. Each opposition serves a particular functional end. For example, the grasp of screw-driving in Figure 3.1b may be interpreted as a combination of 3 components: action of the thumb against side of the fingers which supports the action of fingers against the palm

**(a)** Four task scenarios: turning a dial, writing, opening a tightly closed bottle-cap, screw-driving show that choice of hand surfaces engaged brings different functionality to the grasp.

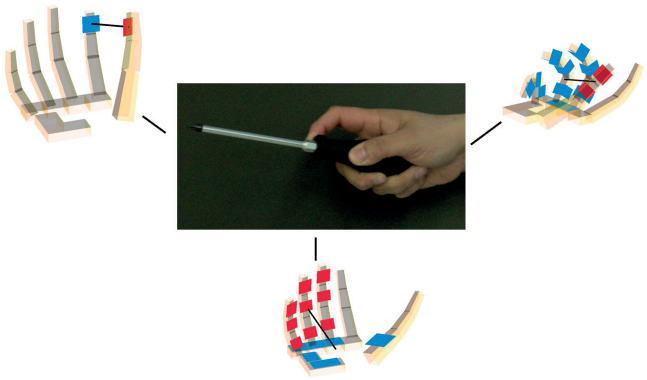

**(b)** A screw-driving grasp may be interpreted in terms of 3 oppositions between hand-parts. Each opposition serves a particular functional role. Action of the thumb against side of the fingers supports the action of fingers against the palm in order to keep the tool gripped firmly. Use of the thumb-tip against the finger-tip enables the tool to be directed appropriately during the task.

in order to keep the tool gripped firmly, while use of the thumb-tip against the finger-tip enables the tool to be directed appropriately during the task. In this chapter we will infer this mix of oppositions from the hand configuration and tactile information present in a grasp demonstration.

This chapter is structured as follows. In section 2 we review the different ways human grasp demonstrations have been modelled with a view to inform robotic grasping. Section 3.4 describes the sensing infrastructure used to capture human demonstrations of grasping. Section 3.5 develops a model for grasp behaviour based on opposition primitives. The opposition space framework is reformulated to be more readily applied in a demonstration context, and extended so that all oppositional roles of the thumb can be recognized as separate components of a grasp. Section 3.6 outlines a general method to discover a Grasp Signature – a combination of primitives with their importance – leveraging prior knowledge contained in the primitive definition. Section 3.7 reports on empirical evaluation of the proposed approach using human demonstrations of grasping conducted over a wide range of hand function. Sections 3.8 and 3.9 discuss limitations, directions for future research and conclude the chapter.

## 3.3 Literature Review

Capturing and analyzing human prehensile behaviour finds application in several fields. In robotic tele-manipulation (Hu et al., 2004) a mapping is needed in order to use the motion of a human hand to control the motion of a dexterous robotic hand. In the field of immersive virtual reality (VR) (Kahlesz et al., 2004) or VR-hand rehabilitation (Zhou et al., 2010) a user is enabled to grasp and manipulate virtual objects. In a robotics or biomechanical context one needs to measure and understand human manipulation in order to transfer these skills to robotic or prosthetic hands.

Several works use visual appearance or hand configuration information to classify demonstrated grasps into the categories of a grasp taxonomy. The taxonomies most often used for this purpose are those of Cutkosky (1989) and Kamakura et al. (1980). In Bullock et al. (2013) a human manually examines the grasp to perform the classification. Alternatively, feature based classification can be employed. Kjellstrom et al. (2008) present a method using visual features extracted from 2D images of the grasp to identify 6 different grasp types. Friedrich et al. (1999) rely on joint information from data glove devices. A neural network based classifier is employed in their approach. Classification performance can be improved by incorporating joint trajectory data during the reaching phase. This also makes it possible to arrive at a classification result even before the grasp is completed. (Ekvall and Kragic, 2005). However, these methods ignore interaction forces between the hand and the grasped object. Hence they are negatively impacted by the fact that similar hand shapes sometimes take on entirely different functions depending on how hand surfaces are engaged. For example, in Friedrich et al. (1999) confusion occurs between three precision grasps: disc shaped, spherical and tripod circular, as these have similar joint configurations. Also in Ekvall and Kragic (2005), confusion occurs between a power grasp (power sphere) and a precision grasp (precision disc) as both have similar hand shapes but the former makes use of finger and palm surfaces while the later uses only the finger-tips.

Several works incorporate the use of tactile information to improve the classification. Aleotti and Caselli (2006) extracts tactile information from virtual reality simulation. In Bernardin et al. (2005) hand surfaces are covered with tactile sensors. Tactile information concatenated with hand configuration is used to train HMMs for grasp recognition. Murakami et al. (2010) show impressive classification results combining tactile and joint information. Additionally, they investigate placement of a smaller number of tactile sensors with comparable results. Faria et al. (2012) cover surfaces of the fingers and the palm with sensors to learn tactile templates for a fixed set of grasps. In this work we recognize that both configuration and tactile information are necessary raw information in order to interpret grasp behaviour. In conjunction with a kinematic reconstruc-

tion of the grasp, we use tactile information to analyze the low level interactions between grasping surfaces of the hand in order to highlight the different oppositional roles a single sensor may be engaged in.

The works discussed above are oriented towards identifying a taxonomy category. While this is a useful starting point, a taxonomy category does not capture how fingers may close to form the grasp or adapt it to different objects while preserving functional roles. A strategy which closes fingers of the hand uniformly does not preserve different axes of oppositional pressure. And these may be important parts of the grasp, associated with task related roles, as was seen earlier for the case of screw-driving (Figure 3.1b). It becomes necessary to consider each class of grasps individually and find suitable heuristics for grasp closure (Romero et al., 2009; Kjellstrom et al., 2008; Ekvall and Kragic, 2007). Avoiding heuristics, Ben Amor et al. (2012) makes use of joint synergy subspaces for each category to train DMP based controllers for human-like grasp formation. However, the approach is demonstrated only for precision grasp types and controllers have to be trained on a case by case basis.

In this work, we use opposition primitives as a means to interpret grasp behaviour. This forms a more general approach to represent grasps spanning a large functional space. Moreover, a primitive based representation can serve as a guide for low-level controllers to complete the grasp by driving opposing hand-parts together. Relatively few works have tried to interpret demonstrated grasps in this manner. Tactile templates employed by Faria et al. (2012) approach this idea. However, the work doesn't show how different components could be separated if they occur together. Kang and Ikeuchi (1993, 1994) present the contact-web representation to differentiate grasps based on the particular hand-surfaces impacting the object. Active virtual fingers are identified by maximizing force coupling (considering similarity between hand-surface force vectors) among the real fingers while favouring a smaller number of virtual fingers. This method makes the inherent assumption that real fingers are exclusively dedicated to a single oppositional role, and cases where different categories of oppositions occur simultaneously are not considered (such as a palm-side combination). However, these assumptions are frequently violated in the context of real-world grasps. In our approach hand surfaces can be simultaneously involved in multiple oppositional roles. We characterize these interactions and assign them a relative importance value. Cooperating oppositional intentions may belong to different opposition categories.

## 3.4 Human grasp data

This section outlines the sensing framework we developed in order to obtain tactile and configuration data from human grasp demonstration. For some time now, sensor gloves (or data gloves) have been a preferred means to observe human grasp behaviour (Dipietro et al., 2008). Advancement in technologies for tactile sensing allow for tactile information to be incorporated as well (Dahiya et al., 2010). Several researches use a data glove and cover the inner part of the hand with tactile sensors (Murakami et al., 2010; Buscher et al., 2012; Faria et al., 2012). This forms the basis of our approach as well. In many commonly encountered tasks such as screw-driving, opening a tight bottle cap, engraving/sculpting, prying and so on, action of thumb surfaces against sides of the fingers and the palm plays an important role and if present cannot be ignored. We collect sensory information from finger sides and palm as well as the frontal surface of the fingers. However, inferring the opposition role of the thumb also means that oppositional geometry of thumb surfaces must be correctly captured. We address this issue through an appropriate kinematic model and calibration technique.

### 3.4.1 'Sensorized' data glove

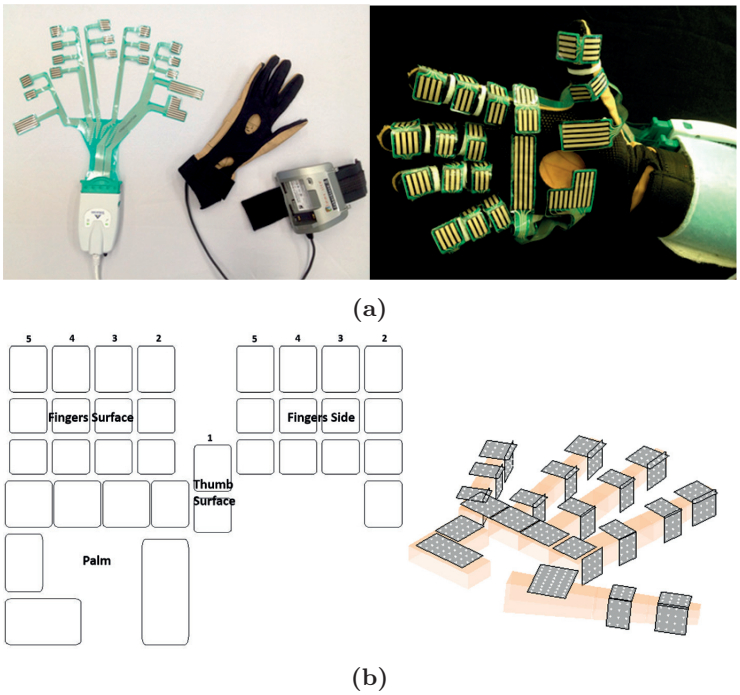


**Figure 3.2:** (3.2a) shows the hardware setup to capture human grasp demonstrations. The raw sensory data is interpreted in terms of 34 sensor units with the large palm patches divided into subunits (3.2b)

We collect human grasp data using the setup presented in Figure 3.2a. It

consists of the Cyberglove, used to measure hand joint angles, and the TekScan sensor array, used to measure the tactile response from the grasping surfaces of the hand.

The Cyberglove has 22 bend sensors strategically located over the hand joints. Since bending can be detected anywhere along the sensor length, the glove can adapt well to different hands sizes. The glove needs to be calibrated in order to transform raw sensor output to hand joint angles. Raw data from the glove is of dimension $\mathbb{R}^{22}$.

The Tekscan sensor array consists of 18 sensors patches which are matrices of pressure sensitive sensing elements or sensels. The patches in one array are strategically located so as to cover the grasping surfaces of the human hand. Two tactile arrays are employed in an overlapping configuration in order to cover the frontal grasping surfaces of the hand as well as all finger-sides which are able to oppose the thumb. We make use of uncalibrated tactile response as only relative force levels are necessary for analysing synergistic use of grasping surfaces. Raw data from the tactile sensory array is of dimension $\mathbb{R}^{581}$.

Data streams from the hand configuration and tactile response are synchronized. The combined data is obtained at a frequency of 200Hz and is averaged over a pre-determined time interval over which the grasp demonstration is maintained. Data from a grasp demonstration is represented in terms of elementary units called ***grasping patches***. A total of 34 grasping patches are identified as shown in Figure 3.2b. Let these be denoted by

$$\mathcal{GP} = \{gp_i\}_{i=1}^{34} \tag{3.1}$$

Each grasping patch is viewed as a single unit of grasping force. The force $\mathbf{f}_i \in \mathbb{R}^3$ associated with a grasping patch $gp_i$ is obtained as the sum of all the sensel activations associated with it and is assumed to be acting normally to the patch at the centroid of sensel activations $\mathbf{p}_i \in \mathbb{R}^3$ (Figure 3.3). The position and orientation of each patch is expressed with respect to a coordinate frame centred at the wrist. Data from a grasp demonstration can therefore be summarized as

$$D = \{\mathbf{p}_i, \mathbf{f}_i\}_{i=1}^{34} \tag{3.2}$$

We consider only hand surfaces that are actively engaged in applying force on the object. Other sources of tactile response arise from artefacts induced due to glove construction. Prior to analysis, the active patches are identified by applying a threshold on the tactile response normalized by the maximum $\|\mathbf{f}_i\|$ detected. While this method works for frontal surfaces of the fingers and the palm it does not always work with finger sides. Due to artificial enlargement of the finger, the tactile signal may be quite large even when the finger side is not actively engaged with the object. For this work, sides of fingers actually impacting the object are identified by visual analysis of the grasp. This could also be achieved automatically by fitting an object approximation given the

tactile information and patch geometry.

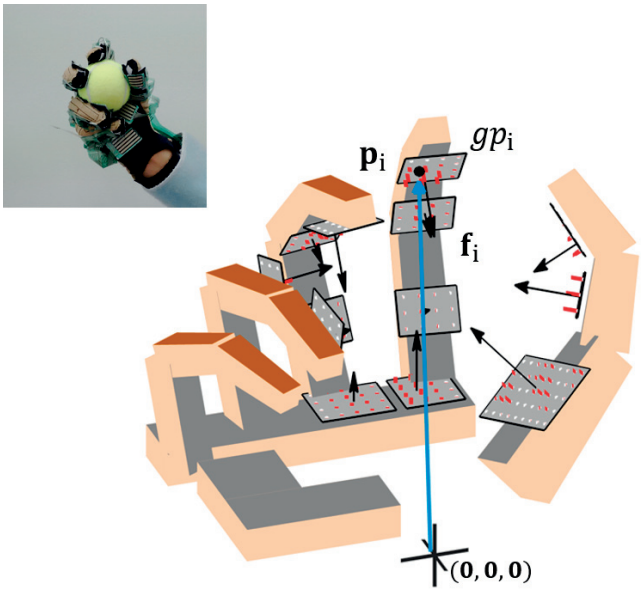


**Figure 3.3:** Grasp demonstration and the raw information captured. Each sensor unit can be represented by a force vector $\mathbf{f}_i$ equal to the sum of all sensel activations and acting at the centroid of pressure $p_i$ defined in a coordinate frame centred at the wrist .

### 3.4.2 Kinematic Model

We define a kinematic model able to achieve most human hand postures and which can be customized to accommodate hands of different sizes. Figure 3.4a presents the kinematic model adopted.

Each finger is modelled as a separate kinematic chain positioned with respect to a coordinate frame located at the wrist. Four revolute joints are used: 2 joints at the metacarpophalangeal junction (MPJ) for flexion and abduction and one joint each at the proximal and distal interphalangeal (IJ) junctions.

The thumb exhibits an ability for pronation/supination at the carpometacarpal junction (CMJ) which needs to be taken into account for accurate positioning. This twisting motion of the thumb is not directly controllable but is a function of the flexion and abduction angle at the CMJ. Modelling this twist becomes even more essential for correctly capturing the different oppositional roles in which the thumb may participate. Thumb-twist has been modelled in Hu et al. (2004); Griffin et al. (2000) by adding a revolute joint with axis along the thumb metacarpal. We choose to locate the additional joint at the metacarpophalangeal junction instead with axis along the proximal phalanx. This is because the thumb-twist effect most influences the orientation of the proximal and distal grasping surfaces.

Link lengths and location of the base of each kinematic chain in the model are set to default values, as provided by Cyberglove, corresponding to an average sized human hand. We customize the kinematic model for each human

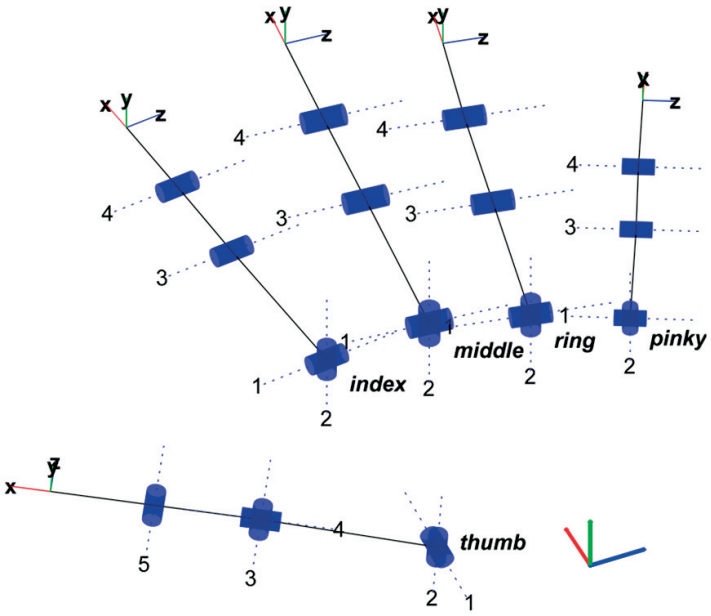


**(a)** Kinematic model for human right hand (dorsal view). Constructed using Robotics Toolbox (?)

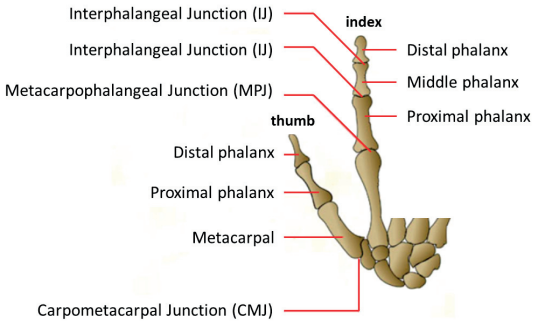


**(b)** Skeletal model of index and thumb fingers with joint nomenclature. Human right hand - dorsal view. Image adapted from http://www.infovisual.info/03/027_en.html

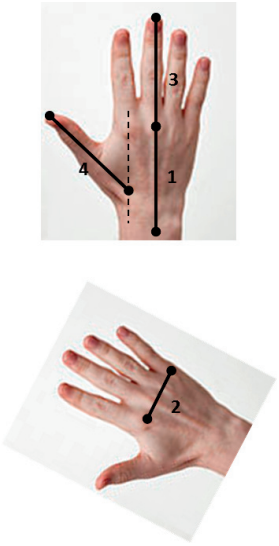

**(c)** Measurements used to scale the kinematic model in 3.4a

**Figure 3.4:** Hand kinematic model

demonstrator using 4 measurements of the subject's hand, Figure 3.4c, to scale the default values. Grasping surfaces of the palm are not controllable in this model. They lie in the plane of the wrist at predetermined locations which also get scaled appropriately according to the hand measurements.

### 3.4.3 Calibration

Careful calibration of the data glove is needed so that the relative geometry of the patches in the kinematic model reconstruction corresponds to the grasp demonstration.

Calibration of the fingers (index, middle, ring, pinky), is done by asking the subject to randomly explore the workspace of the finger joints by moving them between fully opened and fully closed positions. Maximal and minimal joint values are recorded and subsequently mapped to the joint limits of a normal human hand. This method is feasible as the glove sensors for finger joints vary linearly with respect to the finger joint angles.

Thumb calibration is a bigger challenge because there is no sensor embedded in the glove for measuring thumb-twist, and there exists a coupling between the MPJ flexion and abduction sensors which depends on their bend state. Hu et al. (2004); Griffin et al. (2000) use a linear combination of the abduction and flexion angles to approximate the thumb-twist. They observe good positional accuracy of the thumb finger-tip, but no result on orientation of thumb surfaces was reported.

We use a data-driven approach to model the non-linear relationship between the 4 sensors of the glove and the 5 joint angles of the kinematic model. The workspace of the thumb is sampled and position/orientation of the thumb-tip recorded. We use the Optitrack vision system with appropriately placed optical markers (Figure 3.5). For each sample, an inverse kinematic solution is found by minimizing the position and orientation error between the observation and the 6D pose of the thumb-tip as predicted by the forward kinematic model (Figure 3.6). Gaussian mixture regression is then used to model the relationship between the input (glove sensors) and output (joint angles) sets obtained. Regression parameters are obtained through cross-validation on the training set. We obtain a test set error of 0.71 cm in position with a standard deviation of 0.475 cm and 6.62 degrees in orientation with a standard deviation of 4.84 degrees.

**Figure 3.5:** Optical markers are used to track the 6D position and orientation of the thumb-tip during thumb workspace exploration.

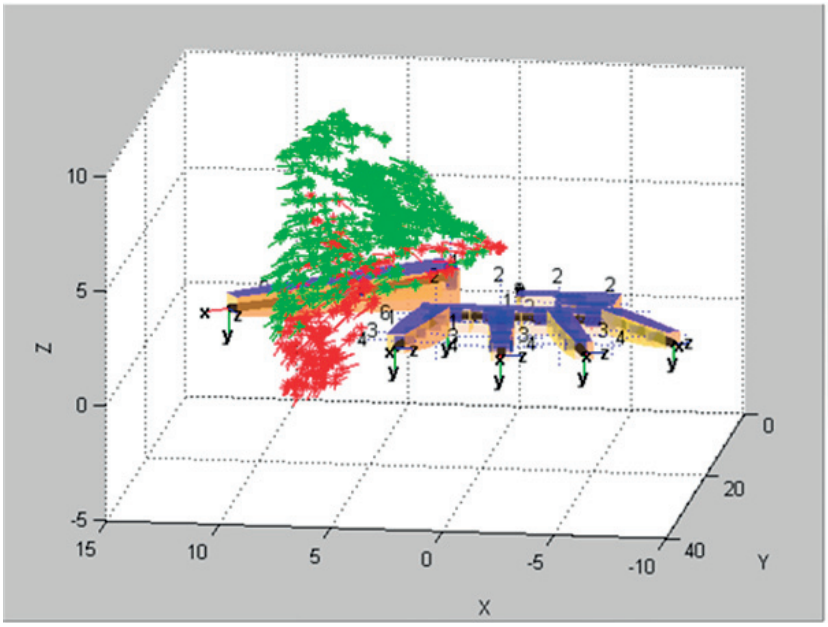


**Figure 3.6:** Forward kinematics applied to thumb-tip pose data obtained after thumb workspace exploration.

## 3.5 Component model for human grasp behaviour

This section defines a model based on opposition primitives which will be used to interpret human grasp behaviour. Opposition concepts introduced in Section 1.2 are defined for use with the sensing infrastructure and extended to consider different oppositional roles of the thumb.

### 3.5.1 Opposition concepts in a sensing framework

The sensing framework outlined in the previous sections imposed a patch decomposition over the grasping surfaces of the hand, i.e. $\mathcal{GP}$ (3.1). The ***grasping patch*** forms the basic unit of information. Information from all patches taken together, $D = \{\mathbf{p}_i, \mathbf{f}_i\}_{i=1}^{34}$ (3.2), constitutes the raw information that is collected from a grasp demonstration.

The key opposition concepts of virtual fingers and opposition primitives, introduced in Section 1.2, can now be defined in terms of grasping patches as follows.

**Definition 3.9** *A **virtual finger** is a subset of grasping patches that work together for the purpose of applying an oppositional force*

**Definition 3.10** *An **opposition primitive** is a pair of virtual fingers between which opposition is kinematically feasible*

For the purpose of extending the opposition space definition we introduce also the concept of a ***hand-part*** to represent the maximum subset of the hand grasping surface which can be given a similar functional role.

**Definition 3.11** *A **hand-part** is the maximal subset of grasping patches that can form a single virtual finger.*

### 3.5.2 Extending the Opposition Space definition

Figure 3.7a presents the hand-parts underlying the original definition of opposition space as proposed in Iberall (1987). Combining these hand-parts into opposing pairs leads to the pad, palm and side opposition categories.

The ability of the thumb to oppose different parts of the hand is responsible for much of human prehensile ability. This becomes an important design consideration when constructing robot hands based on the human model Chalon et al. (2010); Grebenstein (2014). Similarly, we should be able to recognize these different roles when they occur in a grasp demonstration. In this regard, the hand-parts listed in Figure 3.7a, leave some grasping ability unaccounted

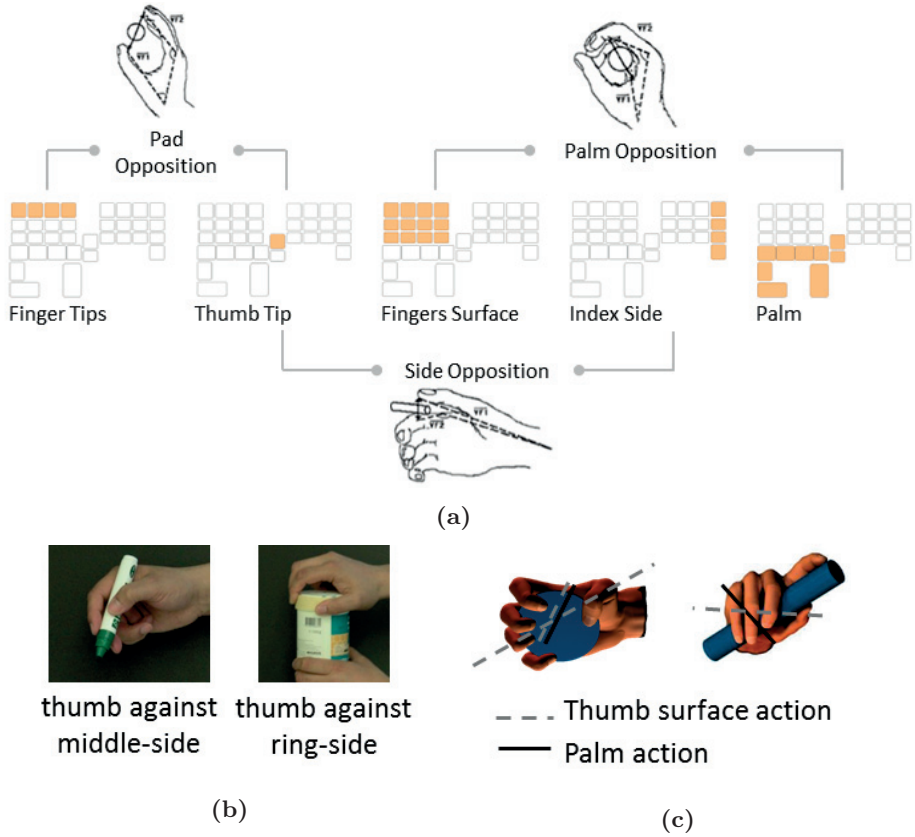


**Figure 3.7:** (3.7a) shows a hand-part decomposition as prescribed by the Opposition Space framework (Iberall, 1987). 3 oppositions are formed when the hand-parts are combined in kinematically feasible ways. (3.7b) and (3.7c) show common scenarios illustrating limitations of this framework in capturing full flexibility of thumb surface usage.

for. *side opposition* accounts only for opposition of the thumb against the index finger side. This implies that thumb usage against other finger sides cannot be recognized. Figure 3.7b shows some examples where this forms an important component of commonly encountered grasps. Another issue is that the oppositional intention of the thumb surfaces is always clubbed with that of the palm. While this is true for some grasps (where the thumb acts as an extension of the palm), in many instances, such as the examples shown in Figure 3.7c, thumb action has quite a different functional meaning and should form a separate component of the grasp. That the original set of hand-parts leaves some grasping capability unaccounted for may also be seen from the fact that the union of oppositions between them is not equal to the entire set of grasping patches.

To address these limitations we add another hand-part, *Thumb Surface*, which separates out the action of thumb surfaces from that of the palm. Also, the *Index Side*, now called just *Side*, is enlarged to cover sides of all fingers. The new set of hand parts is shown in Figure 3.8. They are collectively referred to as $\mathcal{H}$, below, where each hand-part is abbreviated by its starting letter (e.g. Fingers Surface = FS). As will be seen later (Section 3.5.3), these additional hand-parts enable recognition of the different opposing roles of the thumb.

$$\mathcal{H} = \{TT, TS, P, FT, FS, S\} \tag{3.3}$$

Note that for all hand-parts $h \in \mathcal{H}$,

$$h \subset \mathcal{GP}, \quad \bigcup_{h \in \mathcal{H}} h = \mathcal{GP}, \quad \bigcap_{h \in \mathcal{H}} h \neq \varnothing$$

The union of these hand-parts now covers the entire grasping patch set, but their intersection is not empty. The overlapping hand-parts model the fact that individual grasping patches can play multiple functional roles when different oppositions cooperate in delivering the overall functionality of a grasp.

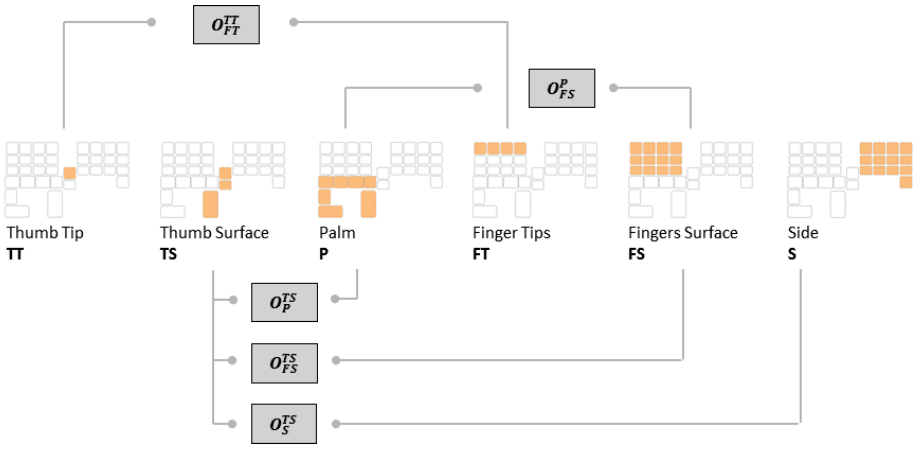


**Figure 3.8:** The new hand-part decomposition leading to an extended definition of opposition space

There are 5 ways in which oppositions between these hand-parts are kinematically feasible. These are shown in Figure 3.8. Let $O_y^x$ be a notation to represent an opposition between the hand-parts $x$ and $y$. Using this notation, the set of hand-part oppositions can be denoted as:

$$\mathcal{O}_{\mathcal{H}} = \{O_{FT}^{TT}, O_{FS}^{P}, O_{P}^{TS}, O_{FS}^{TS}, O_{S}^{TS}\} \tag{3.4}$$

This extends the definition of Opposition Space.

The set $\mathcal{O}_{\mathcal{H}}$ cannot be used directly as a model for grasp intention, since we must first resolve ambiguity related to the different virtual finger possibilities for each hand-part. Each element of $\mathcal{O}_{\mathcal{H}}$ is actually a category of oppositions due to the different ways grasping patches can be grouped together. To resolve these ambiguities, we impose constraints on how virtual fingers can be formed leading to a set of 41 opposition primitives. The following sub-section explains this in more detail.

### 3.5.3 Primitive set for recognizing grasp intention

We impose 2 constraints on grasping patch groupings possible in order to identify a working set of opposition primitives with which to interpret a demonstrated grasp. The first constraint states that:

> *All patches within a hand-part that belong to a real-finger are constrained to be used together.*

Examining $\mathcal{H}$ closely, we see that with the hand-parts $TT, TS$ and $P$, there is no ambiguity, as they all identify a set of grasping patches that are constrained to be used in their entirety. With $FT, FS$, $S$ however, ambiguity exists, as several combinations are possible based on the number of real-fingers that act together with the same oppositional intention. The following introduces notation to denote these possibilities.

Let the index, middle, ring, little fingers be identified by numbers 2-5 and let $\mathcal{F}$ represent all their combinations.

$$\mathcal{F} = \Big\{ f \mid f \subset \{2,3,4,5\}, f \neq \varnothing \Big\}$$

The set of grasping patches comprising a virtual finger can then be denoted by intersecting a hand part $h \in \{FT, FS, S\}$ with real fingers $f \in \mathcal{F}$. For example, $FT234$ denotes the set of grasping patches belonging to tips (distal phalanges) of the index, middle and ring fingers. If we extend the set of cooperating grasping patches to include also the middle and proximal phalanges of the same fingers, then the virtual finger becomes denoted as $FS234$. An opposition primitive is denoted by $O_{VF_2}^{VF_1}$, where $VF_1$ and $VF_2$ are the two opposing virtual fingers given by the virtual finger notation just described. To illustrate this notation,

**Figure 3.9:** Turning a dial. Opposition of the type $O^{TT}_{FT}$. Can be described by primitive $O^{TT}_{FT234}$.

consider the example of the turning-a-dial task of Figure 3.9 where the thumb-tip is used against finger-tips of the index, middle and ring fingers to form the grasp. This may be described as the opposition primitive $O^{TT}_{FT234}$.

Using the first virtual finger constraint stated above, a total of 61 opposition primitives are possible. This can be seen from the fact that the cardinality of $\mathcal{F}$ is 15 ($C^4_1 + C^4_2 + C^4_3 + C^4_4$). In conjunction with $\mathcal{O}_{\mathcal{H}}$, this gives a total of $4 * 15 + 1 = 61$ opposition primitives. However, an examination of grasp taxonomies in the literature made from studies of human grasping behaviour, such as Feix et al. (2009), shows that many of these primitive possibilities are never employed in practice. Motivated by the same studies, we impose a second constraint on virtual finger formation which states that:

*Virtual finger span is contiguous.*

This means that if fingers 2 and 4 are being used with the same oppositional intention, say $O^P_{FS2}$ and $O^P_{FS4}$, finger 3 is required to cooperate with them and the primitive being used is actually $O^P_{FS234}$. With this simplifying assumption there are 10 valid real-finger groupings: 2, 3, 4, 5, 23, 34, 45, 234, 345, 2345 and a total of 41 opposition primitives. Let this primitive set be denoted by $\mathcal{P} = \{P_1, \ldots, P_{41}\}$. These are indicated in Figure 3.10.

The difference of this primitive set with the original opposition space framework is seen in the additional primitives in the bottom half of Figure 3.10 (primitives no. 21-41). These primitives model flexibility of thumb usage (against finger surfaces, against palm, against sides of all fingers) all of which play an important role towards overall hand functionality. The addition of these primitives implies that they can now be recognized as separate intentions in a grasp demonstration.

### 3.5.4 Grasp Signature

A ***grasp signature***, $GS$, is defined as an importance distribution over the set of opposition primitives.

$$GS = \left\{ \mathbf{x} \in \mathbb{R}^{41} \mid x_i \geq 0, \sum x_i = 1 \right\}$$

The grasp signature characterizes the grasping intention underlying a demonstrated grasp. This is a higher dimensional space when compared to 22 DOF joint angles. It should be noted however that joint angles and opposition primitives represent different information. While joint angles model the hand shape by capturing an end-configuration, they do not represent how the hand surfaces are to be used during closure and over the task duration. In contrast, a grasp signature comprised of opposition primitives, uses interaction between hand surfaces to model the latter aspects of grasp formation, leaving the end-configuration to be decided by compliance with the object. Considering all ways hand surfaces may interact, there is inherently more information to represent when compared to all prehensile postures possible. Also, similar to the synergies discovered in the space of joint angles (Santello et al., 1998), it is very likely that there exists low dimensional representations which could account for most of the variance in an interaction space. One candidate for such an interaction space is proposed next.

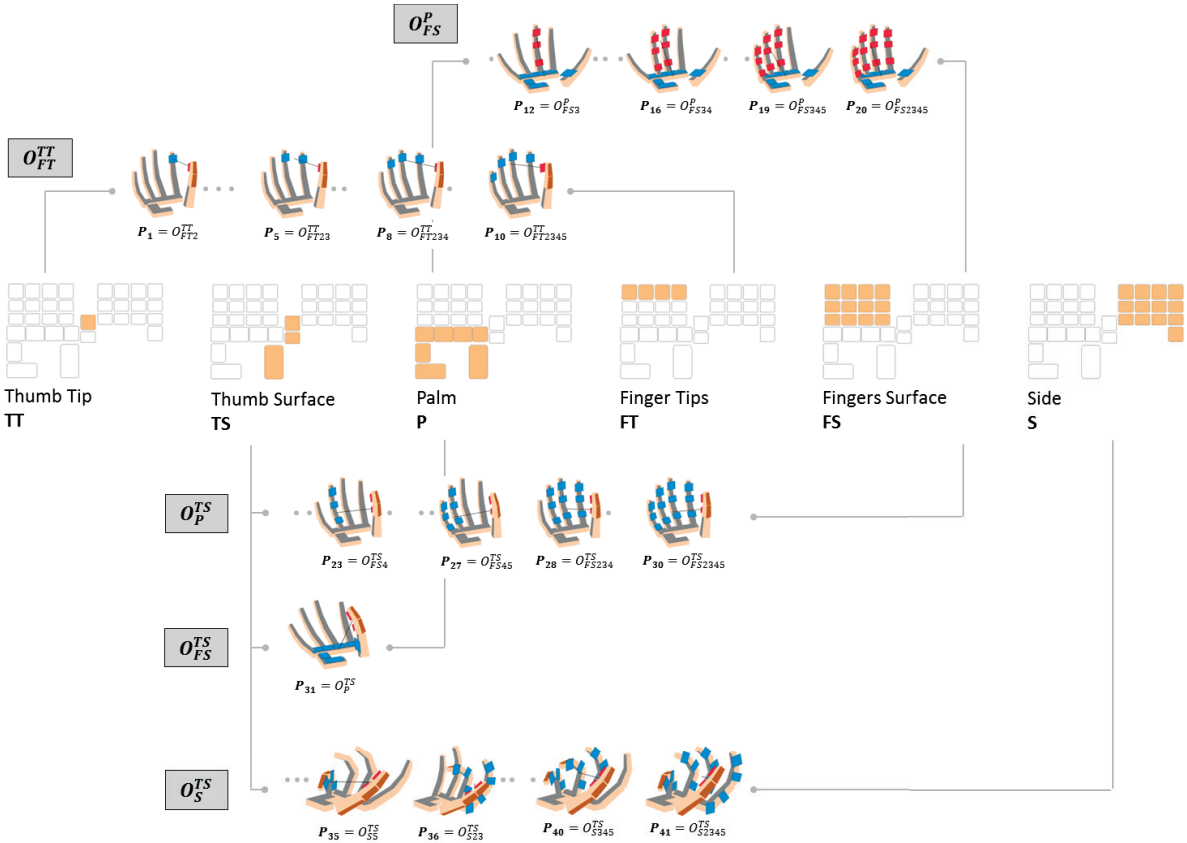


**Figure 3.10:** Shows the set of opposition primitives with which *grasp intention* is interpreted. For the categories $O^{TT}_{FT}, O^{P}_{FS}, O^{TS}_{FS}, O^{TS}_{S}$, there are several ways in which real-fingers may group together with the same oppositional intention. Using the simplifying assumption of contiguous virtual finger span, 10 possibilities may be identified: 2, 3, 4, 5, 23, 34, 45, 234, 345, 2345. For clarity only a selected number of these are shown above.

## 3.6 Inferring a grasp signature

A combination of primitives may be detected from the raw information in a grasp demonstration. We present the patch level opposition (or PLO) representation for combining raw information (configuration, tactile) present in a grasp demonstration. The PLO representation is a 144 dimensional feature based on quantifying the importance of pairwise interactions between grasping patches in the context of a demonstrated grasp. This representation is better suited to expose the different oppositional roles in which a grasping patch participates than if tactile and configuration data are considered in a disconnected manner. Detection of a grasp signature relies on the fact that, if a primitive is an important component of a grasp, it becomes more likely to find "strong" patch level interactions between the patches defined by its opposing virtual fingers.

### 3.6.1 A metric for patch level opposition (PLO)

Given a pair of grasping patches $gp_i, gp_j$, we wish to quantify how relevant is the opposition of $gp_i$ against $gp_j$ to the demonstrated grasp. We propose a metric of opposition strength based on two measures:

*1) The normal force.* The minimum of the two forces $\mathbf{f}_i$ and $\mathbf{f}_j$ is taken.

$$\phi_{force}(\mathbf{f}_i, \mathbf{f}_j) = \min\Big\{\|\mathbf{f}_i\|, \|\mathbf{f}_j\|\Big\} \tag{3.5}$$

*2) Quality of geometrical opposition.* Two angles arising from the relative geometry of the patches are considered and the one having the greater influence is used.

The first is the angle between the normal force vectors.

$$\alpha = cos^{-1}\langle\frac{\mathbf{f}_i}{\|\mathbf{f}_i\|}, \frac{\mathbf{f}_j}{\|\mathbf{f}_j\|}\rangle$$

Patches oppose the best when $\alpha = 180$, Figure 3.11a. The quality of opposition decreases with decreasing $\alpha$. Once $\alpha$ crosses a threshold i.e. $\alpha < \alpha_t$, opposition between the patches is deemed not relevant.

The second is the angle that force vectors make with the line joining patch centroids.

$$\beta_i = cos^{-1}\langle\frac{\mathbf{f}_i}{\|\mathbf{f}_i\|}, \hat{\mathbf{p}}_{ij}\rangle \quad \beta_j = cos^{-1}\langle\frac{\mathbf{f}_j}{\|\mathbf{f}_j\|}, -\hat{\mathbf{p}}_{ij}\rangle$$
$$\beta = \max\Big\{\beta_i, \beta_j\Big\}$$

In contact models used for analytical grasping analysis (Murray et al., 1994), this angle is related to the maximum force that can be applied to a surface before incurring the risk of slipping. $\beta$ should lie within the friction cone of the surface. We use it here to indicate opposition capability even when the angle between the normal force vectors decreases significantly such as in figure 3.11b.

In such cases, opposition is still possible if enough friction exists or if the object is immobilized by other parts of the hand. Smaller the angle $\beta$ greater is the force which can be applied.

As long as opposition is deemed relevant i.e. $\alpha \geq \alpha_t$, the influence of $\alpha$ and $\beta$ on opposition strength can be quantified using the functions $f_\alpha$ and $f_\beta$ as follows:

$$f_\alpha = \mathrm{e}^{\left(-\frac{\pi-\alpha}{\alpha_c}\right)^\gamma}$$
$$f_\beta = \mathrm{e}^{\left(-\frac{\beta}{\beta_c}\right)^\gamma}$$

Values for all parameters are indicated below.

| | |
|---|---|
| $\alpha_t = 1.48$ | opposition is considered only if angular separation between normals is greater than 85°. |
| $\alpha_c = 1.22$ | reduces the effect of $\alpha$ once $\alpha \leq 110°$ |
| $\beta_c = 1.22$ | conservative estimate of a friction cone taken at 70° |
| $\gamma = 1.5$ | determined empirically |

$f_\alpha$ and $f_\beta$ are dominant in different situations. In figure 3.11b, $f_\alpha$ is low but opposition is still possible, $f_\beta$ is the better indicator. In figure 3.11c, $f_\beta$ is low but the patches are well opposed, $f_\alpha$ is the better indicator. The effect of patch geometry on the quality of opposition is defined considering both functions as follows:

$$\phi_{geom}(\hat{\mathbf{p}}_{ij}, \mathbf{f}_i, \mathbf{f}_j) = \begin{matrix} 0 & \alpha < \alpha_t \\ \max\left\{f_\alpha, f_\beta\right\} & \alpha \geq \alpha_t \end{matrix} \tag{3.6}$$

Finally, the metric of opposition strength, $\phi_{plo}$, is defined as:

$$\phi_{plo} = \phi_{geom} \cdot \phi_{force} \tag{3.7}$$

Since $0 \leq \phi_{geom} \leq 1$, $\phi_{plo}$ may be seen as the normal force modulated by the geometrical quality of the opposition.

### 3.6.2 Feasible patch level oppositions (the PLO-space)

There are $C_2^{34} = 561$ pairwise combinations for the 34 grasping patches in $\mathcal{GP}$. Of these, the set of grasping patch pairs for which opposition is kinematically feasible is termed as the PLO-space. Let $O_{PLO} \in \mathbb{R}^{34\times34}$ represent all valid pairwise interactions between grasping patches.

$$O_{PLO}(j,k) = \begin{cases} 1 & \text{patch } gp_j \text{ can oppose } gp_k \\ 0 & \text{otherwise} \end{cases} \tag{3.8}$$

Each primitive $P_i = O_{VF_2^i}^{VF_1^i} \in \mathcal{P}$ defines a set of valid pairwise interactions between grasping patches as a consequence of opposition between its virtual

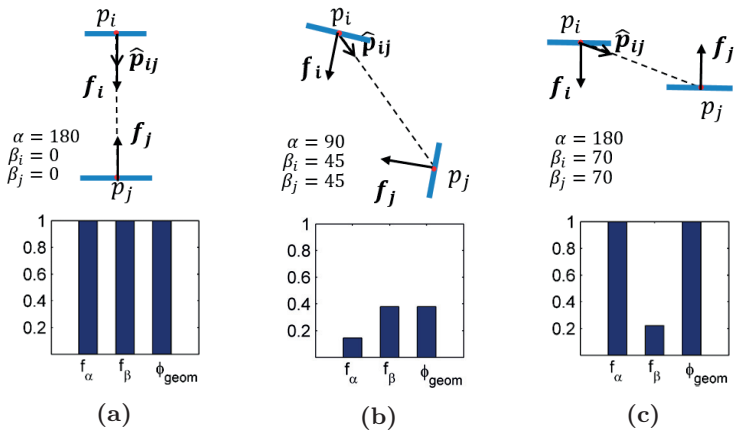


**Figure 3.11:** Angles arising from relative geometry of patches are used to quantify opposition quality. $\alpha$ is angle between the normal force vectors $\mathbf{f}_i, \mathbf{f}_j$. $\beta_i, \beta_j$ are the angles that normal force vectors make with the line joining patch centroids $\hat{\mathbf{p}}_{ij}$

fingers.

$$O^i_{PLO}(j,k) = \begin{cases} 1 & j \in VF^i_1 \text{ and } k \in VF^i_2 \\ 0 & \text{otherwise} \end{cases} \tag{3.9}$$

The PLO-space can be computed as a union of $\mathcal{O}^i_{PLO}$ and is represented by the upper (or lower) triangular portion of Figure 3.12.

$$O_{PLO} = \bigvee_{i \in \mathcal{P}} \mathcal{O}^i_{PLO}$$

This method of determining a PLO-space captures the fact that it is infeasible for each major hand-part to oppose its own self. Further, surfaces of the fingers (excluding the thumb) cannot oppose their sides and distal patches of the fingers cannot oppose the intermediate patches.

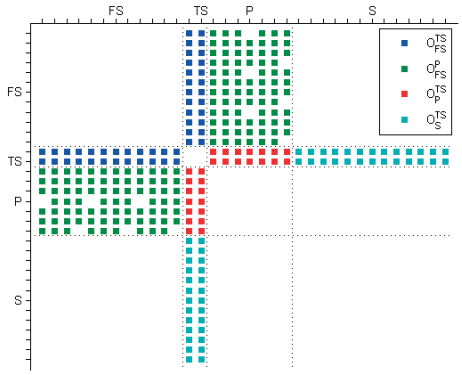


**Figure 3.12:** The space of kinematically feasible patch level oppositions. Each axis represents the set of 34 grasping patches grouped by major hand-part: FS - Finger Front Surface, TS - Thumb Surface, P - Palm Surface, S - Finger Side Surface. Patch level oppositions are color-coded according to the hand parts between which they occur.

Applying (3.7) to (3.8) yields a 144-dimensional feature which can be used to discover the presence of primitives in a grasp demonstration. Figure 3.13 shows the feature computed for demonstrations of commonly encountered precision and power grasps. Notice that multiple oppositional roles of the thumb have been exposed for writing (against finger surface and finger side) and for screwdriving (against finger surface, palm and finger side).

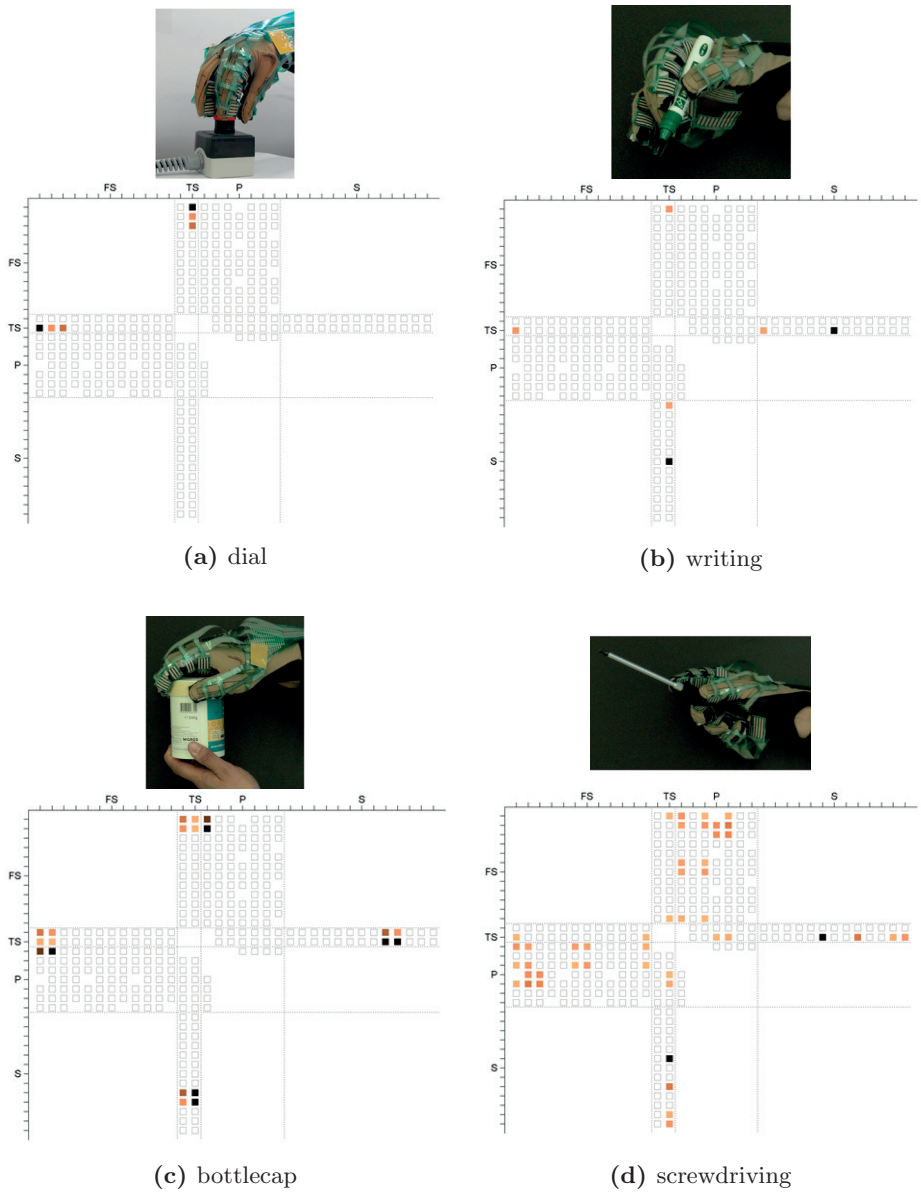


**(a)** dial **(b)** writing

**(c)** bottlecap **(d)** screwdriving

**Figure 3.13:** The space of feasible patch level oppositions (3.12) and examples of instantiating this feature for commonly encountered grasps (3.13a-4.23)

### 3.6.3 Computing a grasp signature

The grasp signature is a distribution over the primitive set corresponding to the importance with which each primitive is manifested in the grasp demonstration. To discover this from hand configuration and tactile force in a grasp demonstration we make use of the intermediate PLO representation. The oppositional roles possible for each finger are examined. These correspond to the set of primitives listed below.

$$\mathcal{X} = \Big\{ O^{TT}_{FT2}, O^{TT}_{FT3}, O^{TT}_{FT4}, O^{TT}_{FT5}, O^{P}_{FS2}, O^{P}_{FS3}, O^{P}_{FS4}, O^{P}_{FS5}, O^{TS}_{FS2}, O^{TS}_{FS3}, O^{TS}_{FS4}, O^{TS}_{FS5}, \quad O^{TS}_{P}, O^{TS}_{S2}, O^{TS}_{S3}, O^{TS}_{S4}, O^{TS}_{S5} \Big\}$$

For each element of $\mathcal{X}$ the opposing hand-parts are known. This prior information can be used to compute primitive likelihood and identify a set of cooperating primitives.

#### Primitive likelihood

Primitive likelihood makes use of a recognition template. The studies by Kamakura et al. (1980), using real world objects, identified tactile signatures commonly encountered when employing certain finger pre-shapes. Similarly Faria et al. (2012) use tactile templates of grasping regions to characterize 7 grasps with which to interpret in-hand manipulations. For an opposition primitive, $O^{i}_{PLO}$ (3.9), defines a template in PLO-space corresponding to the pairwise oppositions that could be generated by it. Further, for any given primitive, using the oppositional intention as a guide, we may identify patches on each opposing hand-part where oppositional pressure is focussed if the primitive is being used. These are termed primary patches. Surrounding patches, act in support of these and are termed secondary patches. Interactions between primary patches have the most importance followed by primary-secondary interactions and then secondary-secondary interactions. Following this reasoning a relevance mask or recognition template for a primitive in $\mathcal{X}$ can defined as in (3.10).

$$\underset{i \in \mathcal{X}}{M^{i}}(j,k) = \begin{cases} 1 & gp_j, gp_k \text{ is a primary patch pair} \\ 0.7 & gp_j, gp_k \text{ is a primary-secondary patch pair} \\ 0.3 & gp_j, gp_k \text{ is a secondary patch pair} \\ 0 & gp_j, gp_k \notin P_i \text{ i.e. } O^{i}_{PLO}(j,k) = 0 \end{cases} \tag{3.10}$$

The recognition template for a primitive is used as a prior knowledge filter to

obtain likelihood of a primitive's presence in a grasp demonstration (3.11).

$$\underset{i\in\mathcal{X}}{\Phi}(i) = \sum_{j,k=1}^{34} M^i(j,k)\cdot\phi_{plo}(\hat{\mathbf{p}}_{jk},\mathbf{f}_j,\mathbf{f}_k) \tag{3.11}$$

$\Phi$ once normalized represents primitive likelihood.

### Primitive compatibility

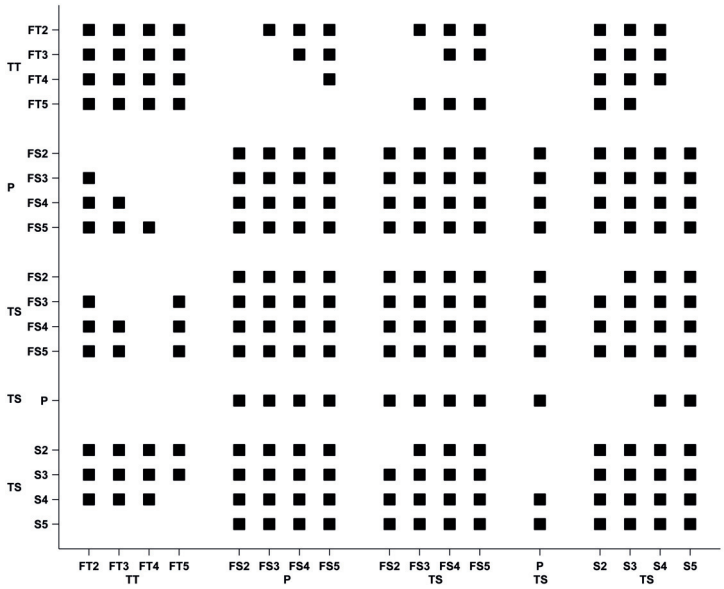


**Figure 3.14:** The opposition compatibility matrix captures co-existence between oppositional intentions at the finger level. Black squares indicate cooperation is possible. White squares indicate incompatibility. Categories $O^{P}_{FS}$, $O^{TS}_{FS}$, $O^{TS}_{P}$, $O^{TS}_{S}$ mostly cooperate but conflicts arise between these and finger-tip opposition $O^{TT}_{FT}$.

Due to the kinematic coupling that exists between the finger joints, choosing one of the primitives in $\mathcal{X}$ as a strong intention makes others infeasible. Coexistence between these oppositional intentions can be pre-analyzed and recorded in a primitive compatibility matrix, Figure 3.14.

### Cooperating primitives in a demonstrated grasp

Using (3.11) and information in Figure 3.14 a set of cooperating primitives can be discovered in an iterative fashion. First the most likely primitive $\psi = \underset{i\in\mathcal{X}}{\max}\Phi$ is chosen. The span of the virtual finger is expanded by selecting all primitives in $\mathcal{X}$ having a non-zero likelihood of opposition with the same hand-part as $\psi$. Normal force of patches contributing to the selected primitives are reduced by strength of the contributing PLOs and $\Phi$ is recomputed. The new likelihood thus incorporates an explanation of the raw data due to the selected primitives. The selected primitives as well as those that are not compatible with the ones selected are excluded from consideration and the process is iterated. The process

terminates when there are no more single finger oppositions likely i.e. $\Phi(i) = 0 \quad \forall i \in \mathcal{X}$.

The grasp signature discovered above is modified to express contiguity of virtual finger span. For example, if fingers 2, 3 and 4 are found to be opposing the palm i.e. $O^P_{F2}$, $O^P_{F3}$ and $O^P_{F4}$ are present, then these are combined and reported as $O^P_{F234}$. If $O^P_{F3}$ is absent, then to ensure contiguity of the virtual finger, palm opposition for finger 3 is added and the primitive $O^P_{F234}$ is reported. Finally, each primitive reported is assigned an importance by summing the PLO strength for each participating finger and taking the average.

## 3.7 Experimental Validation

The system for recognizing grasp behaviour in terms of opposition primitives from raw tactile and configuration data is evaluated using human grasp demonstrations carried out over several grasp scenarios.

A grasp scenario consists of an object-grasp pair. The grasp chosen establishes a particular way hand surfaces are to be used. This can be motivated by how an object should be handled in order to perform a particular task. Alternatively, it can be picked from a grasp taxonomy. The grasp scenario thus communicates a specific intention for grasping to the human subject who will manifest it on an object. Performance of the system is based on whether the recognized signature corresponds to the pre-identified grasp intention. All grasps are demonstrated using the tactile glove described earlier. We differentiate between expert and naïve demonstrator. An expert is one who has a lot of experience with using the tactile glove to grasp objects and is well versed in grasp taxonomy. A naïve demonstrator has no knowledge of either.

A set of experiments are designed to vary different parameters in order to examine the generality and reliability of the system. Parameters to be varied include the grasp itself, the object on which the grasp is manifested or the hand (subject) making the grasp. An underlying theme behind the experiments is that for the same grasp, regardless of whether it is demonstrated by different hands or on different objects, the grasp signature recognized should remain unchanged. However, if the grasp changes in some way, then this change should be correctly reflected in the grasp signature. The change can be small such as the importance given to different grasp components or the number of fingers employed, or large, as when employing a different combination of oppositions.

### 3.7.1 Single expert demonstrator

By using an expert demonstrator we minimize the possibility of misunderstanding the grasp or improperly manifesting it on the object using the tactile glove.

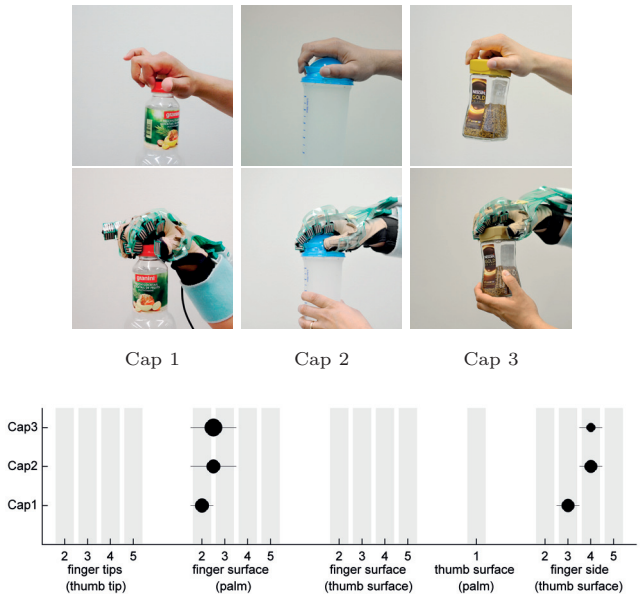


**Figure 3.15:** Similar grasp on different objects. Single demonstrator. Opening a tight bottle-cap with different size/shape. Cap1 and Cap2 are round with diameter 4 cm and 8.5 cm, while Cap3 is square with side 7 cm. The grasp intention is changed slightly for Cap1 to accommodate smaller diameter.
The recognized grasp signatures are plotted below the figure. The y-axis denotes the grasp scenario and the x-axis denotes the different opposition classes. Fingers thumb-index-middle-ring-pinky are numbered 1-5. For each grasp scenario, primitives detected are denoted by filled circles. The circle diameter corresponds to the importance of the primitive in the grasp. The horizontal line in each circle indicates the virtual finger span i.e. the real fingers detected as having the same oppositional intention. This representation allows any subset of the 41 primitives to be presented in a compact manner. For example, recognized signature for scenario Cap2 and Cap3 comprise of the primitives $O^{P}_{FS23}$ and $O^{TS}_{S4}$, whereas for Cap1 the primitives recognized are $O^{P}_{FS2}$ and $O^{TS}_{S3}$.

### Same grasp on different objects

The first scenario involves the task of opening a tight bottle cap. Three different caps are used having different size and/or shape (round, square). The grasp does not need to deliver any motion rather it needs to grip the cap firmly in order to transmit the strong torques and coarse motion generated by the wrist-arm without allowing any slippage. This is done by using the thumb surface against the side of the ring finger supported by the action of finger-tips (index-middle) against the fleshy part of the thumb (Figure 3.15 top half). This intention remains the same for cap 2 and 3 but is changed slightly for cap 1 to accommodate the smaller diameter. The recognized signature (Figure 3.15 bottom half) for each grasp-object pair, when evaluated against the grasp intention just stated, shows that the intention is correctly recognized. Also, change in intention for the small diameter cap has been captured.

Grasp scenarios involving a cutting tool is also taken. Three handles of different diameter and weight are used. The grasp chosen grips the handle firmly using action of fingers (middle−ring) against the palm while directional ability is provided by a tripod grip between thumb, middle-side and index-tip (Figure 3.16). This intention remains the same for tool 1 and 2 but is

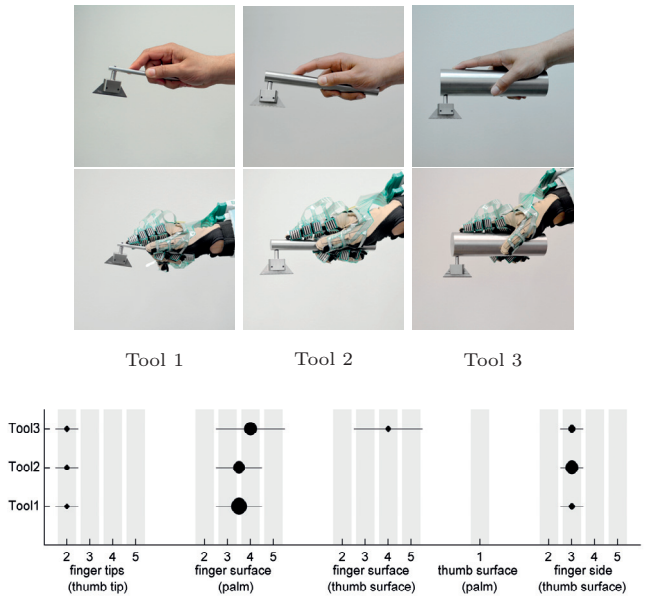


**Figure 3.16:** Similar grasp on different objects. Single demonstrator. Cutting with different diameter/weight handles: Tool 1 (⌀ = 0.8cm, 23gm), Tool 2 (⌀ = 2cm, 500gm), Tool 3 (⌀ = 5cm, 3136gm). The grasp intention is changed slightly for Tool3 to accommodate larger diameter and weight. The recognized grasp signatures are plotted below the figure. See Figure 3.15 for an explanation on how to interpret the plot.

changed slightly to accommodate the larger diameter and weight of tool 3. The recognized grasp signatures compared with the stated intention show that the grasp is well recognized including the change in intention for tool 3.

### 3.7.2 Different grasps on the same object

Opening a tight bottle cap scenario is taken first. The grasp for this was explained earlier in Section 3.7.1. However, when the cap becomes loose a new grasp is employed. The strong action of palm opposition is no longer required and is replaced instead by use of finger tips. Results shown in Figure 3.17 indicate that this different intention is correctly detected from the demonstration.

A cutting tool scenario is also examined. Here the position of the cutting blade is changed to the middle (tool 2) and the top (tool 3) of the handle as shown in Figure 3.18. Entirely different grasps are now required in each case. The grasp for tool 2 uses exclusively side-opposition, whereas grasp for tool 3 uses a combination of palm opposition and side opposition. Examining the recognized grasp signatures, we see that these intentions are well detected.

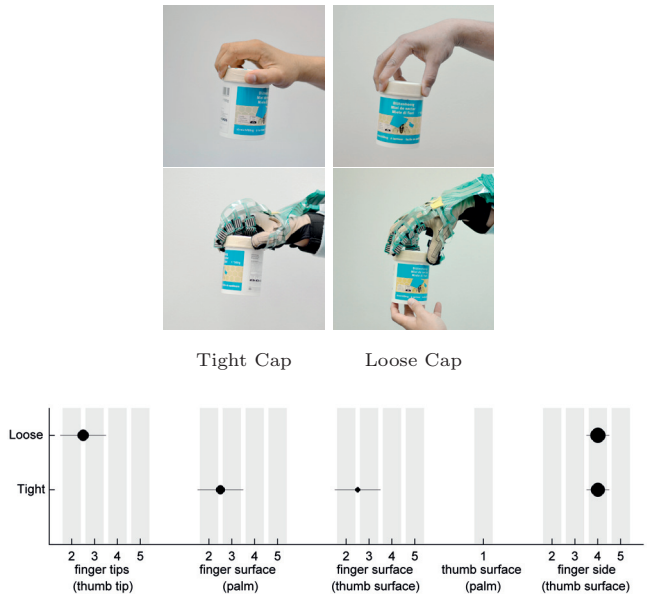


**Figure 3.17:** Different grasps on the same object. Single demonstrator. Opening a bottle-cap when it is tight and when it is loose. Entirely different grasps are required for each case. The recognized grasp signatures are plotted below the figure. See Figure 3.15 for an explanation on how to interpret the plot.

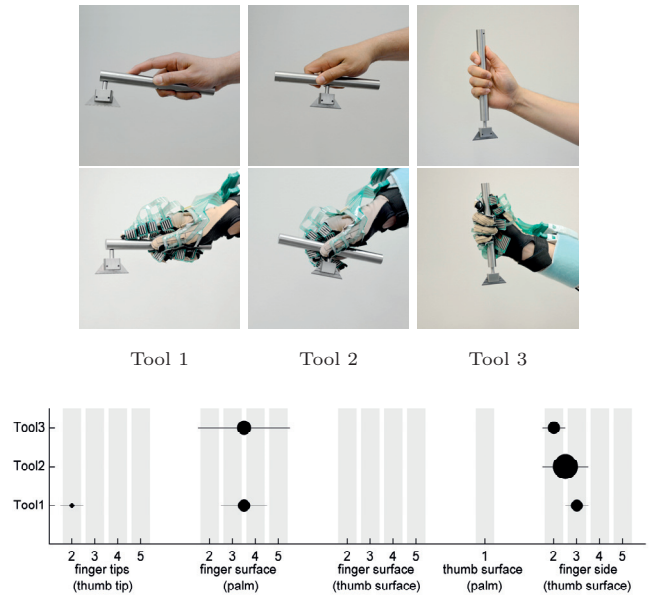


**Figure 3.18:** Different grasps on the same object. Single demonstrator. Cutting with different tools. Tools 1, 2 and 3 use the same handle but have the cutting blade positioned differently requiring entirely different grasps for each case. The recognized grasp signatures are plotted below the figure. See Figure 3.15 for an explanation on how to interpret the plot.

From the above experiment it is seen that the method for grasp recognition performs well when intention is kept the same, is changed in a small way or when completely different. However, only 1 hand is used and relatively few number of grasps are demonstrated. In the next experiment we widen the set of grasps and objects considered. Also, grasps are demonstrated by several naïve subjects

who do not have experience using the tactile glove nor are knowledgeable about grasp taxonomy.

### 3.7.3 Multiple naïve demonstrators

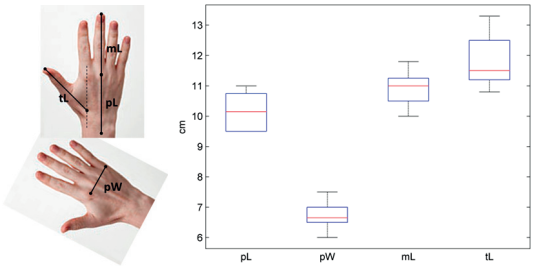


**Figure 3.19:** Dimensions for measuring hand size and dispersion of hand size data across the 10 subjects. For each dimension, the vertical line indicates extremes, box covers $25^{\text{th}}$-$75^{\text{th}}$ percentiles and the red line denotes the median.

The performance of grasp recognition is evaluated using a 10 naïve demonstrators. The subjects were male (between 21-30 years of age) with different hand sizes as summarized in figure 3.19. Grasp scenarios are taken from the taxonomy from Feix et al. (2009) which represents a comprehensive summary of several grasp taxonomies proposed in the literature. Ten grasps are selected to cover a wide range of hand functions. These range from high precision grasps, to intermediate grasps mixing power with the ability to control force and torque at a tool tip, to high power grasps. Grasps selected are presented in Table 3.1. Other than wide range of function, we may note that scenarios 5, 6 and 7 test the case where different grasps are manifested on the same object. Also, scenarios 7, 8, 9 are all examples of power grasp with directional ability. Different grasp components provide the directional capability in each case.

#### Method

1. A grasp scenario is communicated to the human subject using a picture of the grasp-object pair and a high level description of the way hand surfaces are to be employed. Table 3.1 lists the instructions used. Based on these instructions an expected signature is constructed for each grasp scenario.

2. The subject tries out the grasp, following the instructions first with the ungloved hand. The subject is then given the opportunity to practice with the gloved as many times as desired. Once the subject is comfortable with creating the grasp with the gloved hand, tactile and configuration data are recorded. One record is taken for each grasp scenario.

3. Subjects did not always adhere to the communicated intention. For example, for grasp no. 4 in Table 3.1, some subjects preferred not to use the little finger

although this is unambiguously indicated in the figure. Clear deviations of this sort, exhibited on the communicated intention, are noted at the time of demonstration and are reflected in the expected signature.

4. Detected grasp signatures for each grasp scenario are then compared with the expected signature.

### Results

The 10 subjects and 10 grasp scenarios constitute a total of 100 trials in all. Figures 3.21- 3.30 present the recognition results. For each grasp scenario the results show the expected signature in red (deviations are noted in blue[1]) followed by the detected signatures.

We see that in 87 trials the recognized signature matches the expected exactly, thus indicating that the system is good at detecting the expressed grasp intention from tactile and configuration data over a wide range of ways in which the hand may be utilized to generate grasps. Cases where mismatch occurred were investigated and are noted below. In the following (X-a.b.c) should be read as scenario-X, subjects-a,b,c.

a) In 9 trials although the grasp was demonstrated correctly, tactile signal was too weak. This resulted in the virtual finger span being smaller than expected (1-9, 2-5, 6-1.6, 7-10), or certain components not getting detected at all (1-2.3, 5-5.10).

b) In 4 trials, confusion occurs where oppositions are detected which have clearly not been demonstrated (6-9, 7-4.6.8). In all these cases, $O^P_{FS2}$ is detected but it is clear that the index finger is employed differently.

c) In 23 trials, an additional component of the type $O^{TS}_F$ is detected when not expected. This is seen in scenarios 3 and 7-10. This can be explained due to the natural tendency to include this component when the power grasp $O^P_F$ is being exercised as a strong intention, which is the case in all these scenarios.

Examination of the confusions detected (point b) showed that these were caused due to patches which exhibited geometrical opposition but whose tactile response came from some other involvement. When two patches oppose geometrically and also exhibit tactile response, the system assumes mutual opposition and quantifies opposition strength. The system cannot tell if the tactile response is due to other causes. Recognition of the correct signature relies on the fact that the intention being demonstrated results in oppositions that are stronger, causing the correct primitives to be prioritized. However relying solely on geometry and interaction force can result in confusion and other indicators of opposition would need to be considered.

[1] Out of 100 trials, 10 deviations from the communicated intention were noticed.

| | Scenario | Description |
|---|---|---|
| 1 |  | **Power grasp.** Object is encaged and grasped firmly. |
| 2 |  | **Power grasp.** Object is encaged and grasped firmly. |
| 3 |  | **Power grasp including finger side.** Object is encaged and grasped firmly. |
| 4 |  | **Fingertip grasp.** |
| 5 |  | **Fingertip grasp with side support.** |
| 6 |  | **Tripod grasp.** Tripod is made using fingertip and finger side. |
| 7 |  | **Directional power grasp.** Directional ability is provided using thumb and finger side. |
| 8 |  | **Directional power grasp.** Directional ability is provided using thumb and finger tips. |
| 9 |  | **Directional power grasp.** Directional ability is provided using thumb, finger side and finger tips. |
| 10 |  | **Power grasp with dexterous ability.** Dexterous ability is provided using thumb and finger tip. |

**Table 3.1:** Grasp scenarios covering a range of hand function. Scenarios and figures (except for 8,10) are taken from Feix et al. (2009)

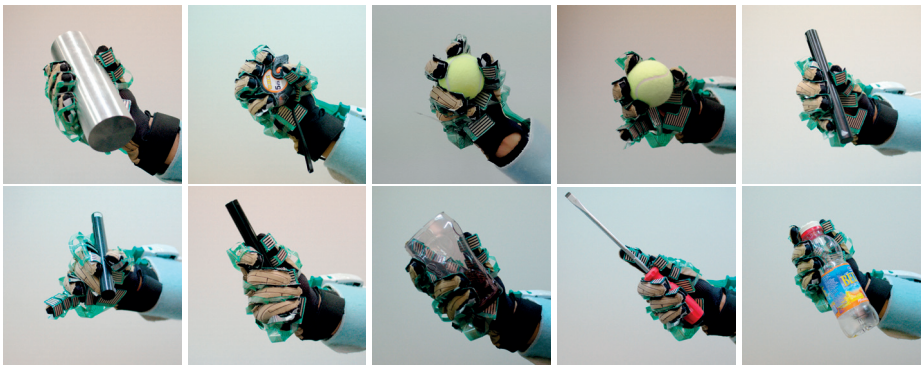

**Figure 3.20:** Grasp scenarios in Table 3.1 demonstrated on objects using the tactile glove.

Although the system reports on importance of the grasp components recognized, we have no basis for examining the detected importance. For static grasping there is no cause for giving importance to different grasp components. Importance only becomes relevant in a task context when the capabilities brought to the grasp by a component are exercised in response to task demands that occur. This may also be partly responsible for tactile signal being absent or very weak for some components even though they were demonstrated. For example, side stabilization in scenario 5.

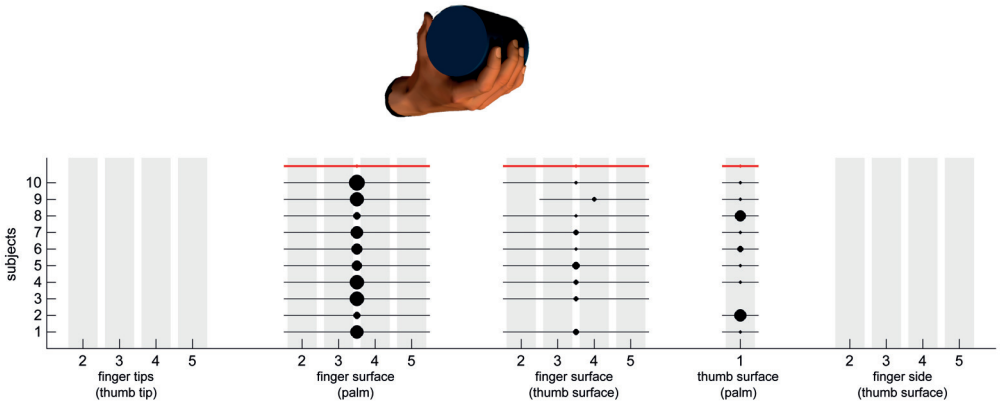


**Figure 3.21:** Scenario 1

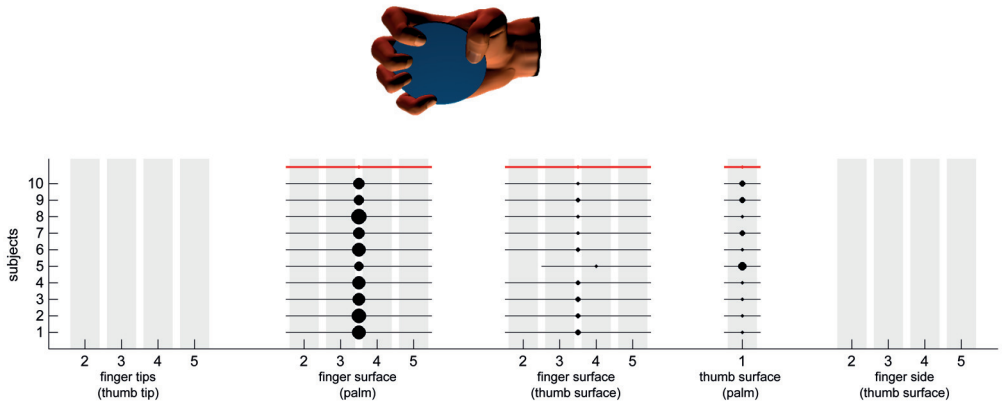


**Figure 3.22:** Scenario 2

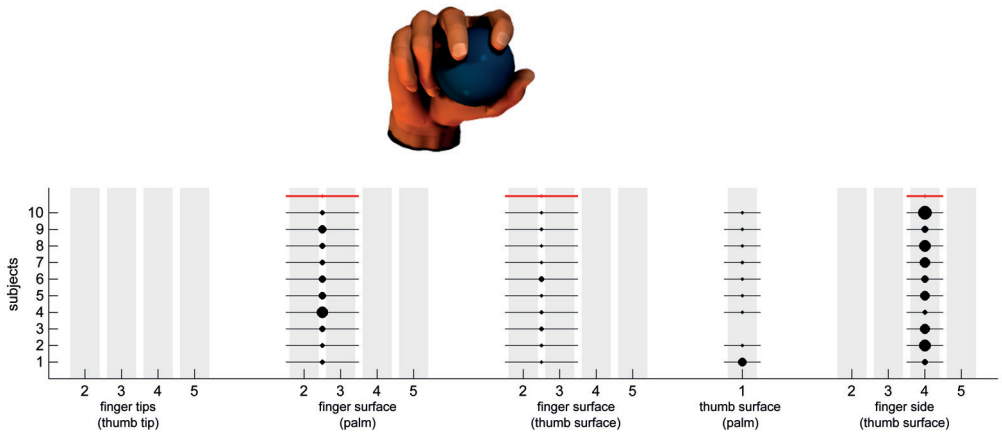


**Figure 3.23:** Scenario 3

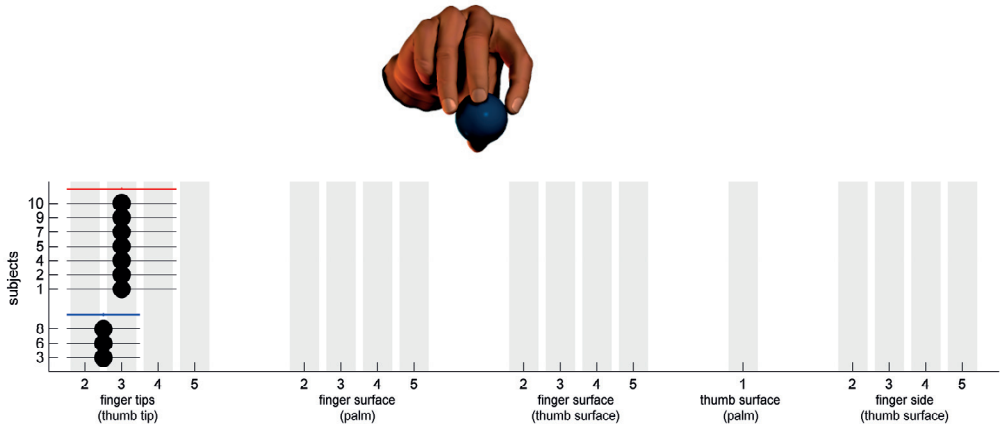


**Figure 3.24:** Scenario 4

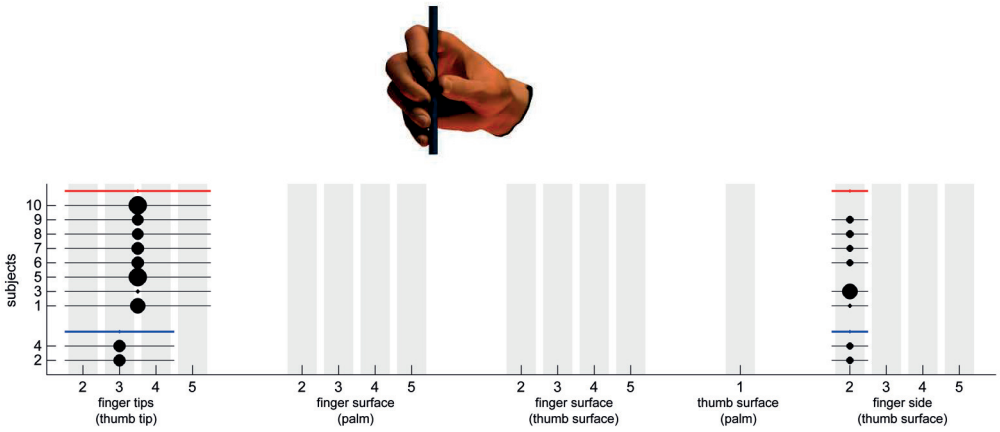


**Figure 3.25:** Scenario 5

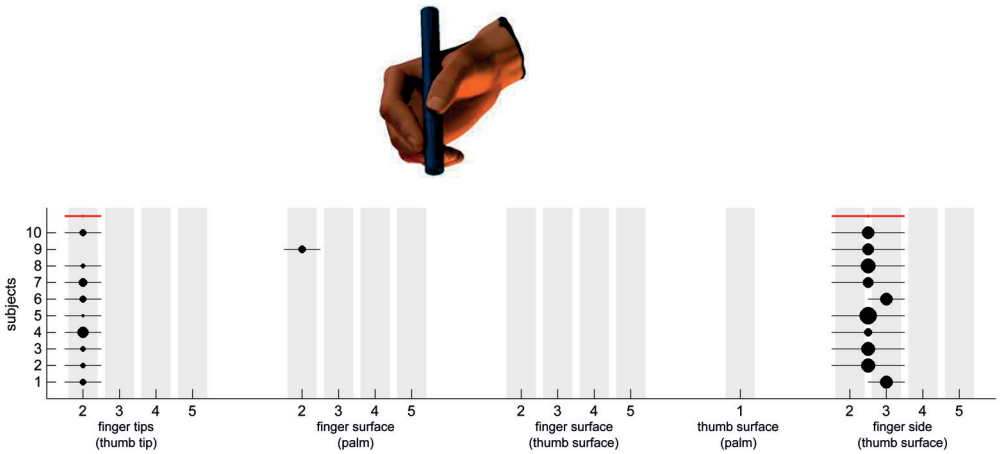


**Figure 3.26:** Scenario 6

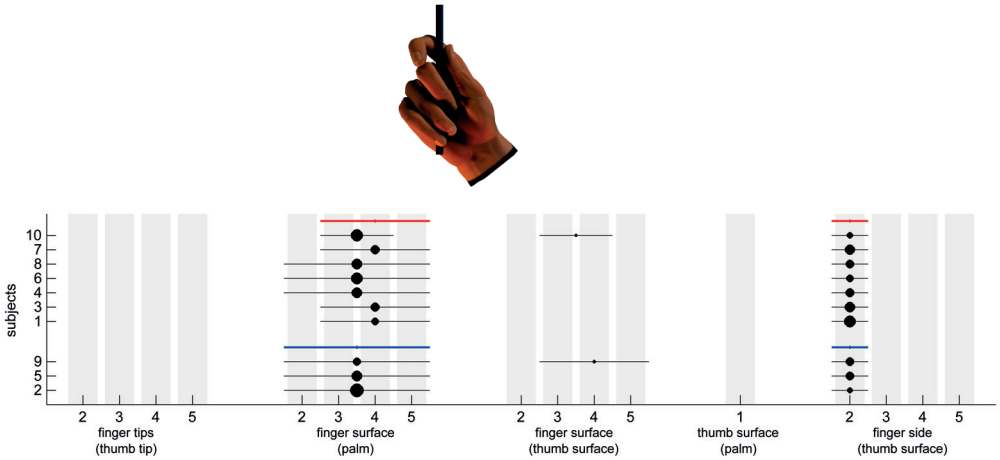


**Figure 3.27:** Scenario 7

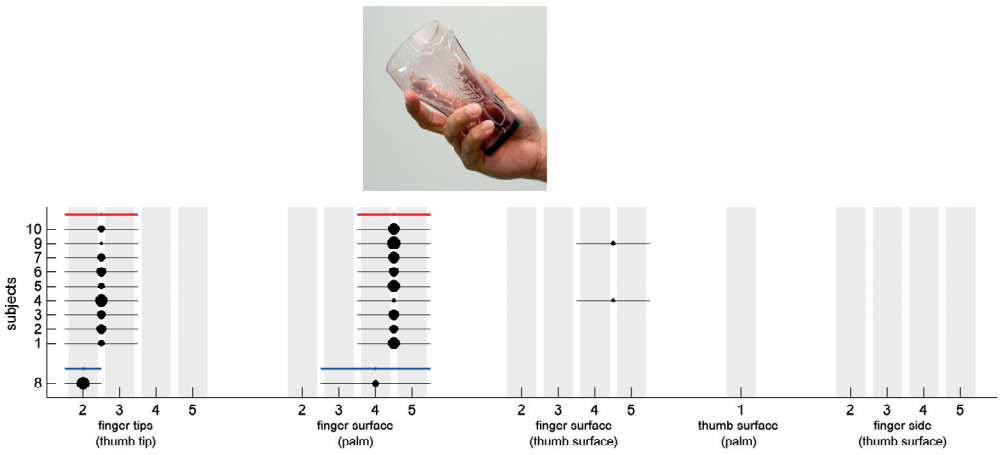


**Figure 3.28:** Scenario 8

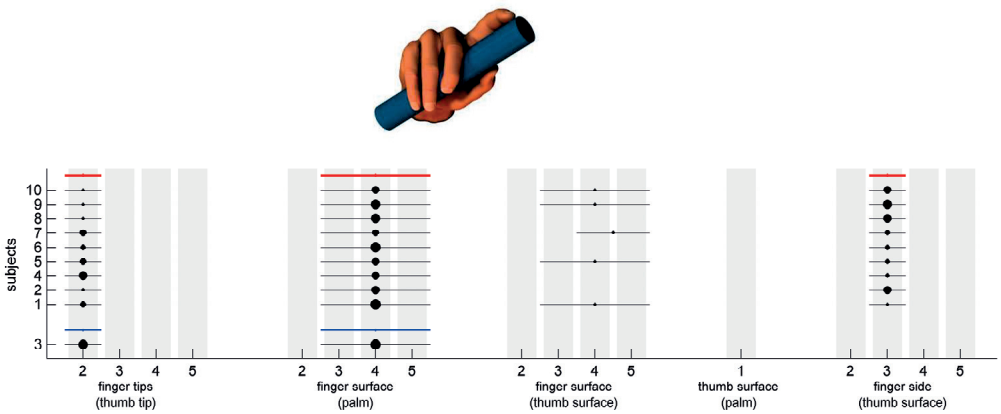


**Figure 3.29:** Scenario 9

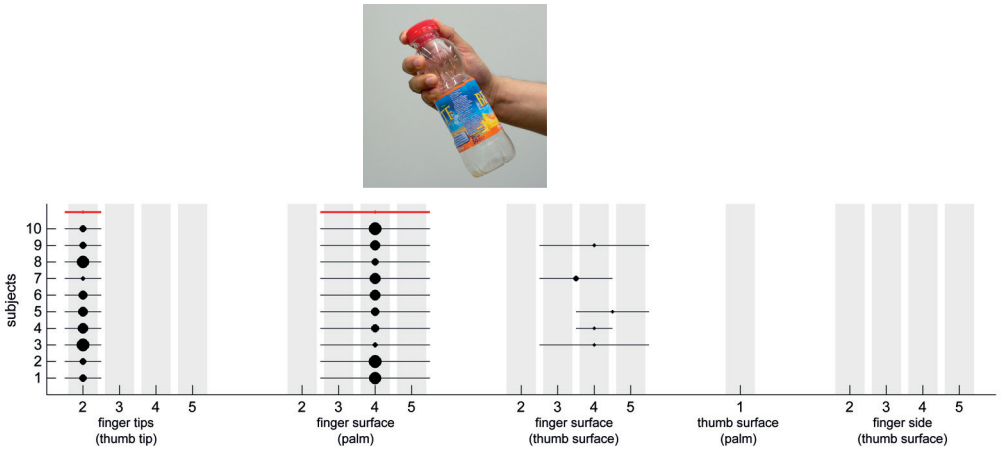


**Figure 3.30:** Scenario 10

## 3.8 Discussion: limitations, applications and future directions

The present work is limited to static grasping whereas hand-parts become more actively engaged and the importance of grasp components becomes relevant only when actually performing a task. The techniques as presented in this chapter would need to be modified and improved for correct and stable detection of grasp signature given the different variations introduced in configuration and tactile data when actually performing a task. Also, we rely only on opposition between two hand-parts. Consequently, we are not able to recognize non-prehensile grasps, such as the hook or flat-palm grasps, which work against gravity. Similarly, with prehensile grasps, components where hand-parts work solely against task forces cannot be recognized. Examples of these would be finger extension for applying cutting force, pressing a button or resting the side of the palm against a surface during writing.

Despite these limitations, the present work has important application in communicating task relevant meaning of a grasp. Let us revisit again the problem posed in the introduction where we have selected a taxonomy category for performing a given task. A demonstration of the grasp now emphasizes the important grasp components that are cooperating. Using the methods described, this can be recognized for a wide range of grasps in the space of human prehensile ability. The grasp signature becomes input to an Opposition Space controller which does not focus on achieving similar configuration nor contacts but recreates the relevant oppositions in order of the importance that was demonstrated. In response to perturbations or task demands, the controller can apply pressure purposefully by emphasizing the oppositions that comprise the grasp. When adapting the grasp to an object with different properties, the problem lies with positioning oppositions appropriately. A grasp controller focuses on finding configuration and contacts to serve this high level intention.

To map the grasp to a robot hand, a correspondence problem must be solved. This can be tackled at the level of Opposition Space. We must first define opposition primitives for the robot hand under consideration and then establish a mapping between the human and robot primitive sets. This mapping may impose additional constraints on virtual finger formation for the human which can be used to further streamline the primitive set developed in Section 3.5.3. Thus grasp signatures can be discovered in terms of the robot hand under consideration.

We proposed a new way to look at raw information from a grasp demonstration (configuration, tactile) by combining them into an intermediate patch-level opposition (PLO) representation. This representation highlights different roles of a single sensor patch in the grasp which otherwise get overlapped when raw information for patch is considered alone. It was shown to be useful when iden-

tifying the most likely primitives present in the grasp. Seen objectively, the PLO is a 144 dimensional feature. In future, data-driven models could be used to capture PLO correlation with other components of a task scenario namely, object properties, force/torque and motion, leading to automatic generation of grasp signature in response to task requirements.

Recognizing grasp signature over an entire task duration is also a direction for future work. From a demonstration perspective, the signatures detected may be used as a means to segment task sequences based on the grasp employed. Also, a set of grasp signatures detected over several trials and subjects can be used as basis for grasp adaptation. From a control viewpoint, real-time characterization of the hand-object interaction in terms of grasp signature can provide the appropriate control inputs for task relevant properties of a grasp to be maintained and adapted over the task duration.

## 3.9 Conclusions

In a grasp demonstration, individual grasping surfaces of the hand are employed so as to leverage their particular functional qualities in order to provide overall grasp function in terms of generating and controlling forces, torques and motion. In this chapter we characterized grasp behaviour using the concepts of Opposition Space, where virtual fingers in opposition form a set of opposition primitives. These concepts were expressed in a manner suitable for a demonstration framework. Extensions were proposed to cover the additional oppositional roles assumed by the thumb frequently encountered in everyday grasps. A general method was proposed by which the specific combination of primitives present in a grasp demonstration could be identified. Using a single expert demonstrator, scenarios testing the same grasp expressed on different objects, and different grasps on the same object were recognized successfully. A recognition rate of 87% was achieved with multiple naive demonstrators over a wide range of categories taken from a grasp taxonomy.

This chapter discovered primitives present in a demonstrated grasp. It raises the question whether a grasp can be formed from components based on capabilities assessed against task requirements. For opposition primitives we can estimate these capabilities and express them in a hand-centric virtual frame. Positioning this frame in an object has a three-fold effect, it constrains : the hand configuration, the wrist-pose exposed to the arm and the extent to which task demands on the hand will be satisfied. In the next chapter we leverage these abilities in an holistic approach to task-oriented configuration of the hand and the arm.

Chapter 4

# Opposition primitives for task-oriented hand-arm configuration

## 4.1 Foreword

Flexibility for grasp formation available to anthropomorphic hands can be represented in terms of opposition primitives. Previous chapters have used opposition primitives to interpret human grasps that have already been formed. In this chapter we consider using primitives to aid in the formation of grasps. We tackle task-oriented configuration of hand-arm systems for tasks where the arm generates force and motion in well known directions but is constrained by the ways stable grasps can be found. Here, a strategy of choosing the strongest grasp that is reachable by the arm does not always result in optimal arm configurations. Instead, we advocate a component based approach to grasp formation by which the larger context of arm action is considered before the whole hand is committed to the grasp. For this, we establish a 'functionally aware' wrist-pose space, using the different oppositional intentions possible for the hand, to serve as the link between the hand and the arm. We take advantage of the fact that configuration and contact proceed from oppositional intention, to position the hand with respect to the object and quantify robustness in the task directions before the grasp is formed. We also exploit the ability of weaker components, which impose fewer constraints on the hand, to explore a wider region of the object-relative wrist-pose space as compared with stronger enveloping formations. The final hand-arm configuration is optimized over the identified wrist-pose space by trading-off robustness in the grasp with ability of the arm to perform the task. We evaluate our approach using 4 commonly encountered tasks, namely: cutting, hammering, screw-driving and opening a bottle cap. We compare our approach with traditional ways of generating configuration for arms connected with dexterous hands.

## 4.2 Introduction

Robots designed for interaction with real world environments are being increasingly endowed with anthropomorphic hand-arm systems (Asfour et al., 2006; Borst et al., 2007; Kaneko et al., 2008). With these, they are expected to grasp and manipulate objects and tools in a variety of task settings. Due to the complexity involved with reasoning in a high dimensional space, common

approaches deal with the configuration of hand and arm as separate problems. Hand configuration is found using an enveloping strategy where the objective is to maximize overall robustness. The commonly used force-closure metrics (Ferrari and Canny, 1992) discover grasps which counter external perturbation from all directions through minimum force applied through the object contacts. When presented with a task scenario, arm configuration is decided by choosing the best grasp (from a force closure sense) that is reachable by the arm.

Considering overall grasp robustness in this way is appropriate when there is no notion of the task to be performed in the environment. This constraint can be relaxed when the directions in which perturbations are expected to occur during the task are known beforehand (Li and Sastry, 1988; Li et al., 2007; El-Khoury et al., 2015). Grasp that are specialized for robustness in the task directions become suitable.

When the arm takes a dominant role in the delivery of task requirements, the hand, acting as the interface between arm and tool, must be able to transmit force and motion generated by the arm to where it is required. Tasks such as opening a tight bottle cap, or tasks involving tool use, such as cutting, hammering or screw-driving, are cited as examples. For these tasks, the hand and arm cannot be viewed as isolated systems. The hand configuration adopted will constrain wrist-pose and thereby the possible arm configurations. A strategy that blindly chooses the best force-closure grasp available is liable to constrain the arm to configurations that are not optimal for generating required force and motion to achieve task goals.

Under these conditions, opposition primitives offer two advantages. Firstly, they offer a principled way to expose a variety of sub-grasps that specialize the hand for robustness in different task directions, and whose task relevance can be quantified before the grasp is completed. Secondly, a larger wrist-pose space can be discovered than if we are limited to the strongest force-closure grasps. Our objective in this chapter is to leverage these properties to trade-off overall stability in the grasp with the ability of the arm to deliver force and motion required for achieving task goals.

The remainder of the chapter is organized as follows. In Section 4.3 we review the literature for generating stable grasps with and without a task context as well as approaches for task-oriented configuration of the hand-arm system together. Section 4.4 formalizes the oppositional intention encoded in a primitive definition and uses this to generate an object relative wrist-pose space. Sections 4.5 and 4.6 show how the wrist-pose space identified can be used to reason functionally about task performance of hand-arm configuration. Section 4.5 establishes a task model based on essential directions in which force and motion are required to accomplish external task goals. A common language to combine and rank the task performance of the hand and the arm is presented assuming that directional quality for force and motion generation can be quantified. In Section 4.6, methods to quantify directional quality for the hand and

arm are presented combining several advances in the literature. Section 4.7 evaluates the proposed framework for the human hand-arm model in the context of cutting, hammering, screw-driving and opening a bottle-cap tasks. Section 4.8 shows how the proposed framework can be applied to robotic systems that are similar but not identical to the human hand-arm system. Section 4.9 presents the conclusions of the chapter.

## 4.3 Literature Review

We review approaches that have been adopted in the literature to tackle the problems of stable grasp generation with dexterous hands, generating grasps that are suitable for the task and finding task oriented hand-arm configurations.

### 4.3.1 Stable grasp generation

Grasp generation with multi-fingered hands has been studied for several decades and several attempts to summarize the various techniques developed exist in the literature. Analytical formulations of the grasping problem are reviewed in Shimoga (1996); Bicchi and Kumar (2000). Sahbani et al. (2011) differentiate between the analytical and empirical approaches which leverage learning from data. Bohg et al. (2013) discuss the latter in detail separating the cases where the object is known, unknown or partially known. Here we look at grasp generation from the perspective of how the different flexibility available to the hand is employed.

Using physical and contact models (Prattichizzo and Trinkle, 2008), contact-level approaches for grasp generation attempt to find an optimal set of contact locations on an object so that force applied at the contacts ensures robustness to any external perturbation (Ding et al., 2001; Zhu and Wang, 2003). Variations on this sacrifice some robustness in the interests of improving run-time performance (Borst et al., 1999; El-Khoury and Sahbani, 2009) or consider hand constraints (Borst et al., 2003; El-Khoury et al., 2013; Saut and Sidobre, 2012; Hang et al., 2014b) or uncertainties in object pose or robot control (Roa and Suárez, 2009; Krug et al., 2010). Nevertheless, these approaches are only validated for a few contacts (such as seen in finger-tip grasps) as computation becomes increasingly complex with more contacts.

For situations in which large forces have to be resisted, more contacts become a necessity. A common strategy relies on enveloping or caging type grasps to maximize the use of hand surface area. Here contacts are discovered after the grasp is made. The problem is finding an approach vector which is likely to result in a stable grasp after hand-closure is completed. The 6D object relative hand-pose space can be systematically sampled for approach vectors (Pelossof et al., 2004). However, a large number of these may not result in stable grasps. The commonly used approach to avoid this, is to exploit structural cues in the object geometry to find suitable approach directions. For this, Roa et al. (2012)

examines local curvature to find suitable locations for opposing types grasps. Michel et al. (2004) formulates a convex optimization problem using opposing facets of the object to find a set of natural grasping axes suitable for planning enveloping grasps. Another approach uses a union of inscribed balls to find the medial axis transform. This forms an object skeleton with information that can be used to design heuristics for planning approach directions (Przybylski et al., 2011). Shape approximation follows the same idea but instead of extracting structural properties, the object is approximated with shapes whose geometrical properties are known and hence approach directions can be planned. For this, a variety of shapes are employed such as bounding boxes (Huebner and Kragic, 2008), cones, cylinder, spheres (Miller et al., 2003), superquadrics (Goldfeder et al., 2007) and so on.

Focus on enveloping or caging grasps tends to ignore the variety of prehensile postures available to anthropomorphic hands. Consequently a wide range of hand-functionality remains unexplored and not brought to bear against task requirements. Ways of incorporating human grasping principles into grasp generation have been investigated in the literature. Joint synergies underlying human grasps of common daily use objects have been extracted (Santello et al., 1998). These now form low-dimensional subspaces over which human-like grasps can be discovered (Ciocarlie and Allen, 2009). However, approaches based on general synergies cannot find particular hand configurations and hand surface contacts needed for the functional requirements of a task, for example the tripod grasp for using a pen. In this case Ben Amor et al. (2012); Bernardino et al. (2013) learn specialized synergy spaces. The approach is applied only for precision grasp types. Grasp pre-shapes, taken from taxonomies, are a convenient way by which the particular functional qualities associated with different human grasp behaviour can be leveraged. Several works, follow the so-called knowledge-based approach to grasp planning. They use an intuitive understanding of the grasp capability of a taxonomy category, to develop heuristics for matching grasp pre-shape with object geometry (Harada et al., 2008) and also for accomplishing a given task (Cutkosky, 1989; Stansfield, 1991; Bekey et al., 1993; Morales et al., 2006). In Prats et al. (2010), rule-based planning with pre-shapes is combined with task specification formalism for robotic manipulators, to automatically specify and control physical interaction tasks in household environments.

In this chapter we adopt the latter approach for task-oriented grasp planning which starts from a knowledge of the ways the hand can be used and different functionality that can be engaged. Then ways to apply the hand to an object in task context are sought. Opposition primitives form the bridge between grasp formation, hand function and task requirements. Hand function is explored in a principled way at the planning stage. This differs from object centric methods where approach directions are sampled first and the hand is essentially used as a gripper which uniformly closes fingers till object contact. In these approaches no notion of hand function is entertained till the hand is closed. However, by

then it becomes too late to engage different functionalities possible. We differ also from other knowledge based approaches since we do not employ rule-based methods and heuristics to decide the grasp. Instead, information encoded in the oppositional intention is used to position the hand in the object, quantify its directional capabilities and match them to the task requirements.

### 4.3.2 Task-oriented grasp generation

Task-oriented grasp selection is almost always done in post-grasp manner. The focus is on finding a quality measure whereby a generated grasp can be assessed against task requirements.

In most cases one prefers to find grasps that display overall robustness to external perturbation (Morales et al., 2006; Ciocarlie and Allen, 2009; Goldfeder et al., 2007; Huebner and Kragic, 2008; Roa et al., 2012; Przybylski et al., 2011). The $\epsilon$-ball measure (Ferrari and Canny, 1992) is commonly used. This quantifies the direction in which the grasp is weakest by finding the radius of the largest 6D ball that can be inscribed inside the Grasp Wrench Space (GWS). Pollard (1994) suggests that the Object Wrench Space (OWS) is more physically relevant. Unlike the GWS, this only allows object torques generated by forces acting on the object surface. However, estimating the OWS is more difficult. Borst et al. (2004) presents method to approximate the OWS with an ellipsoid and compute a robustness measure.

In several cases, directions along which disturbances are expected during task execution are known. Borst et al. (1999, 2005) propose methods to compute distance to the GWS boundary. These distances give a measure of robustness for a particular task direction. Measures for different task directions are linearly combined according to task-relevance. Haschke et al. (2005); Li et al. (2007) find maximum applicable wrench for different task-directions given a set of contacts. Whereas in Haschke et al. (2005) these measures are linearly combined, in Li et al. (2007), the task-direction where the grasp is weakest is used to determine grasp quality. Li and Sastry (1988) construct a task-ellipsoid taking the known task directions as the principal axes. Grasp quality is measured as the largest task ellipsoid which can fit in the GWS.

Task relevant directions are manually defined in the works mentioned above by examining object-world interaction. These directions can also be discovered automatically through human demonstration of the task. El-Khoury et al. (2015) use a tool instrumented with a 6-axis force-torque sensor to automatically generate task ellipsoids for tasks such as cutting and screw-driving. Aleotti and Caselli (2010) use different grasps demonstrated for the same task to build a union of grasp wrench spaces known as the functional wrench space (FWS). A task oriented measure is obtained by comparing the GWS of candidate grasps to the FWS for the task.

In this chapter we assume that tools are grasped by their handles (Sahbani

and El-Khoury, 2009). The directions for which force and motion are required (at the tool end-effector e.g. cutting-edge, hammer-head) to accomplish the task are known and therefore directions along which perturbations are expected on the handle during task execution may be inferred. Following existing approaches, distance to the grasp wrench space boundary is used as the means to quantify task-oriented ability of a grasp hypothesis. But we make use of oppositional information to improve accuracy of the grasp wrench space approximation. Firstly, oppositional intention is used to inform hand-closure and identify hand surfaces likely to impact the object. Then contacts are differentiated on the ability to exert normal pressure through them using a mix of criteria that involves kinetostatic analysis, oppositional intention and hand-object geometry. These factors influence the shape of the grasp wrench space and the quality measures derived from it.

### 4.3.3 Combining hand configuration with arm configuration

In the large body of work dealing with robotic arm configuration considers the tool as rigidly fixed to the arm. All DOF for force and motion at the end-effector are the same from a grasp perspective. This assumption is no longer valid when the arm is connected to a dexterous hand. The problem of stable grasping must also be addressed.

With real world systems, such as ARMAR-III, Justin, HRP3 and DLR hand-arm, the common approach taken is to first pre-compute an object relative grasp hypothesis cloud (using the methods described in Section 4.3.1). At run-time an inverse kinematic (IK) problem is solved for each grasp hypothesis to find the most stable grasp reachable by the arm. IK computation is expensive. Thus, research has focussed on methods to optimize the search for reachable grasps. Berenson et al. (2007) combines grasp quality with features of the local environment and robot kinematics to develop rapidly computable reachability scoring functions that can rank grasps without performing expensive IK. Arm trajectories are found for the most promising of these. The work is extended in Berenson and Srinivasa (2008) where the arm is directed to regions of an object relative pose space. This is more suitable for cluttered environments where a single precomputed pose is unreachable but its neighbours are. Alternatively, as described in Vahrenkamp et al. (2012), IK computation can be performed in an offline manner to obtain reachability maps over a discretized workspace of the arm. Expensive IK computation still has to be performed for a given wrist-pose at run-time, but only if it has a high likelihood of being reachable. The authors show that this can have an order of magnitude improvement in speed of finding a valid hand-arm configuration. Vahrenkamp et al. (2010) integrates grasp generation with RRT-based motion planning techniques used to find an

arm trajectory to the object. This obviates the need for inverse kinematic computation since feasible grasps are found during the motion planing process.

The methods discussed above are suitable for pick and place kinds of tasks. However, when the task requires directed force and motion in a few specialized directions to accomplish task goals, such as in cutting, hammering, there is no guarantee that the arm configuration selected will be well suited for this purpose. Consequently, task execution may be either impossible or inefficient. In Vahrenkamp and Asfour (2015) a measure of manipulability was also stored in the precomputed reachability maps. Grasp selection now returns hand configurations for which the arm has most manoeuvrability. This is a desired general attribute to have for operation in a real-world environment.

In this chapter we optimize arm configuration with a specific task in mind. The ability of the arm to transmit force and motion in task relevant directions is quantified. This gives us a measure of how well the task can be performed. The ability of the arm to perform the task is traded off against robustness in the grasp to arrive at a suitable hand-arm configuration.

## 4.4 Primitives as bridge between hand-function and arm-function

The interface between the hand and the arm lies at the wrist. Each primitive encodes an oppositional intention, which when positioned in the object also constrains the wrist-pose. Since primitives by their definition are specialized for robustness in certain directions, they bring different hand capabilities to the grasp. We use primitives as the bridge between the hand and the arm so that a variety of wrist-poses can be exposed which also span a large space of hand functionality. In this way, hand function is incorporated at the grasp planning stage. The following subsections will identify a primitive basis for grasp construction and discuss the generation of a functionally relevant wrist-pose space.

### 4.4.1 Basis for grasp construction

In Chapter 3 we identified 5 categories of oppositions possible for the anthropomorphic hand. These are listed below and shown in Figure 4.1.

$O^{TT}_{FT}$ thumb-tip against finger-tips
$O^{P}_{FS}$ finger-surfaces against palm
$O^{TS}_{FS}$ thumb-surface against finger-surface
$O^{TS}_{P}$ thumb-surface against palm
$O^{TS}_{S}$ thumb-surface against finger-sides

Primitives are chosen from these categories to form a basis for grasp construction. In Figure 4.3 13 primitives are identified for the human hand. Later on (Section 4.8), a primitive basis is defined in the context of a robot hand.

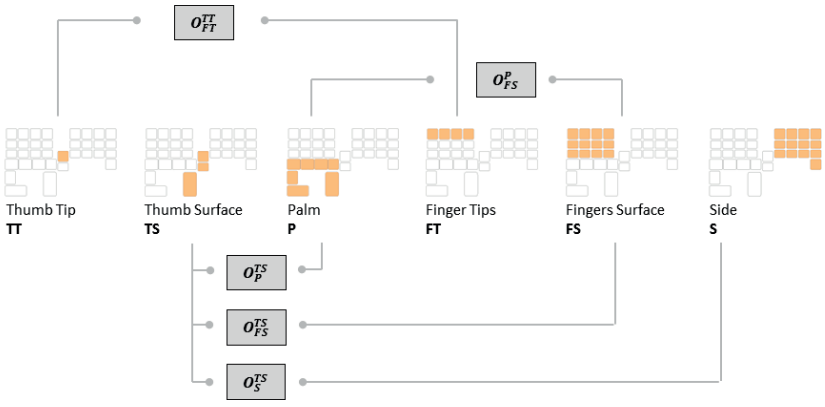


**Figure 4.1:** Opposition categories possible for the anthropomorphic hand.

Each primitive encodes an oppositional intention which derives from the particular manner in which hand-parts are used against each other. This intention can be formalized by a pre-shape ($\phi_{pre}$), two virtual fingers ($VF_1$, $VF_2$), an opposition vector ($\overrightarrow{o}$) and the primitive reference frame ($PRF$). These concepts are defined below. Figure 4.2 provides an illustration.

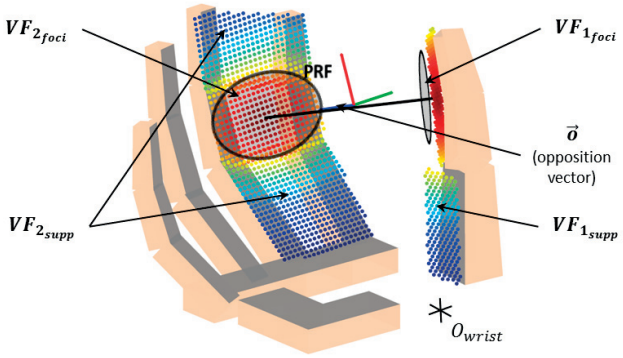


**Figure 4.2:** Encoding the oppositional intention of a primitive.

| | |
|---|---|
| $O_{FT}^{TT}$ | 1. $O_{FT2}^{TT}$ 2. $O_{FT23}^{TT}$ 3. $O_{FT234}^{TT}$ |
| $O_{FS}^{P}$ | 4. $O_{FS23}^{P}$ 5. $O_{FS234}^{P}$ 6. $O_{FS345}^{P}$ |
| $O_{FS}^{TS}$ | 7. $O_{FS23}^{TS}$ 8. $O_{FS234}^{TS}$ 9. $O_{FS345}^{TS}$ |
| $O_{P}^{TS}$ | 10. $O_{P}^{TS}$ |
| $O_{S}^{TS}$ | 11. $O_{S23}^{TS}$ 12. $O_{S234}^{TS}$ 13. $O_{S345}^{TS}$ |

**Figure 4.3:** Primitive basis for the human hand. For each primitive, grasping patches of $VF_1$ are highlighted in red while grasping patches of $VF_2$ are highlighted in blue. Focus regions are coloured black and Supporting regions are coloured white.

For any anthropomorphic hand we may define a coordinate frame centered at the wrist $O_{wrist}$. We may also define a decomposition of the grasping surface of the hand into elementary grasping patches $\mathcal{GP}$.

**pre-shape ($\phi_{pre}$)** is a vector of joint angles corresponding to the initial configuration of the hand from which the opposing hand-parts are drawn together to manifest the oppositional intention.

**virtual fingers ($VF_1,\ VF_2$)** identify the opposing hand-parts in terms of elementary grasping patches ($\mathcal{GP}$). Each virtual finger is expressed as a tuple of two sets $foci, supp \in \mathcal{GP}$. The patches $foci$ denote the places where oppositional pressure is intended to be focused. The patches $supp$ act in a supporting fashion.

$$VF = \Big\{ foci, supp \Big\} \ \mid \ foci, supp \in \mathcal{GP} \quad foci \cap supp = \varnothing$$

**opposition vector ($\overrightarrow{o}$)** is the unit vector along the line determined by joining the centroid of patches $VF1_{foci}$ to the centroid of patches $VF2_{foci}$.

**primitive reference frame (PRF)** is a coordinate frame defined with respect to $O_{wrist}$. The purpose of PRF is to localize the oppositional intention in a hand-centric manner. It forms a handle by which the intention can be applied to an object. The PRF is centered at the mid-point between $VF1_{foci}$ and $VF2_{foci}$. The opposition vector ($\overrightarrow{o}$) is taken as the z-axis and a right-handed system is built around this. $T^{wrist}_{PRF}$ denotes the transform for this coordinate system with respect $O_{wrist}$.

### 4.4.2 Functionally relevant wrist-pose space

Considering that a primitive basis also spans different functional ability, positioning the oppositional intention can be used as a principled way to explore the object relative wrist-pose space while exposing to the arm, grasps that are specialized for robustness in different directions.

#### Planing primitive-based grasps

A grasp hypothesis identifies an object relative wrist-pose and a preshape configuration for the finger-joints from where the fingers can close onto the object. For an opposition primitive this implies matching the primitive's grasping surface to the object grasping affordance. Suitable orientations for the opposition vector may be found by examining the structural properties of the object, for directions where the object will allow oppositional pressure to be exerted by a given primitive. Structures like natural grasping axis (Michel et al., 2004), medial axis transform (Przybylski et al., 2011), shape primitives (Miller et al., 2003), can all be applied for this purpose.

In this chapter we make the assumption that a tool is grasped by its handle. The handle itself is modelled as a cylinder. A coordinate frame, known as the Grasp Reference Frame (or GRF), is positioned in the handle to denote the graspable region. This is the region that will be subject to oppositional pressure by the hand. The surfaces of a cylinder afford the application of oppositional pressure in a direction perpendicular to the principal axis (see Figure 4.4a). We sample a set of 12 orientations (increments of 30°) for the opposition vector in the plane perpendicular to the principal axis and passing through the GRF origin. Additionally, for each orientation, 12 rotations of the hand are sampled using the opposition vector as the rotation axis. We thus have a total of 144 transformations of a primitive with respect to the grasp reference frame ($T_{PRF}^{GRF}$). Let this set be denoted by $\mathcal{T}$.

Given a primitive basis $\mathcal{P}$, all combinations of $\mathcal{T} \times \mathcal{P}$ generate a wrist-pose space.

$$\mathcal{W} = \left\{ T_{wrist}^{GRF} = T_{PRF}^{GRF} (T_{PRF}^{wrist})^{-1} \right\}_{\mathcal{T} \times \mathcal{P}} \tag{4.1}$$

$$\begin{array}{ll} T_{PRF}^{wrist} & \text{is defined by } p \in \mathcal{P} \text{ (Section 4.4.1)} \\ T_{PRF}^{GRF} & \in \mathcal{T} \end{array}$$

Most approaches in the literature do not regard hand-closure as an important step. When no prior oppositional intention exists, hand-closure is a simple matter of uniformly closing the finger joints until contact with the object is made or joint limits are reached. With an opposition primitive, the objective is to establish oppositional pressure between the foci regions of each virtual finger ($VF1_{foci}$, $VF2_{foci}$). This is crucial to the functionality brought to the grasp (and hence the task relevance). Care must be taken on how these surfaces are brought together. As can be seen in Figure 4.4c for the primitive $O_{FT234}^{TT}$, uniform closure of the finger joints will violate the oppositional intention. The thumb and finger-tips turn inward instead of remaining opposed to each other. Instead, we establish a closed pose for each primitive so that linear interpolation between the preshape and closed poses, establishes oppositional pressure between the foci regions[1] (Figure 4.4a). $T_{PRF}^{wrist}$ (which depends on the wrist-relative pose of the foci regions) is recomputed at each time-step during hand-closure and is used to adapt the object-relative wrist pose $T_{wrist}^{GRF}$ according to (4.1). This ensures that the opposition vector is always oriented in the graspable region as indicated by the grasp hypothesis (Figure 4.4e). The final wrist pose exposed to the arm is denoted by the spherical marker and two perpendicular lines, along the palm and normal to it. Examples for other primitive categories can be found in Figure 4.14.

The full object relative wrist-pose space exposed to the arm using this

[1] This heuristic is sufficient for the purpose of simulation. For the real robot hand, a control strategy to achieve hand closure under oppositional intention is described in Section 4.8.1

method is shown in Figure 4.5. Wrist-poses corresponding to the different primitive categories are highlighted in each sub-figure (a)-(e). We see that each way of generating oppositional pressure by the hand causes a different part of the object relative pose space to be explored. Additionally, by virtue of its oppositional intention, each pose is linked with a grasp which is specialized for robustness in a few DOF and for which explicit instructions exist to control and adapt this functionality over the task duration. These instructions have to do with maintaining the specific oppositional and co-operational constraints among the grasping surfaces of the hand. Later on, when the robustness of the grasp is matched with task requirements, maintaining these constraints is given a task relevance. i.e. preserving oppositional intention also implies better ability to withstand specific task wrenches that will be encountered.

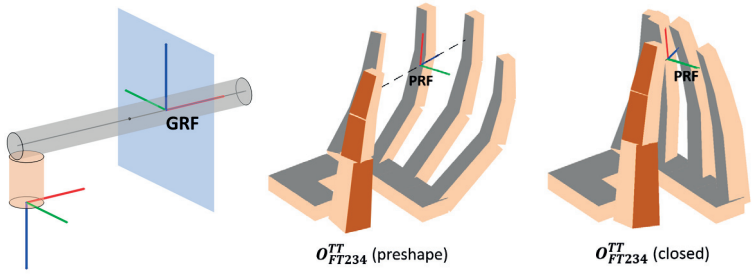


**(a)** Grasp Reference Frame (GRF) and Primitive Reference Frame (PRF)

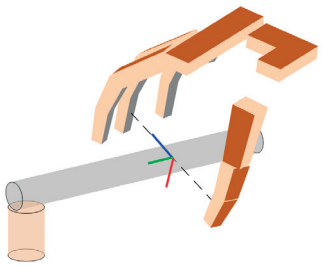

**(b)** PRF positioned with respect to the GRF forms a grasp hypothesis.

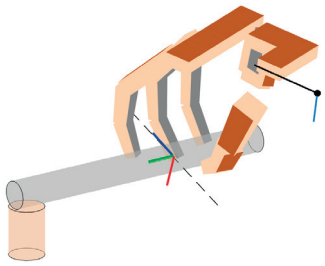

**(c)** Uniform closure of finger joints violates oppositional intention.

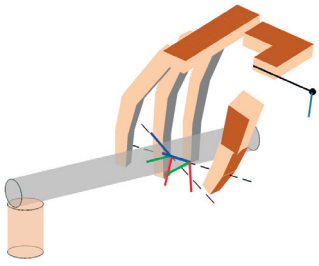

**(d)** Hand closure respecting oppositional intention, but the grasp hypothesis is violated

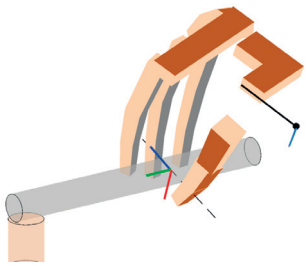

**(e)** Hand closure respecting oppositional intention. Wrist-pose is adapted to maintain grasp hypothesis.

**Figure 4.4:** Generating a wrist pose space using opposition primitives.

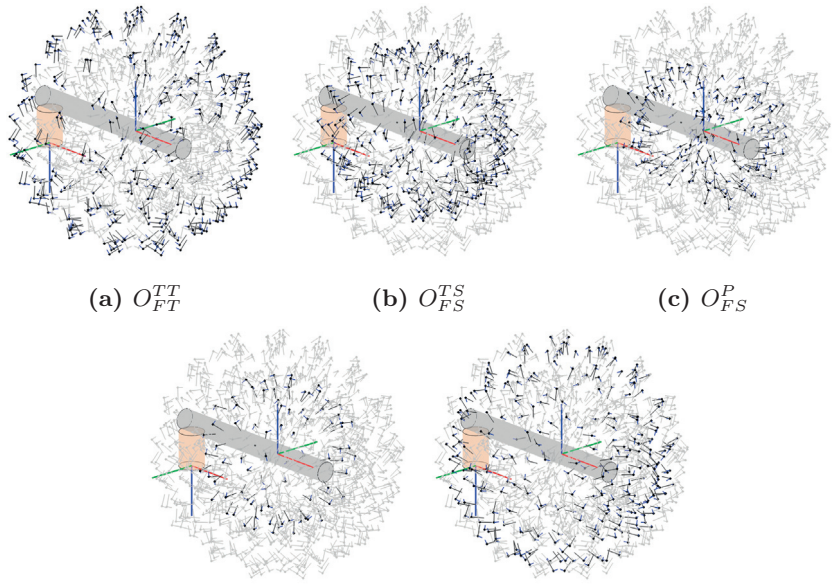

**(a)** $O^{TT}_{FT}$ **(b)** $O^{TS}_{FS}$ **(c)** $O^{P}_{FS}$

**(d)** $O^{TS}_{P}$ **(e)** $O^{TS}_{S}$

**Figure 4.5:** Wrist pose space exposed to the arm by positioning oppositional intention in the graspable region. Each opposition category exposes a different part of the object relative wrist-pose space.

### Planning enveloping grasps

To contrast with a primitive based approach, a common way to plan grasps employs the enveloping strategy. Here the objective is to identify the $k$-strongest grasps of an object. Overall robustness from a force closure perspective is the criterion.

The best envelope of a cylindrically shaped object is found when the surface of the palm is parallel to the principal axis of the cylinder (Figure 4.6a). This heuristic is similar to the one used by Miller et al. (2003), which is incorporated into the GraspIt! simulator and used by several authors to generate stable grasp hypotheses. As shown in Figure 4.6a, an open pre-shape with fingers extended is used. We fix a PRF in the palm and take the outward normal ($\hat{z}_{PRF}$) as the approach direction. To generate a wrist-pose connected with a valid grasp, the hand approaches along a pre-selected direction for $\hat{z}_{PRF}$ till contact with the palm is detected. Hand closure does not follow any oppositional intention but the fingers, followed by thumb, close uniformly till joint limit or contact with object or hand is encountered.

To plan grasp hypotheses, the plane perpendicular to the cylinder axis and passing through the GRF is sampled for possible approach directions. 12 samples are taken (increments of 30°). For each approach direction, 10 rotations between ±30°are sampled for each sense of the palm w.r.t the cylinder (see Figure 4.6a). Figure 4.6b shows the object relative wrist-pose space explored by this method. In contrast to the primitive-based approach it has much less variety. This is due to the fact that only the most stable grasps were sought and

only one way of applying the hand was explored.

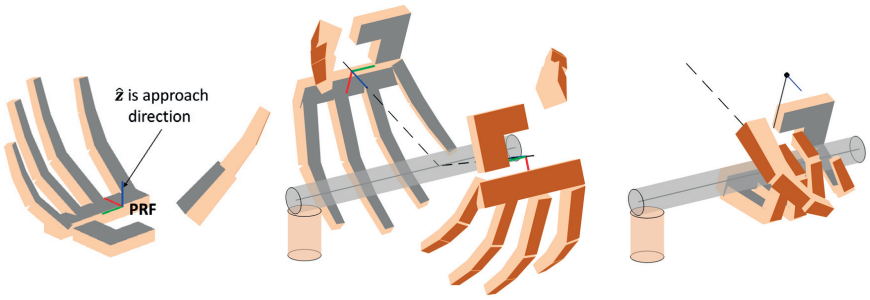


**(a)** Preshape for enveloping grasp. The PRF is fixed in the palm. $+\hat{z}$ is the approach direction. Best envelope of a cylindrical handle is obtained when the cylinder axis is parallel to the palm as shown.

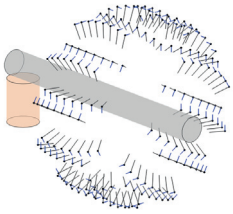

**(b)** Grasp hypotheses for enveloping type grasps.

We have till now used the oppositional intention to expose an object relative wrist pose space and contrasted this with a strategy that prefers the strongest enveloping grasps of an object. We now give task relevance to the identified wrist-poses, from a hand and arm perspective.

## 4.5 Task-Oriented configuration of hand-arm system

In this section we use the wrist-pose space, discovered in the previous section, to identify the $n$-best hand-arm configurations for the task. A task model is first defined which is instantiated in the context of 4 commonly encountered tasks. Then, a method to combine and rank task performance of the hand and the arm is presented.

### 4.5.1 Task Model

Our objective in defining a task model is to arrive at a common description by which the functional abilities of the hand-arm can be compared with the functional requirements of the task. We identify 2 criteria that are needed to identify suitable configurations both from a task perspective and a hand-arm perspective. These are:

1) The directions in which force and motion are relevant for achieving desired external effects in the environment. There are termed task requirements.

2) The relative importance of force and motion directions with respect to each other. These enable to privilege some particular force/motion directions that are most crucial to perform the task.

Additionally, we consider arm requirements separately from hand requirements. For the class of tasks being considered, the arm assumes responsibility for generating the external force and motion, required for achieving task goals, at the tool end-effector . The hand grips the tool handle and is responsible for maintaining a stable grasp. It does not generate any motion. Rather, it should be specialized for resisting force and torque disturbance induced in the handle as a consequence of arm action.

Even though task requirements are different, a common definition scheme can be used to encode task requirements for both hand and arm. Functional dimensions considered are force, torque, linear velocity, angular velocity. Task relevant directions are denoted by $\boldsymbol{f}$, $\boldsymbol{\tau}$, $\boldsymbol{v}$, $\boldsymbol{\omega}$ which are vectors $\mathbb{R}^3$. A task definition $\Lambda$ is defined as follows.

$$\Lambda = [\, \Gamma_{n\times 12},\ \alpha_{n\times 1} \,] \tag{4.2}$$

$n =$ number of task requirements
$\Gamma_i = \left[\boldsymbol{f^T}\ \boldsymbol{\tau^T}\ \boldsymbol{v^T}\ \boldsymbol{\omega^T}\right]$ ; $i^{th}$ task requirement
$\alpha \in \mathbb{R}^n$ ; importance of task requirements
$\sum \alpha_i = 1$

Task directions for the arm are defined with respect to a coordinate frame centered in the tool end-effector. This is termed the end-effector reference frame

or ERF. This is where the force and motion generated by the arm are delivered in the environment. Task directions for the hand are defined with respect to a coordinate frame centered in the tool handle (the GRF). The overall task combines requirements defined separately for hand and for arm as

$$\Lambda = [\Lambda_{hand}\ ,\ \Lambda_{arm}] \tag{4.3}$$

Using this definition, manually constructed task models for the tasks of cutting, hammering, screw-driving and opening a tight bottle cap are described next. These models can also be learned from human demonstration, as was shown in our earlier work (El-Khoury et al., 2015), where we use force/torque ellipsoids to model the task based on information obtained from a sensorized tool over the task duration. However, the earlier work did not consider motion requirements.

Note that, in the following, the terms downward, forward, backward are used to describe force and motion directions with respect to the tool end-effector reference frame. It should be emphasized that the task model is independent of where the task is performed in the environment. For e.g. in Section 4.8.3 we will examine hammering against a wall and against the ceiling.

### Cutting

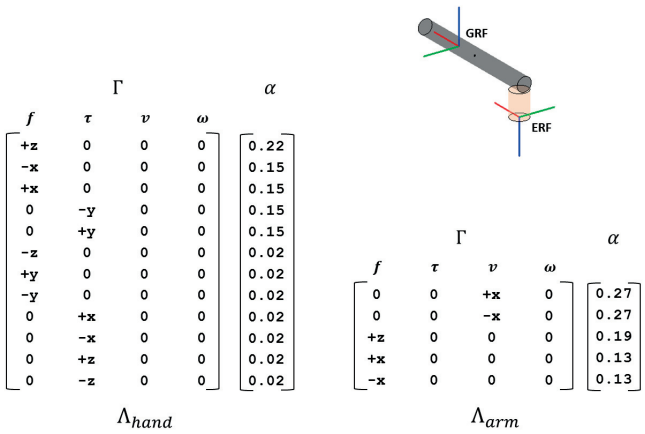


**Figure 4.7:** Task definition for cutting. $x = [1\ 0\ 0]$, $y = [0\ 1\ 0]$, $z = [0\ 0\ 1]$, $0 = [0\ 0\ 0]$

For the task of cutting, the arm needs to generate of force and motion in the forward/backward ($\pm x$) direction. Downward $+z$ cutting force is also required. In this particular definition, motion generation is given more importance than force generation. This would be the case when cutting something soft. Other importance distributions may be applicable depending on what is being cut.

From a hand perspective, cutting action of the arm appears as force and torque disturbances on the grasp reference frame (GRF). To withstand the

downward cutting force and forward/backward motion, the grasp must be particularly robust to force disturbance in $+z$ and $\pm x$ and the torque this induces around $\pm y$. These requirements are given most importance. Additionally, a small degree of importance is added for all other directions to prefer grasps that have larger overall stability.

### Hammering

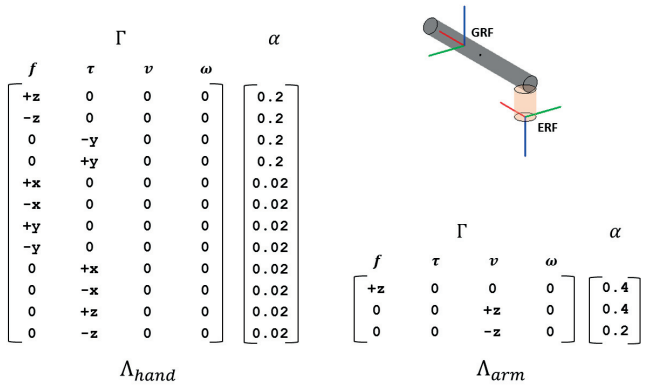


**Figure 4.8:** Task definition for hammering. $x = [1\ 0\ 0]$, $y = [0\ 1\ 0]$, $z = [0\ 0\ 1]$, $0 = [0\ 0\ 0]$

For the arm generation of downward $+z$ force and motion assumes primary importance. Motion in the upward $-z$ direction is also required to reset the tool for a new hammering sequence, but it is of lesser importance.

For the grasp, the action of hammering induces large force disturbances at the GRF in the $\pm z$ directions as well as large torque disturbances around $\pm y$. It is important that the grasp be particularly robust against these disturbances. Additionally, small degree of importance is added for all other directions to prefer grasps that have larger overall stability.

### Screw-driving

For screw-driving, arm requirements may be characterized by the generation of downward force $\pm z$ and driving torque and motion around the $z$ axis.

For the grasp these appear at the GRF as force disturbance in $+x$ and torque disturbance around $\pm x$. This is given most importance. As in the other tasks, a small degree of importance is added for all other directions to prefer grasps that have larger overall stability.

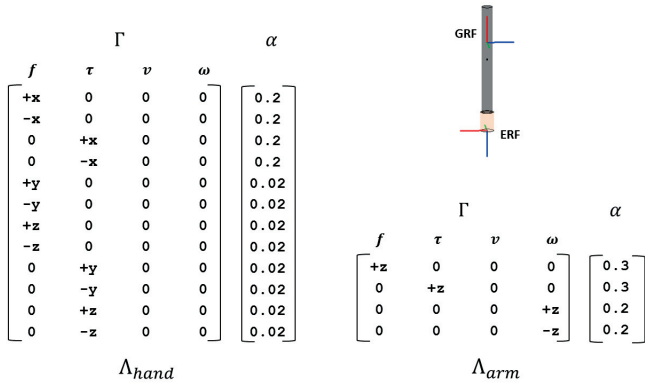


**Figure 4.9:** Task definition for screw-driving. $x$ = [1 0 0], $y$ = [0 1 0], $z$ = [0 0 1], 0 = [0 0 0]

### Opening a tight bottle cap

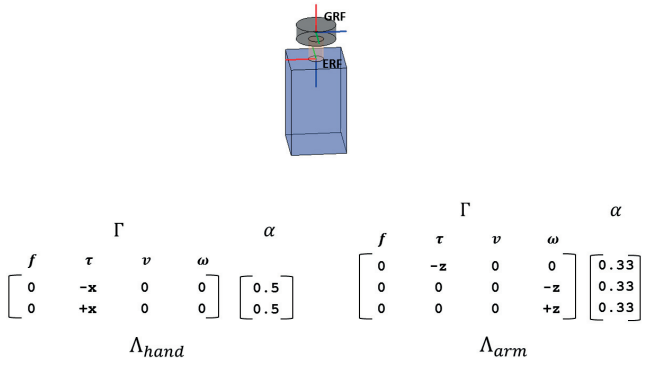


**Figure 4.10:** Task definition for opening a tight bottle cap. $x$ = [1 0 0], $y$ = [0 1 0], $z$ = [0 0 1], 0 = [0 0 0]

Arm requirements are focused on the generation of twisting torque around $-z$ and angular motion around $\pm z$. These are given most importance in the task definition.

For the grasp, unscrewing of the cap appears as a strong torque disturbance around $\pm x$. The grasp must be particularly robust against this. The bottle itself is assumed to be rigidly fixed hence we do not add any other stability requirements.

## 4.5.2 Task Suitability metric

A metric of task suitability assesses an object-hand-arm configuration for its suitability towards task requirements. Notwithstanding the vast hand-arm configuration space, a relatively small number of configurations are exposed due to the application of oppositional intention. We are therefore interested in a relative measure which is able to rank task suitability of a small subset of hand-arm configurations. The method described below is based on the idea of linear

combination of directional qualities for known task directions (Chiu, 1988; Borst et al., 2005; Haschke et al., 2005).

Consider that we have metrics $Q_{hand}(\Gamma, \theta_h)$ and $Q_{arm}(\Gamma, \theta_a)$, for the hand and the arm respectively, that return a scalar measure of quality given a task requirement $\Gamma$. $\theta_h$ represents parameters describing the hand-object relationship and $\theta_a$ represents parameters describing the arm configuration. For a known configuration $\theta_h/\theta_a$ and a set of task requirements $\Lambda_{hand/arm}$, a task-oriented quality measure may be defined which linearly combines quality the configuration for each task requirement, using the measure $Q_{hand/arm}$ and relative importance $\alpha$.

$$Q_{\Lambda_{hand/arm}} = \sum_{i=1}^{n} \alpha_i Q_{hand/arm}(\Gamma_i) \tag{4.4}$$

For an object-hand-arm configuration $\{\theta_h, \theta_a\}$, and task description $\Lambda$, $Q_{\Lambda_{hand}}$ and $Q_{\Lambda_{arm}}$ are evaluated separately and then combined to obtain a single task-oriented quality measure as follows.

$$Q_{\Lambda} = \lambda_1 Q_{\Lambda_{hand}} + \lambda_2 Q_{\Lambda_{arm}} \tag{4.5}$$

The choice of $\lambda_1$ and $\lambda_2$ trades off the importance of the arm v/s the hand in doing the task. By favouring $\lambda_2$ we can allow for a less efficient hand configuration to be chosen if the ability of the arm to do the task is improved by this.

Some form of normalization is required so that the measures $Q_{hand/arm}(\Gamma)$ can be combined. This is because functional dimensions $\boldsymbol{f}$, $\boldsymbol{\tau}$, $\boldsymbol{v}$, $\boldsymbol{\omega}$ have different units and methods for $Q_{hand/arm}(\Gamma)$ return values that are incompatible in scale. Normalization factors are found separately for each functional dimension and consist of the maximum $Q$ value encountered. The normalization factors are computed once using the range of hand-arm configurations sampled in the context of one task. Thus task-oriented quality as measured by (4.5) cannot be seen as in absolute terms but offers a means to rank a set of hand-arm configurations for a task.

### 4.5.3 Algorithm

Computing the $n$ most suitable hand-arm configurations is performed in two phases. The first phases is done only once and computes a wrist-pose space for a given primitive basis and object/tool. Each wrist-pose is associated with a grasp hypothesis and task-related functionality measure. The second phase is done each time a task is to be performed. The tool is positioned in the world according to where the task is to be performed. This also transforms the wrist-pose space. Arm configuration is optimized over the wrist-pose space to find the $n$ best hand-arm configurations. The algorithm is described below. Figure 4.11 provides an illustration.

PHASE 1: COMPUTING A WRIST-POSE SPACE

**input** primitive basis $\mathcal{P}$ and an object/tool.

**output** $\mathcal{C}_H = \left[p, T^{GRF}_{PRF}, \mathfrak{f}\right]_1^n$

$p \in \mathcal{P}$ is a primitive, $T^{GRF}_{PRF}$ defines an orientation for the opposition vector and $\mathfrak{f} \in \mathbb{R}^{12}$ records quality of the grasp hypothesis $\left\{p, T^{GRF}_{PRF}\right\}$ for force and torque generation along each axis-aligned direction $\{\pm x, \pm y, \pm z\}$.

The algorithm has the following steps:

1) Generate a set of orientations $\mathcal{T}$ for the opposition vector, with respect to the GRF, using the method described in Section 4.4.2.
   Perform steps $2-5$ for each grasp hypothesis $\left\{p, T^{GRF}_{PRF}\right\} \in \mathcal{P} \times \mathcal{T}$

2) Position wrist, using (4.1) to find $T^{GRF}_{wrist}$. Perform collision detection and discard hypothesis if hand intersects with the object and this is not resolved by opening of the aperture between opposing surfaces.

3) Close aperture preserving oppositional intention (Section 4.4.2) to a distance of 2cm from the object surface. Estimate hand surfaces likely to contact with the object.

4) Compute $Q_{hand}(\Gamma)$ for force and torque along axis aligned directions $\{\pm x, \pm y, \pm z\}$. This yields a grasp functional measure vector $\mathfrak{f} \in \mathbb{R}^{12}$.

5) Augment $\mathcal{C}_H$ with the tuple $\left\{p, T^{GRF}_{PRF}, \mathfrak{f}\right\}$.

PHASE 2: COMPUTING $n$ BEST HAND-ARM CONFIGURATIONS

**input** object/tool with pre-computed $\mathcal{C}_H$, task definition $\Lambda$, where to perform task in the world $T^W_{ERF}$, arm model.

**output** $\mathcal{C}_{H-A} = \left[p, T^{GRF}_{PRF}, \theta_a, Q_{\Lambda_{hand}}, Q_{\Lambda_{arm}}, Q_{\Lambda}\right]_1^n$

$\left\{p, T^{GRF}_{PRF}\right\}$ is a grasp hypothesis. $\theta_a$ is a reachable arm configuration. $Q_{\Lambda_{hand},\Lambda_{arm},\Lambda}$ are task-oriented quality measures.

The algorithm has the following steps:
Perform steps $1-4$ for each $\left\{p, T^{GRF}_{PRF}, \mathfrak{f}\right\} \in \mathcal{C}_H$

1) Obtain wrist-pose in the world : $T^W_{wrist} = T^W_{ERF}\ T^{GRF}_{ERF}\ T^{GRF}_{wrist}$
   $T^W_{ERF}$ is supplied as input, $T^{GRF}_{ERF}$ is known from object geometry and $T^{GRF}_{wrist}$ comes from the grasp hypothesis.

2) Analyze reachability of arm using inverse kinematics. If not reachable, discard hypothesis. Otherwise obtain a valid arm configuration $\theta_a$ which connects the arm to the hand at the wrist.

3) Compute $Q_{\Lambda_{hand}}$, $Q_{\Lambda_{arm}}$ and $Q_{\Lambda}$ using equations (4.4) and (4.5) together with the supplied task definition $\Lambda = [\Lambda_{hand}\ ,\ \Lambda_{arm}]$. Here, pre-recorded task-oriented quality $\mathfrak{f}$ is used for the hand whereas $Q_{arm}(\Gamma)$ (for each $\Gamma_i \in \Lambda_{arm}$) needs to be computed for the current $\theta_a$.

4) Augment $\mathcal{C}_{H-A}$ with the tuple $\left\{p, T^{GRF}_{PRF}, \theta_a, Q_{\Lambda_{hand}}, Q_{\Lambda_{arm}}, Q_{\Lambda}\right\}$.

5) Sort $\mathcal{C}_{H-A}$ by $Q_{\Lambda}$. The first $n$ entries correspond to the $n-best$ hand-arm configurations for the task.

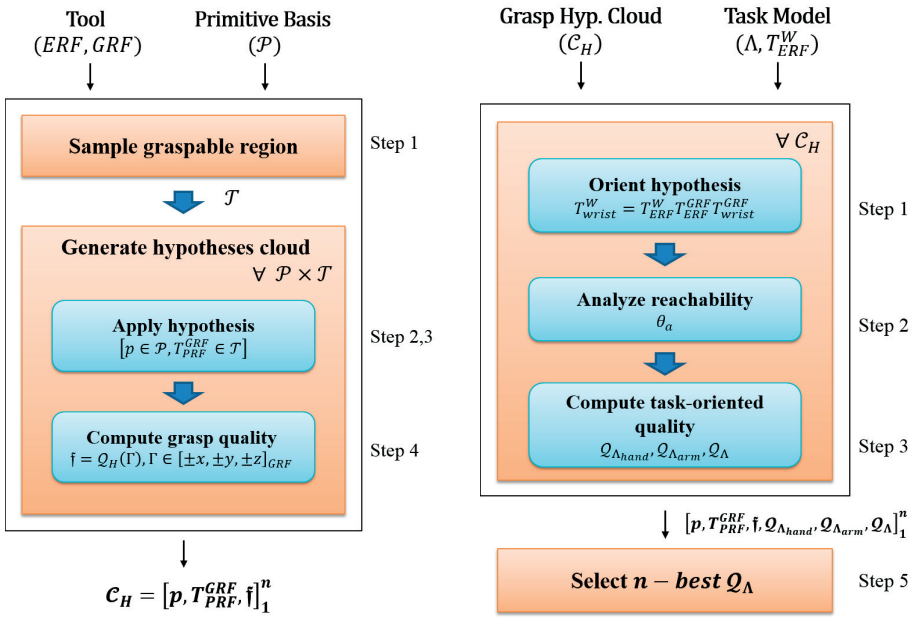


**(a)** Phase 1. Performed once per tool.

**(b)** Phase 2. Performed for each task pose in the world $T^{W}_{ERF}$.

**Figure 4.11:** Algorithm for determining $n-best$ hand-arm configurations for the task.

## 4.6 Characterization of directional quality for hand and arm

Previous sections have assumed existence of quality measures $Q_{hand}(\Gamma)$ and $Q_{arm}(\Gamma)$ for a known task requirement $\Gamma$. In this section we describe methods to quantify the ability for force and motion generation for the hand and the arm. Measures for the hand are based on Grasp Wrench Space (GWS) approximation. Measures for the arm are based on manipulability ellipsoids. We combine several advances in the literature regarding theses approaches. Extensions are made to improve accuracy of measurement in some cases.

### 4.6.1 Hand Quality

Hand quality is estimated by approximating the Grasp Wrench Space (GWS) by a convex hull and estimating distance to the GWS boundary (Ferrari and Canny, 1992; Borst et al., 2005). Grasp wrench space computation is well studied. However, simplifications introduced by common approaches, for the purpose of computational speed, introduce errors which compromise both the accuracy and physical relevance of the measurements. Here we briefly review the notion of grasp wrench space and outline the solutions adopted to overcome these problems.

#### Grasp Wrench Space

To differentiate grasps from one another we need a measure of quality. The grasp wrench space provides a way to differentiate between grasps based on their ability to resist arbitrary force and torque disturbance. The grasp wrench space is defined as the space of object wrenches which can be generated on an object through forces exerted at a set of object contacts. Consider $k$ object contacts. The force $\boldsymbol{f}_i$ exerted at contact $c_i$ produces an object wrench $w_i$ where

$$w_i = \begin{pmatrix} f_i \\ c_i \times f_i \end{pmatrix} = \begin{pmatrix} f_i \\ \tau_i \end{pmatrix} \tag{4.6}$$

Origin is usually taken as the object centre of mass. The space of object wrenches $\mathcal{W}$ is

$$\mathcal{W} = \left\{ w \;\middle|\; w = \sum_{i=1}^{k} w_i,\ w_i = \begin{pmatrix} f_i \\ \tau_i \end{pmatrix}, f_i \in \mathcal{FC}_i \right\} \tag{4.7}$$

$\mathcal{FC}_i$ represents friction cone constraints at contact $i$ which limit the tangential component of the contact force to be within a fraction $\mu$ of the normal component. $\mu$ is the coefficient of friction.

The linear nature of the relationship between $w_i$ and $f_i$ in (4.6) implies that increasing contact force results in proportionate increase in the object wrench

due to the contact force. The GWS is therefore defined in a normalized fashion by limiting some norm of the contact forces to unity.

$$f = \left[f_1^T f_2^T \dots f_k^T\right] \quad ; \quad \|f\| \leq 1 \tag{4.8}$$

Distance to the boundary of $ConvHull(\mathcal{W})$ in a direction $\boldsymbol{d}$ is a measure of how efficient a grasp is with respect disturbance along $\boldsymbol{d}$. A small value implies that more effort is required from the joints to scale the wrench space sufficiently to counter the disturbance. Larger the value, more efficient is the grasp against disturbance along $\boldsymbol{d}$.

In practice, computing $\mathcal{W}$ involves discretizing the friction cones at each contact point and computing the convex hull over the object wrenches due to these (Ferrari and Canny, 1992). A sparse discretization is used for rapid computation, especially when number of contacts are large (as is the case with power grasps). This can introduce large errors (30%) in the wrenches that are allowed through the contacts. At least 8 cone generating vectors are required for reasonable error ( 8%) (Borst et al., 2005). A more serious problem exists however with taking the convex hull over discretized contact friction cones as this limits the sum of all contact forces to unity. Several authors have pointed out that this is not physically relevant for an anthropomorphic hand in which contacts are made through several independently powered grasping surfaces. The more correct approach requires computing $ConvHull(\mathcal{W})$ by taking the Minkowski sum over the contact friction cones. Unfortunately, increasing the number of cone generating vectors and taking the Minkowski sum becomes computationally intractable.

### Physically relevant wrench space measure for a known direction

Quality measure for the hand is given by

$$Q_{hand}(\Gamma, C) = dist(\Gamma, C) \tag{4.9}$$

where $\Gamma$ is a 6D task wrench direction[2] and $C = [c_i]_1^n$ is a set of contacts. $\Gamma$ and $C$ are expressed with respect to the GRF. The function $dist(\Gamma, C)$ (denoted as $d_\Gamma$) evaluates distance to wrench space boundary in a manner similar to Borst et al. (2005) and is outlined in the following steps.

1) Initially $d_\Gamma = \epsilon$ and $\mathcal{W} = \bigcup_{i=1}^n \mathcal{W}_i$ denotes a set of object wrenches. Each $\mathcal{W}_i$ is the set of object wrenches due to the discretized friction cone at the contact $c_i$. 4 cone generating vectors are used.

2) Compute a new $d_\Gamma$ as the distance to boundary of $ConvHull(\mathcal{W})$ in the direction $\Gamma$.

[2] For consistency in the algorithm description. In practice, the 3D force and torque direction requirements are considered separately with 3D projections of the 6D wrench space

3) Find a combination of object wrenches by sampling force vectors from the contact friction cones such that the convex hull is expanded most in the direction $\Gamma$. This can be expressed as the following optimization.

$$W' = \underset{w_i}{\text{argmax}} \ \Gamma^T \sum_{i=1}^{n} w_i$$

where each $w_i$ is an object wrench due to a force vector drawn from the ***non-discretized*** friction cone at contact $c_i$. $W'$ is found as per the method described in Borst et al. (2005).

4) Set $W = W \bigcup \bigoplus W'$ and repeat steps 2 and 3 till the difference between successive $d_\Gamma$ is less than $\epsilon$.

Since non-discretized friction cones are sampled at each iteration, the method allows all forces admitted by friction constraints at the contact point. Also, by taking the Minkowski sum of the object wrenches due to the sampled force vectors, the resulting wrench space approximation allows each contact capable of influencing the wrench space in the task direction, to exert unit force. However, as discussed next, we further differentiate the contacts based on the ability to exert normal force through them.

### Contact Differentiation

Differentiating contacts based on how much normal force can be exerted through them is an often ignored aspect but which has direct influence on the shape of the wrench space and hence the boundary-distance quality measure. Consider for example contacts on the finger-tips. Normal forces that can be exerted through them are much smaller if the fingers are extended and used against the thumb in a pinch-like fashion, as opposed to when fingers are curled in order to oppose the palm. This follows directly from the kinematics. In the first case normal force is due to action of 1 joint at the finger base, whereas in the second all 3 finger joints contribute. Additionally, even if a large normal force can be exerted through a contact, the way in which it cooperates in the higher level oppositional intention (focus of pressure or supporting role) decides how much of that is actually applied.

We quantify the ability to exert normal force through a contact $c_i$ using 3 criteria discussed below.

1) ***kinetostatic*** ($n_i^{kin}$) A contact can be seen as the end-point of kinematic chain starting from the finger-base. As we will discuss in more details in Section 4.6.2 for the arm context, the ability to transmit normal force can be quantified through manipulability analysis.

$$n_i^{kin} = \boldsymbol{x}^{\boldsymbol{T}} \tilde{J}_{i_{trans}}(q) \tilde{J}_{i_{trans}}^T(q) \boldsymbol{x} \tag{4.10}$$

where $\tilde{J}_{i_{trans}}(q)$ is the translational Jacobian of surface point $c_i$, for hand configuration $q$, penalized for joint limits[3] and $\boldsymbol{x}$ is the direction of the surface normal. $n_i^{kin}$ is normalized by the maximum value seen for all hand surfaces over the open-closed space of all primitives.

While normal force is actively controllable for frontal surfaces of fingers and thumb, this capability is present to a smaller degree for finger-sides and palm. However, the latter offer resistance to any force exerted against them. Thus the normal force ability attributed to finger-sides and palm is taken as the average of all actively controllable surfaces which oppose them after hand-closure is completed.

2) ***oppositional intention*** ($n_i^{opp}$) Since we use a primitive based approach to grasp formation, we always know the higher level oppositional intention that is operating. Contribution of contacts in the foci regions are differentiated from those in the supporting regions using the heuristic below.

$$n_i^{opp} = \begin{cases} 1 & ; c_i \in \{VF1_{foci}\ ,\ VF2_{foci}\} \\ 0.7 & ; c_i \in \{VF1_{supp}\ ,\ VF2_{supp}\} \end{cases} \tag{4.11}$$

3) ***geometry*** ($n_i^{geom}$) Contacts that are closer to and more normally oriented to the object surface are associated with better ability to exert force. Define

$$\delta_{c_i} = \frac{|\vec{o}_{c_i}|}{\beta} + \left(1 - \frac{\hat{n}_{c_i} \cdot \vec{o}_{c_i}}{|\vec{o}_{c_i}|}\right)$$

where $\vec{o}_{c_i}$ is the vector joining contact $c_i$ to the closest point on the object surface, $\hat{n}_{c_i}$ is the hand surface normal and $\beta$ is a scaling parameter required to bring the range of useful linear distances in the same range as angle cosines. $n_i^{geom}$ can be defined as follows

$$n_i^{geom} = (1 - \delta_{c_i}) \tag{4.12}$$

This measure is the same as the one defined in Ciocarlie and Allen (2009).

Each of the criteria listed above results in a factor between $[0, 1]$. These criteria are combined to arrive at a scaling factor reflecting the ability to exert normal force through contact point $c_i$, given by

$$n_i^{scale} = n_i^{kin} * n_i^{opp} * n_i^{geom} \tag{4.13}$$

Eq. (4.13) is used to bound the normal component of the friction cone associated with contacts in $C$ . Figure 4.12 shows the effect of contact scaling on a grasp hypothesis after hand-closure.

[3]The method for penalization is same as that employed for the arm and is described in Section 4.6.2

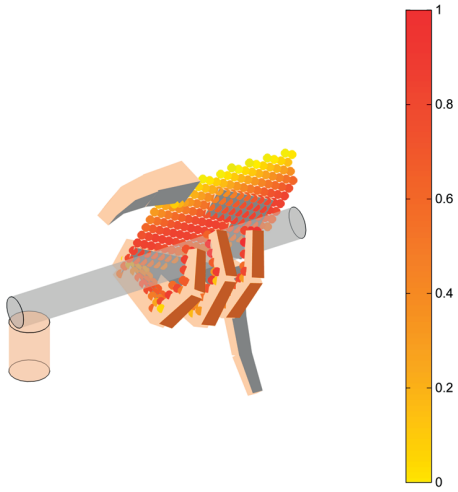


**Figure 4.12:** Scaling normal force ability of contacts according to their location and usage.

## Examples

Figure 4.14 applies the method to characterize task-oriented quality of primitive-based grasp hypotheses to different opposition categories. The task here is taken as force in the downward direction which is needed to counter the upward reaction, encountered on the graspable region, when using the tool as a hammer or for cutting. The GWS approximation approach described above differentiates well between the primitives (Figure 4.13). The best grasp for the task is the enveloping type seen with $O^{P}_{FS234}$, however others such as $O^{TS}_{P}$ and $O^{TS}_{S234}$ are also good and may perhaps suffice depending on the task being performed, especially when they are combined with other components. Importantly, the manner of generating opposition differs and causes a different region of the wrist-pose space to be explored.

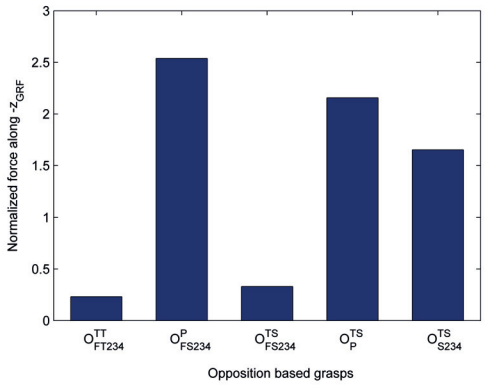


**Figure 4.13:** Normalized force capability in the $-z$ direction of the GRF is compared across primitives from different opposition categories. This is measured as distance to the wrench space boundary (magenta lines in Figure 4.14). Primitive notation introduced in Chapter 3 is used. For e.g. $O^{TT}_{FT234}$ refers to tips of index, middle and ring fingers acting in opposition to the thumb-tip. $P$ refers to Palm, $FS$ to Finger Surface, $TS$ to Thumb Surface and $S$ to Finger Side.

| primitive | preshape | closed | GWS |
|---|---|---|---|
| $O^{TT}_{FT234}$ | 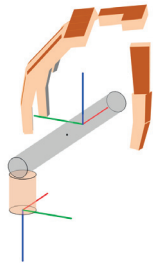 | 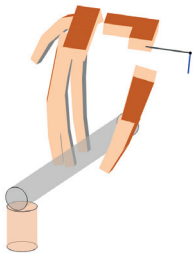 | 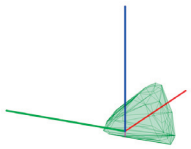 |
| $O^{P}_{FS234}$ | 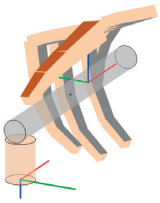 | 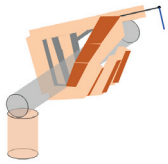 | 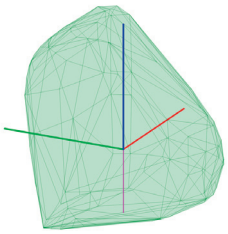 |
| $O^{TS}_{FS234}$ | 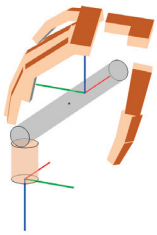 | 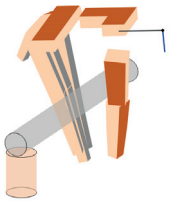 | 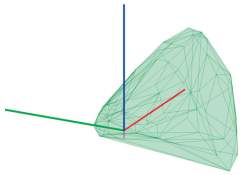 |
| $O^{TS}_{P}$ | 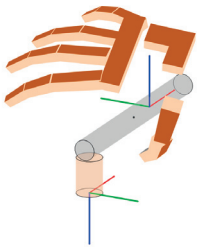 | 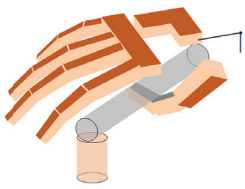 | 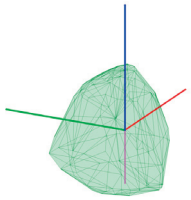 |
| $O^{TS}_{S234}$ | 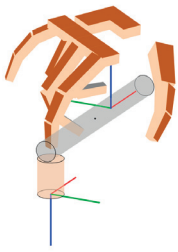 | 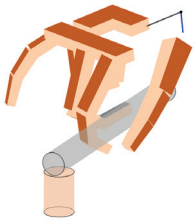 | 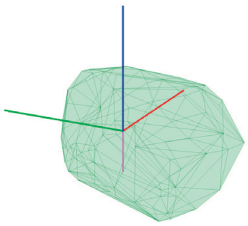 |

**Figure 4.14:** GWS approximation after positioning primitives in the GRF (the grasp hypothesis) and hand-closure according to the oppositional intention while respecting grasp hypothesis. One primitive from each category in Figure 4.3 is displayed.

### 4.6.2 Arm Quality

Manipulability ellipsoids (Yoshikawa, 1985) are used to quantify the ability of the arm to transmit force and velocity at the end-effector. This is a commonly followed approach in the literature (Patel and Sobh, 2014). Here, the arm is seen as a mechanical transformer of energy. Joint force and joint velocity effort are viewed as a normalized hyper-sphere in joint space and mapped to an hyper-ellipsoid in task space using the manipulator Jacobian.

$$\|J(\theta_a)^{+}v\|^2 \leq 1 \tag{4.14}$$

$$\|J(\theta_a)f\|^2 \leq 1 \tag{4.15}$$

Eq. (4.14) denotes the velocity ellipsoid while Eq. (4.15) denotes the force ellipsoid. $J \in \mathbb{R}^{6\times n}$ is the manipulator Jacobian for the current arm configuration $\theta_a \in \mathbb{R}^n$. $v, f \in \mathbb{R}^6$ denote generalized force and velocity at the end-effector.

With manipulability ellipsoids, distance to the ellipsoid boundary in a particular direction $\Gamma$ quantifies the mechanical gain for unit effort in the joints. We use the square of this distance as a measure for a given manipulator configuration to transmit force or velocity in a desired task direction (Chiu, 1988).

$$Q_{arm}(\Gamma, \theta) = \left(\Gamma^T E\, \Gamma\right)^{-1} \tag{4.16}$$

$E$ denotes the manipulability ellipsoid. Depending on whether force or velocity abilities are being examined, $E = JJ^T$ or $E = {J^+}^T J^+$. In the above and also following discussion, $J$ should be understood to mean $J(\theta_a)$.

#### Considering the effect of joint limits

Manipulability ellipsoids defined in (4.14) and (4.15) suffer from inaccuracies near joint limits. This is because the ability of a manipulator to transmit force and motion at the end-effector gets diminished when joint limits are encountered. However, mere proximity to joint limits does not necessarily pose a problem as long as the joint moves away from the limit during task execution.

We adopt the approach of Vahrenkamp and Asfour (2015) to accurately reflect the effect of joint limits on manipulability ellipsoids. The arm Jacobian is penalized in an element-wise fashion, depending on whether joint limits will be encountered for a given task direction. An augmented Jacobian is constructed using the task direction $\Gamma$.

$$\tilde{J}(\Gamma) = L(\Gamma) \cdot J$$

$L(\Gamma)$ is a penalization matrix which acts on each element of $J$.

$$L_{i,j}(\Gamma) = \begin{cases} p_j^- & \text{joint } j \text{ encounters lower limit} \\ p_j^+ & \text{joint } j \text{ encounters upper limit} \end{cases}$$

In the above, $i$ $(1 \leq i \leq 6)$ represents the output translational or rotational

dimension and $j$ $(1 \leq j \leq n)$ represents the arm joint. $p_j^-$ and $p_j^+$ are functions which assume a value 1 in the middle of the joint range and go to 0 at the boundaries. Since the sense of joint movement is directly related to a task space direction, a separate penalized Jacobian must be computed for every direction of interest.

The net effect of the above is that the resulting manipulability ellipsoid becomes squashed in the problematic task directions. This leads to a transmission gain which is a more accurate indicator of the manipulator force and motion generation abilities.

### Separating rotational and translational components

Manipulability ellipsoids of Eq. (4.14) and Eq. (4.15) operate in the 6D space of generalized force and velocity. However, rotational and translational components have different units as well as operating ranges that are generally not compatible (referred to as non-commensurate). Weighting matrices are sometimes used to bring these subspaces into relation with each other (Finotello et al., 1998; Vahrenkamp and Asfour, 2015). However, special reference velocities need to be identified experimentally. The use of scaling to overcome the inconsistency between units introduces arbitrariness by which the manipulability measures change with the scale factors and also with change of the origin (Doty et al., 1992). In Doty et al. (1995), the authors propose a weighted generalized inverse of the manipulator Jacobian which is application specific and which allows the use of 6D non-commensurate vectors without these difficulties. Overall manipulability characteristics are considered.

We prefer to address rotational and translational performance of the manipulator separately (Yoshikawa, 1990; Lee, 1997). This fits well to our earlier decisions in task-modelling where linear and angular task requirements were identified separately and quality measures were normalized separately for each linear/angular force/velocity space before being combined (Section 4.5). 3D ellipsoids constructed from the relevant rows of the Jacobian are used for manipulability analysis. The penalized Jacobian $\tilde{J}(\Gamma)$ and its pseudo-inverse can be represented in a partitioned manner as follows

$$\tilde{J} = \begin{bmatrix} \tilde{J}_{trans} \\ \tilde{J}_{rot} \end{bmatrix} \qquad \tilde{J}^+ = \begin{bmatrix} \tilde{P}_{trans} & \tilde{P}_{rot} \end{bmatrix}$$

Manipulability ellipsoids are defined for the different translational and rotational components of force and velocity as follows.

$$\begin{aligned} E_f &= \tilde{J}_{trans}\tilde{J}_{trans}^T & E_v &= \tilde{P}_{trans}^T\tilde{P}_{trans} \\ E_\tau &= \tilde{J}_{rot}\tilde{J}_{rot}^T & E_\omega &= \tilde{P}_{rot}^T\tilde{P}_{rot} \end{aligned}$$

These ellipsoids replace the ones in (4.16).

## 4.7 Application to human hand-arm system

We apply our approach to both human and robotic hand-arm models. In this section we discuss the simulation setup and results for the human hand-arm model. The tasks of cutting, hammering, screw-driving and opening a bottle-cap are considered. Task models for these were defined earlier. We examine normalized task-oriented quality for the hand and arm for the configurations discovered by our approach and contrast this with a strategy that maximizes robustness through enveloping grasp formation. We consider 3 aspects for comparison: overall variation in grasp quality, quality of arm configuration for the strongest grasps discovered and grasp quality corresponding to the best arm configurations for the task.

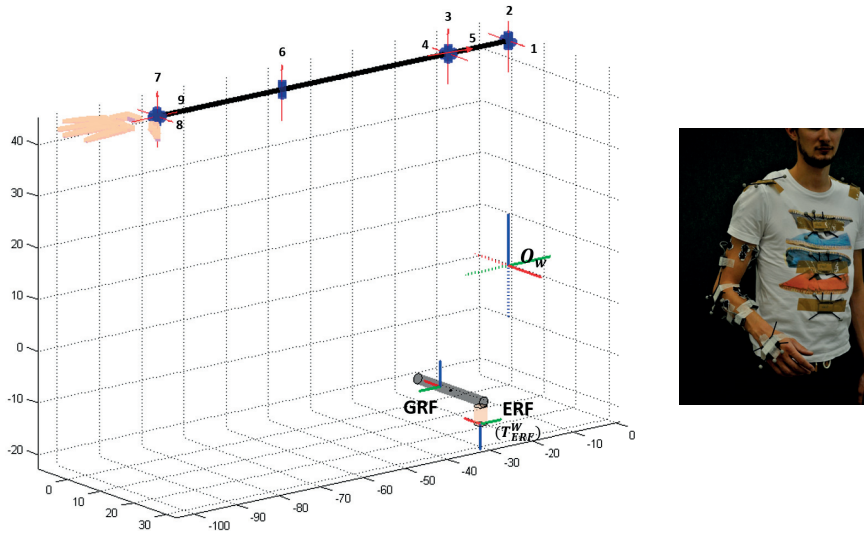


**Figure 4.15:** Kinematic model of the human hand-arm system. The hand has 21 DOF. The arm has 9 DOF. Optical markers are used to instantiate the model and also obtain the tool pose relative to the arm. Origin is taken as the base of the torso

### 4.7.1 Simulation setup

We use an anthropomorphic hand-arm system modeled on the human (Figure 4.15). Our goal in defining the model is be able to generate grasps from the different primitive categories, quantify their task-oriented capability and model their effect in constraining wrist-pose, so that we can examine the effect of a primitive-based grasp strategy versus an enveloping grasp strategy on quality of the arm configuration to do the task. The hand model was described earlier in Chapter 3. It has 21 DOF. The arm is modelled by a 9DOF kinematic chain anchored at the neck. Joints 1 and 2 model the lifting/lowering of the shoulder and rotation of the shoulder about the neck. The shoulder has 3 degrees of freedom (joints $3-5$), 1 DOF for the elbow (joint 6 ) and 3 DOF for the wrist (joints $7-9$).

Link lengths and transform for the base of the kinematic chain are obtained from human measurements. A human is instrumented with optical markers for this purpose. The origin ($O_W$) is taken as the marker at base of the torso. Both the arm base transform and the tool pose in the world ($O^W_{ERF}$) are expressed with respect to this reference frame. To obtain $O^W_{ERF}$, the tool is first positioned according so as to cut something placed on a table. The human is instructed to adopt a suitable position with respect to the tool, facing the table, so that the graspable region can be accessed comfortably.

### 4.7.2 Simulation Results: Cutting task

We present results of the simulation with the human hand-arm model. The cutting task is discussed here in details. Results for the other tasks are summarized later on.

| Grasp Intention | Hypotheses | | |
|---|---|---|---|
| | generated | valid | reachable |
| primitive | 1872 | 1188 | 148 |
| enveloping | 240 | 192 | 27 |

**(a)** Grasp Hypotheses

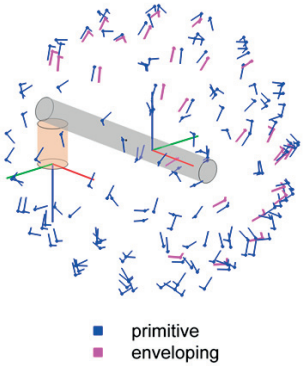


**(b)** Reachable wrist-pose space.

**Figure 4.16:** Grasp hypotheses generated for the cutting tool and wrist poses reachable by the arm.

Referring to Table 4.16a, Phase 1 (in Section 4.5.3) generates a wrist-pose space associated with the cutting tool consisting of 1188 object-relative wrist-poses across all the primitives in the human hand primitive basis (Section 4.4.1). In Phase 2 (Section 4.5.3), these are examined for reachability by the arm. A total of 148 wrist-poses are reachable. For the enveloping approach, a total of 192 grasp hypotheses were generated of which 27 are reachable. Figure 4.16b shows that a larger portion of the object-relative wrist-pose space is explored with the primitive strategy.

For each hand-arm hypothesis, task-oriented qualities are computed for the hand $Q_{\Lambda_{hand}}$, the arm $Q_{\Lambda_{arm}}$ and the hand-arm configuration taken together $Q_\Lambda$. The task definition for cutting i.e. $\Lambda = \Lambda_{cutting}$ (Section 4.5.1) is used. In Figure 4.17, normalized task-oriented hand quality v/s normalized task-oriented arm quality is plotted for the hand-arm configurations discovered. In this way the range of qualities examined becomes clearly visible. Color codes are used to indicate the intention underlying the grasp.

Figure 4.18a summarizes the information from a grasp quality perspective.

Whereas all grasps resulting from the enveloping strategy are of high quality, the primitive based approach exposes different bands of hand quality to the arm. With the primitive-based approach, the weakest grasps for cutting are formed by using finger-tips alone $O_{FT}^{TT}$ ($Q_{\Lambda_{hand}} \in [0 - 0.1]$), and the strongest ones are formed by fingers against palm $O_{FS}^{P}$ ($Q_{\Lambda_{hand}} > 0.3$). Oppositions involving thumb action against finger-surface $O_{FS}^{TS}$, palm $O_{P}^{TS}$ and side $O_{S}^{TS}$ occupy an intermediate range ($Q_{\Lambda_{hand}} \in [0.1 - 0.3]$). The several high quality exceptions seen for thumb-side action are further investigated; when the opposing surfaces are well aligned with the object these constitute high quality grasps.

With the enveloping approach, all grasps lie in a narrow band of high quality $Q_{\Lambda_{hand}} \in [0.6 - 0.7]$. This is to be expected because the strongest parts of the hand are used, and the planning strategy seeks the best envelope of the graspable region, which maximizes the surface area of the hand in contact with the object. However we can also observe that, for these grasps, the arm configuration is not well suited to the task. This fact is highlighted in Figure 4.18b, which shows arm quality for the 20 best grasps, with 10 taken from each strategy (primitive-based, enveloping). Grasps associated with the enveloping strategy or $O_{FS}^{P}$ primitive (which is closely related to enveloping) lie below the lower threshold of arm quality considered to be good for the task. A possible reason for this could be that cylindrical caging of the handle positions the wrist at right angles to the cylinder axis. This in turn constrains the arm such that elbow and shoulder joints are close to their limit. The extended and lowered (close to torso) elbow is not suited for exerting downward force and forward/backward motion (Figures 4.17 e, f).

Other opposition types allow for the elbow to be bent and raised which is a better configuration for delivering the cutting requirements (Figures 4.17 b- d). Figure 4.18c summarizes the top 20 arm configurations[4]. We can see that, with primitives, several good quality arm configurations for low to mid quality grasps are exposed: finger-tip $O_{FT}^{TT}$ ($Q_{\Lambda hand} = 0.1$), thumb-palm $O_{P}^{TS}$ ($Q_{\Lambda hand} = 0.3$) and thumb-side $O_{S}^{TS}$ ($Q_{\Lambda hand} = 0.4$). However, none of the strongest grasps ($Q_{\Lambda_{hand}} > 0.4$) factor here.

[4]We limit to a maximum of 3 per primitive type, arm configurations whose grasp quality is less than half the grasp quality range.

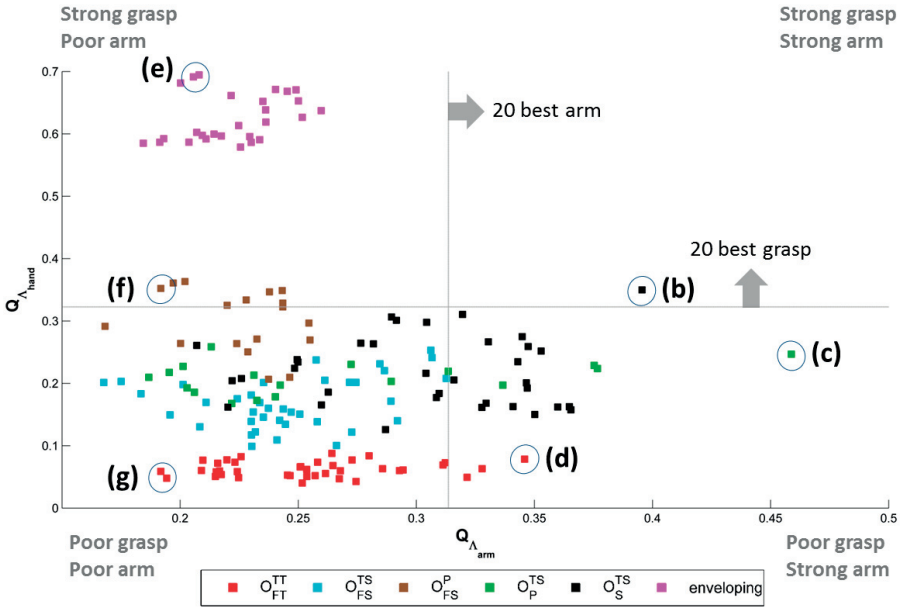


(a) Hand-arm configurations for cutting from a task-oriented quality perspective

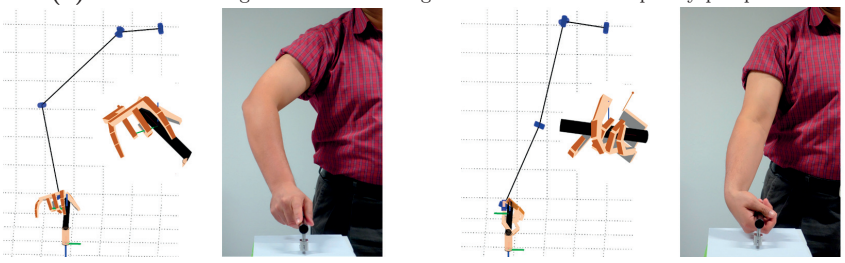

(b) $Q_{\Lambda_{hand}} = 0.406,\ Q_{\Lambda_{arm}} = 0.395$



(e) $Q_{\Lambda_{hand}} = 0.689,\ Q_{\Lambda_{arm}} = 0.208$

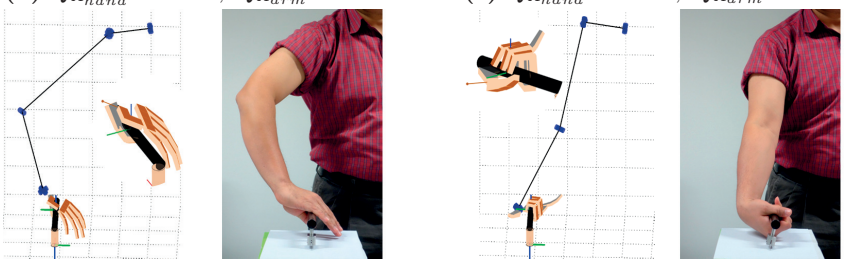

(c) $Q_{\Lambda_{hand}} = 0.288,\ Q_{\Lambda_{arm}} = 0.458$



(f) $Q_{\Lambda_{hand}} = 0.413,\ Q_{\Lambda_{arm}} = 0.191$

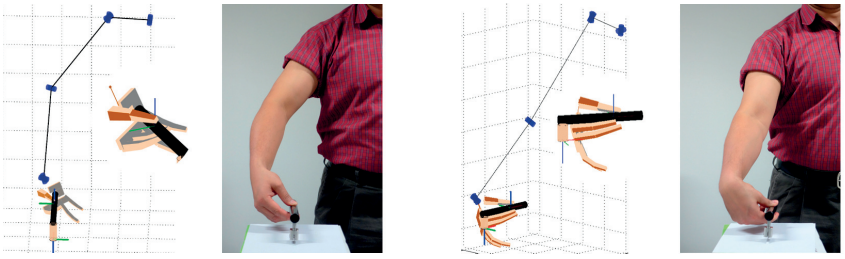

(d) $Q_{\Lambda_{hand}} = 0.094,\ Q_{\Lambda_{arm}} = 0.345$



(g) $Q_{\Lambda_{hand}} = 0.192,\ Q_{\Lambda_{arm}} = 0.07$

**Figure 4.17:** Results for the cutting task. (a) plots normalized task-oriented grasp quality against normalized task-oriented arm quality for the hand-arm configurations discovered for cutting. Points above the horizontal line indicate the top 20 grasp configurations while points to the right of the vertical line indicate top 20 arm configurations. The best hand-arm configuration for cutting lie in the top-right corner. Thresholds values for the lines are identified as discussed in Section 4.7.2. (b)-(g) visualize the selected configurations with the same label. The insets show the graspable region zoomed and re-oriented for better visualization.

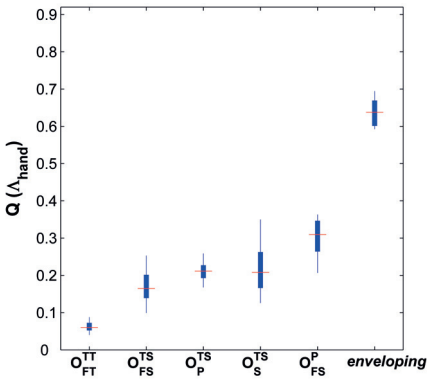


**(a)** Task-oriented grasp quality associated wrist-pose exposed to arm.

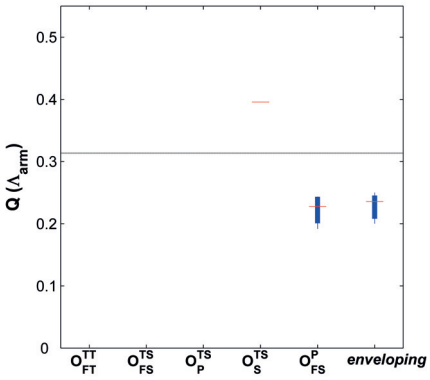


**(b)** Highest quality grasps. 20 grasps with the highest quality are selected with 10 taken from each strategy (primitive-based, enveloping). The y-axis plots arm quality associated with these configurations. The horizontal line shows the lower threshold for good arm configurations.

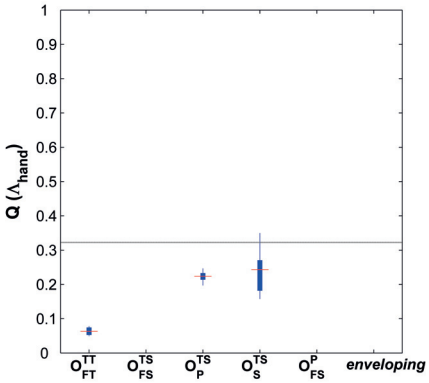


**(c)** Highest quality arm configurations for cutting. 20 configurations with the highest quality are selected. The y-axis plots grasp quality associated with these configurations. The horizontal line shows the lower threshold for good quality grasps.

**Figure 4.18:** Summary of Figure 4.17 for the Cutting task. The figures show variation in hand-quality over all grasp intentions ( 4.18a), quality of arm configurations for the strongest reachable grasps ( 4.18b), the hand quality corresponding to the best arm configurations for the task ( 4.18c). The figures show that the strongest quality grasps are associated with poor arm configurations, whereas good arm configurations are associated with lower quality grasps and these are found by the primitive-based approach.

### 4.7.3 Simulation Results: Hammering, Screw-driving, Open-cap Tasks

Results are also obtained for hammering (Figure 4.22), screwdriving (Figure 4.23) and Open-cap (Figure 4.24) tasks, in the same manner as the cutting task. Key points are summarized in Figures 4.19, 4.20 and 4.21, for : hand-quality variation, arm quality for the strongest grasps and hand-quality for the arm configurations best suited for the task.

Although the same scale has been used in these figures, we note that the plots represent task-oriented quality and hence cannot be compared across different tasks. The quality measures employed are customized according to task requirements (Section 4.5.1) and hence are different across tasks . Nevertheless

| Task | Grasp | Hypotheses | | |
|---|---|---|---|---|
| | Intention | generated | valid | reachable |
| Hammering | primitive | 1872 | 1188 | 149 |
| | enveloping | 240 | 192 | 27 |
| Screwdriving | primitive | 1872 | 1188 | 164 |
| | enveloping | 240 | 192 | 18 |
| Open-Cap | primitive | 1872 | 884 | 113 |
| | enveloping | 1728 | 628 | 66 |

**Table 4.1:** Grasp hypotheses for the Hammering, Screwdriving and Open-Cap tasks.

they can be used to examine how well the primitive-based and enveloping-based strategies serve task requirements, for the different tasks.

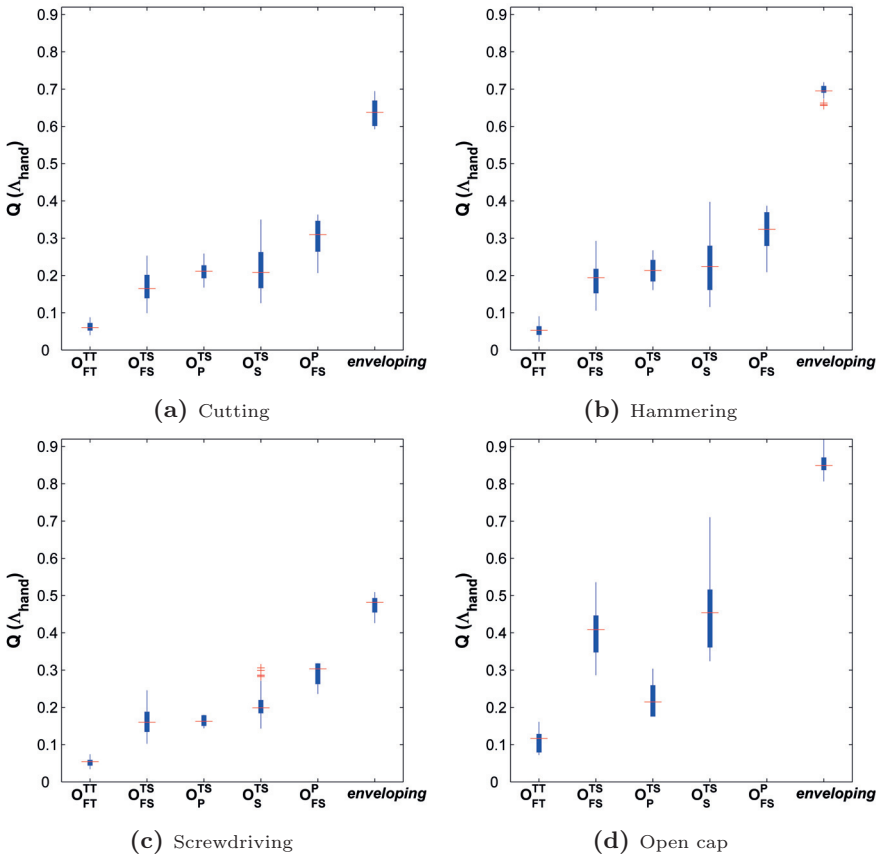


**(a)** Cutting **(b)** Hammering

**(c)** Screwdriving **(d)** Open cap

**Figure 4.19:** Task-oriented grasp quality associated with wrist-pose exposed to arm.

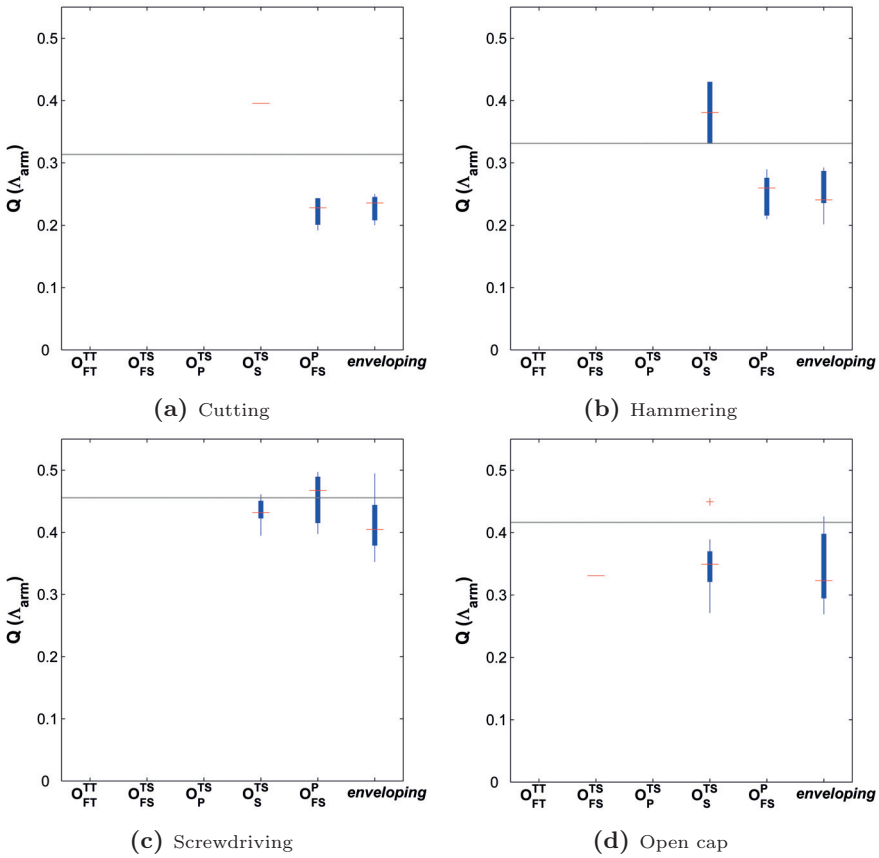


**(a)** Cutting **(b)** Hammering

**(c)** Screwdriving **(d)** Open cap

**Figure 4.20:** Highest quality grasps. The y-axis plots arm quality associated with these configurations. The horizontal line shows the lower threshold for good arm configurations.

From a grasp quality perspective, Figure 4.19 shows that the method can successfully differentiate between different grasp intentions according to task-oriented grasp quality even though we don't have precise configuration and contact. Across all tasks, the strongest reachable grasps are always found using the enveloping strategy, finger-palm opposition $O^P_{FS}$ and thumb-side opposition $O^{TS}_S$, in that order. An exception occurs for the open-cap task – there are no $O^P_{FS}$ grasps – which is discussed later. From Figure 4.20, we see that the first two intentions, which are caging type grasps (enveloping, $O^P_{FS}$) constrain the arm poorly for cutting and hammering whereas $O^{TS}_S$ exposes good wrist-pose while also offering relatively good grasps. For screw-driving and open-cap tasks, the tool handle is positioned differently. Here, a caging strategy does offer the best wrist-pose for arm configurations suited for turning torque and/or downward force. But the primitive based strategy also does equally well. Moreover, it uncovers a range of hand qualities for good arm configurations. With screw-driving for example, finger-tip or finger-surface grasps are found, these have lower hand quality but may be suited for a delicate screw-driving kind of job. Similarly, with the open-cap tasks, these kinds of grasps can be suitable for caps with lower friction properties or when the initial turn of the cap has been taken

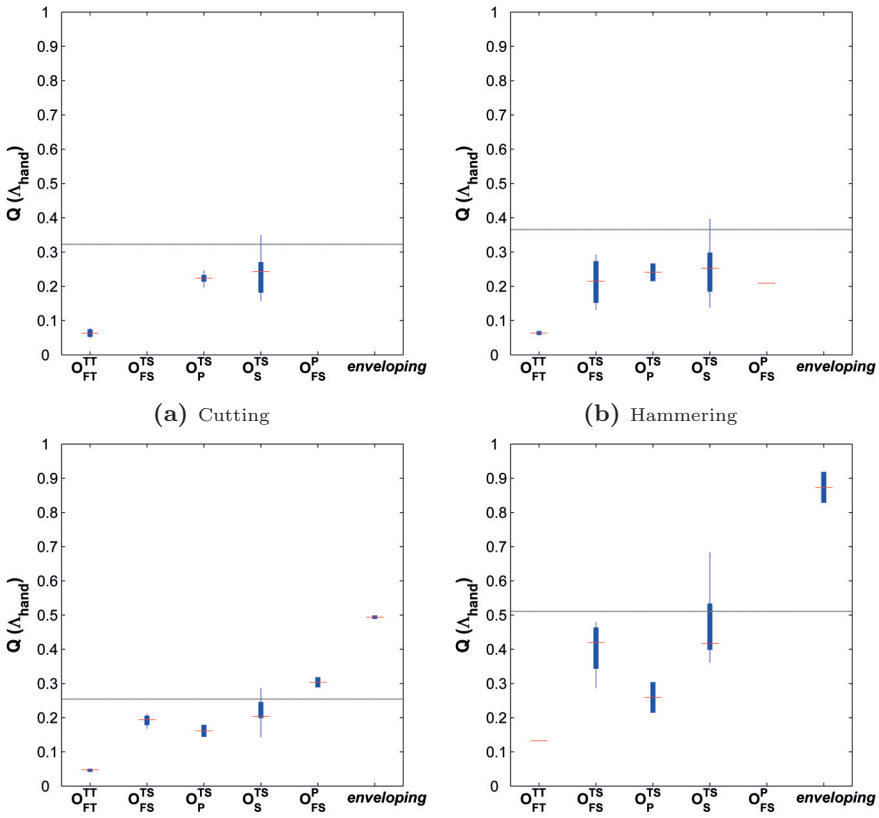


**(a)** Cutting **(b)** Hammering

**(c)** Screwdriving **(d)** Open cap

**Figure 4.21:** Highest quality arm configurations for cutting. The y-axis plots grasp quality associated with these configurations. The horizontal line shows the lower threshold for good quality grasps.

and lower friction conditions exist.

A notable exception occurs for the strongest reachable grasps discovered in the open-cap task (Figure 4.19d). No grasps of the type $O^P_{FS}$ are seen. This may seem strange given that for the enveloping strategy, several grasps were found. It becomes apparent however, when we consider that primitive-based grasp hypotheses derive from application of oppositional intention. For this particular case, it is establishing opposition between foci regions of the palm and finger-surfaces on the cap rim. Having this focus lowers the wrist so that it becomes inaccessible to the arm and thus no reachable grasps are discovered. In contrast, the enveloping strategy is not associated with oppositional intention. We may therefore search all round the cap for approach directions from which to close the hand. Several reachable wrist-poses are uncovered. However they come with a disadvantage. This is made clear by the hand-arm configurations shown in Figure 4.24. The absence of an underlying intention makes it difficult to maintain or adapt the grasp over the task duration. The grasp becomes susceptible to slip under strong turning torque and avoiding this may require substantial effort from the joints. Comparing with the primitive based approach, the thumb-side $O^{TS}_S$ grasp discovered is serving a direct oppositional intention

planned on the cap. This can be more easily adapted (rotated) while maintaining grasp quality. Further, it can be combined with a $O^P_{FS}$ kind of intention to strengthen thumb-side in case strong turning torque is generated by the arm.

The results demonstrate that the strongest reachable grasp is not associated with good arm quality. This means that we must always trade-off task-oriented grasp quality with task-oriented arm quality to achieve the best hand-arm balance for task goals. From Figures 4.17, 4.22a, 4.23a and 4.24a, this is true when we are using an enveloping strategy or a primitive-based strategy to generate grasp hypotheses. However, the primitive-based strategy exposes a wider range of hand quality, across all tasks, as opposed to a small range of high quality grasps found with the enveloping strategy. Also, judging from the pose space associated with reachable grasps, the primitive-based strategy exposes a wider range wrist-poses over which to optimize the arm configuration.

### 4.7.4 Discussion

A key point with a primitive-based approach is that we are reasoning with grasp components and oppositional intentions and not fully formed hand-configurations. Each component is considered as the dominant intention in the grasp and positioned in the graspable region. However, this does not preclude the addition of other components. By adding components which cooperate and which are allowed by the object grasping affordance, we may build up the capabilities of the grasp such that it meets robustness requirements in the task directions. But working on a component basis gives more flexibility to position each one in the graspable region so as to uncover wrist-poses that are better suited for the arm. If we make enveloping/caging the primary goal then we are in essence using only one component and flexibility in grasp formation available to the hand remains unexplored.

The is borne out by the results of Figure 4.17. Note that the best arm configuration is associated with a thumb-palm $O^{TS}_P$ type of intention. This by itself cannot be considered a complete grasp. However, working with this intention alone, with the other fingers considered out of the way, offers a better flexibility for positioning this intention around the graspable region. This uncovers the best arm configuration from a task perspective but is associated with a mid-quality grasp. Now the grasp can be completed for example by wrapping the other fingers in a supporting fashion, or even changing to a 'nearby 'component, to strengthen the grasp while preserving the wrist-pose exposed to the arm. This way of identifying a good hand-arm configuration with a dexterous hand may be more advantageous to working with only the strongest grasps or optimizing the arm blindly over the object-relative pose space without any knowledge of what kind of hand functionality can be leveraged and what quality of grasps these may lead to.

The proposed approach is built around task relevant directions for force/torque

and motion. Lacking here is a sense of absolute values. The approach adopted seeks the best grasp and arm configuration adapted for the task relevant directions and hopes that in doing so the configuration selected will be able to generate the actual force/torque and motion requirements required. If we incorporate a sense of absolute values required both in the task requirements and in hand/arm quality, we may make better choices, choosing configurations that just meet, as opposed to overly exceed, task requirements. For example, from Figure 4.18c, even a finger tip grasp has a very good arm configuration for the task. By stiffening the intermediate joints, a finger-tip kind of grasp could conceivably meet task requirements for some delicate cutting job with a fine tool. This may be the only possibility if the operation has to be performed in a confined or recessed area where more powerful hand configurations are not achievable.

The proposed approach samples the object-relative region in the planning phase. A coarse sample is taken with the objective to find the good regions from a hand and arm perspective. A logical next step is to perform a local adaptation for the best hand-arm configurations identified. Adaptation can be done in two ways both of which result in adapting the wrist-pose so as to optimize arm functionality while retaining grasp robustness along the task directions. We can change how oppositional intention is positioned or change the intention itself, adapting the foci of opposition and/or virtual finger span. And, as discussed earlier, we can add new components to strengthen a weak grasp or move to a 'nearby' component, where nearby is defined by a transition which results in minimal change to the wrist-pose.

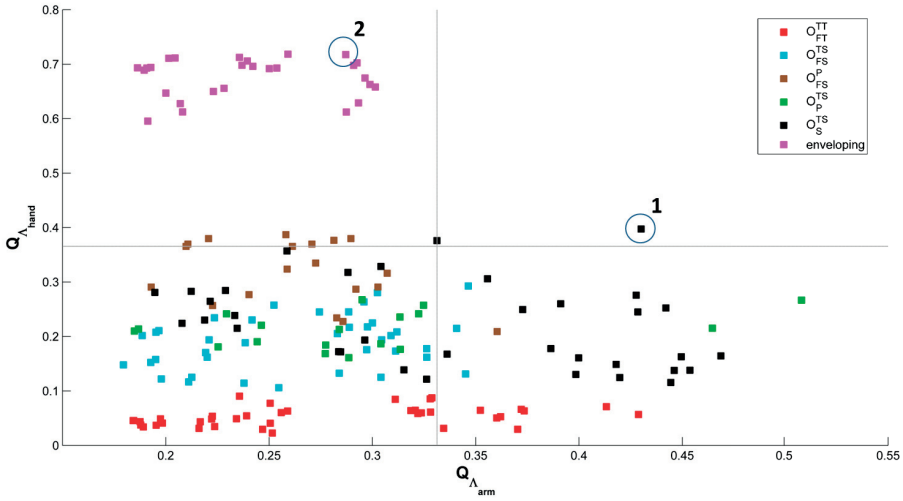


**(a)** The figure plots normalized task-oriented grasp quality against normalized task-oriented arm quality for the hand-arm configurations discovered for hammering. Points above the horizontal line indicate the top 20 grasp configurations while points to the right of the vertical line indicate top 20 arm configurations. The best hand-arm configuration for hammering lie in the top-right corner.

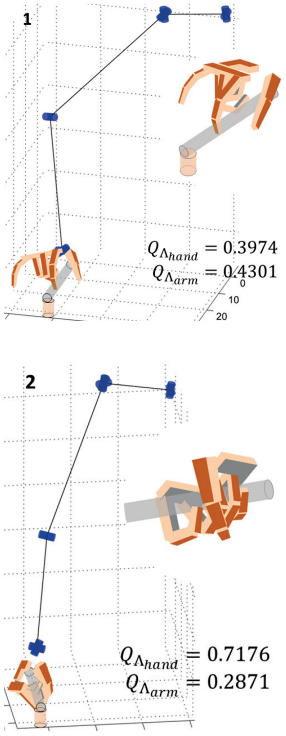


**(b)** Best hand-arm configurations for the task.

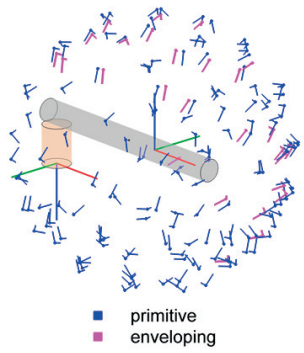


**(c)** Reachable wrist-pose space.

**Figure 4.22:** Results for Hammering

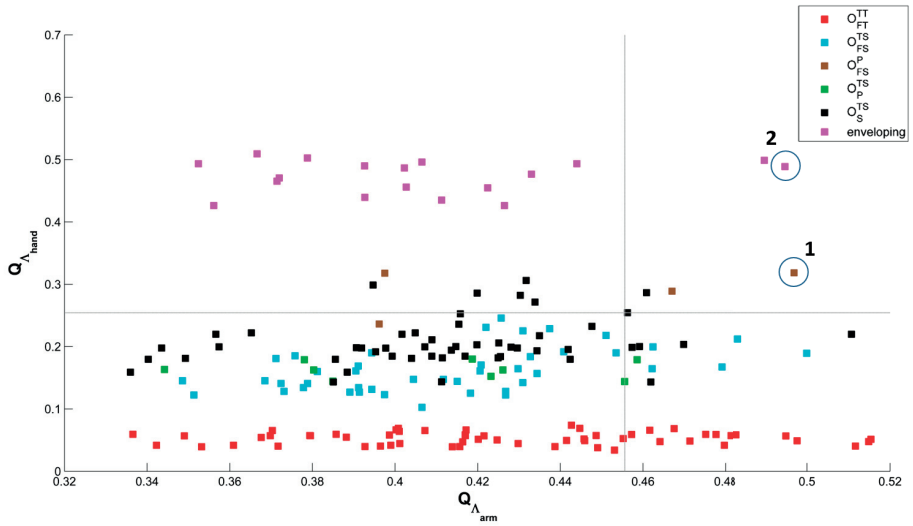


**(a)** The figure plots normalized task-oriented grasp quality against normalized task-oriented arm quality for the hand-arm configurations discovered for screwdriving. Points above the horizontal line indicate the top 20 grasp configurations while points to the right of the vertical line indicate top 20 arm configurations. The best hand-arm configuration for screwdriving lie in the top-right corner.

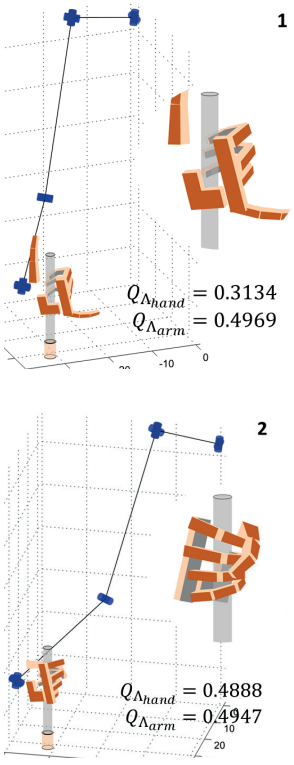


**(b)** Best hand-arm configurations for the task.

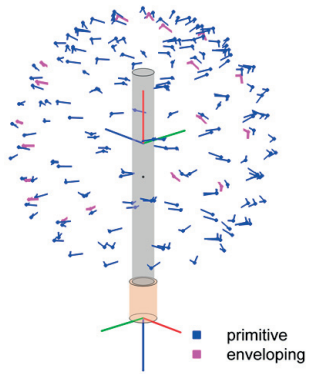


**(c)** Reachable wrist-pose space.

**Figure 4.23:** Results for Screwdriving

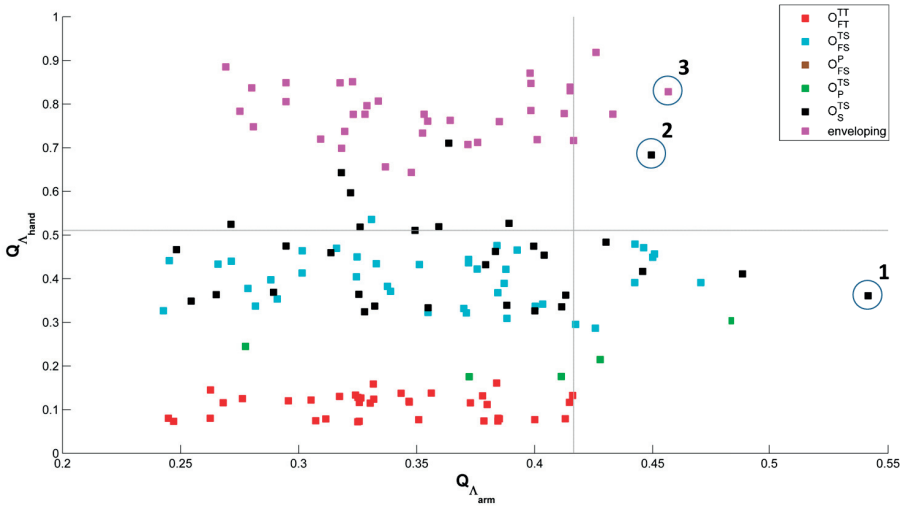


**(a)** The figure plots normalized task-oriented grasp quality against normalized task-oriented arm quality for the hand-arm configurations discovered for opening a bottle cap. Points above the horizontal line indicate the top 20 grasp configurations while points to the right of the vertical line indicate top 20 arm configurations. The best hand-arm configuration for opening a bottle cap lie in the top-right corner.

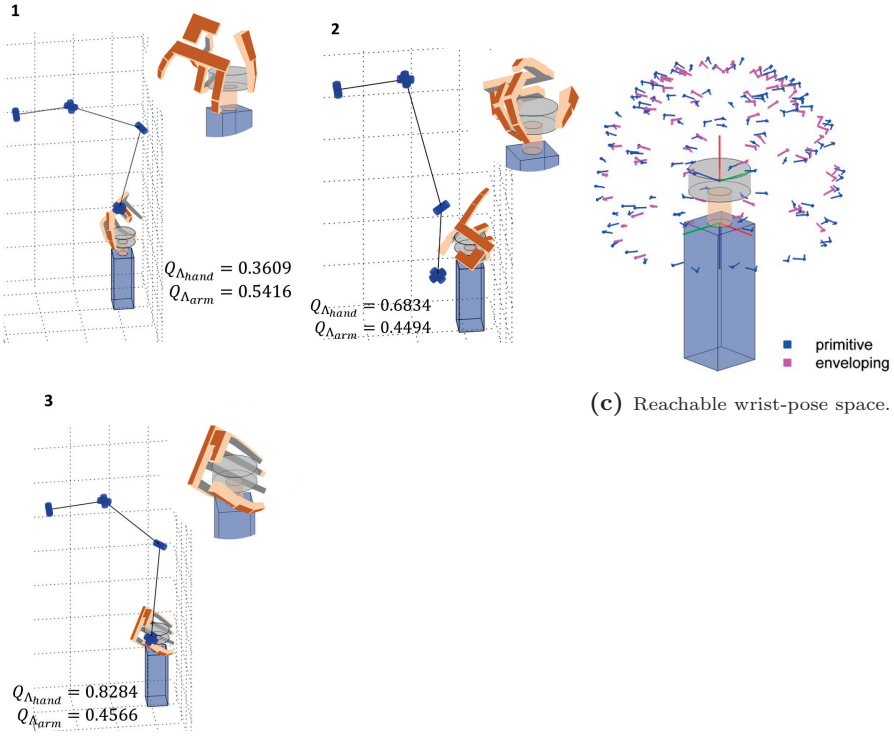


**(c)** Reachable wrist-pose space.

**(b)** Best hand-arm configurations for the task.

**Figure 4.24:** Results for Opening a bottle cap.

## 4.8 Application to robotic hand-arm system

In this section we address how the proposed framework can be applied towards task-oriented configuration of anthropomorphic hand-arm systems that are similar to humans but not identical. The proposed framework is not tied to a particular morphology for the hand or the arm. It can be applied to any hand-arm system based on the following two abstractions:

1. A primitive basis for the hand. This represents the flexibility available for generating oppositional pressure within the hand that we wish to leverage towards the task.

2. A generic representation for the robotic arm on which inverse kinematics computation can be applied in order to obtain an arm configuration for a given wrist-pose.

We apply the framework in the context of the KUKA-LWR arm connected with the Allegro hand. The tasks of hammering and opening a bottle-cap are considered. A primitive basis for the Allegro hand is defined. The $n$-best hand-arm configurations are identified in simulation using the proposed framework and then executed on the real robot platform.

### 4.8.1 Experimental setup

The KUKA-LWR is 7-DOF robotic manipulator. Its workspace and size allow for it to be mounted on a humanoid torso and used in an anthropomorphic manner (Borst et al., 2007). In our case the KUKA-LWR is mounted on a table. The arm is torque-controlled at 1000Hz to generate task relevant force and motion at the end-effector. The Allegro hand[5] is a 16-DOF anthropomorphic hand composed of palm and 4 fingers (one of which acts as a thumb). Each finger has 4 independent torque-controlled joints. The hand is controlled at 333Hz separately from the arm. Hand pre-shape and arm reaching operate simultaneously and hand closure is initiated once these phases have completed. The frontal surfaces of the fingers are covered with Tekscan[6] tactile patches which are sensory arrays containing 12-60 sensory elements (or taxels) depending on the size of the patch. Tactile data is used to detect the fingers impacting the object and the locations of contact. Tactile data is received at the rate of 200Hz and incorporated into hand closure (discussed in more details later in this section).

We consider the tasks of Open-Cap and Hammering. The experimental setup is shown in Figure 4.25. The origin ($O_W$) is taken as the base of the KUKA-LWR arm. The tool pose in the world ($O^W_{GRF}$,$O^W_{ERF}$) is obtained by means of visual markers attached to the tools. For the Open-Cap task, the

[5] http://www.simlab.co.kr/Allegro-Hand.htm
[6] https://www.tekscan.com/products-solutions/systems/grip-system

**(a)** Finger surfaces of the Allegro hand are covered with Tekscan tactile sensors to detect object contact and contact location.

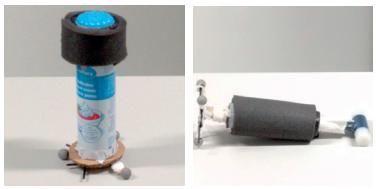

**(b)** Objects used for the tasks of Open-Cap and Hammering. In each case, the graspable region is padded to increase size and compliance for grasping with the Allegro hand. Optical markers and the OptiTrack system are used to track object pose.

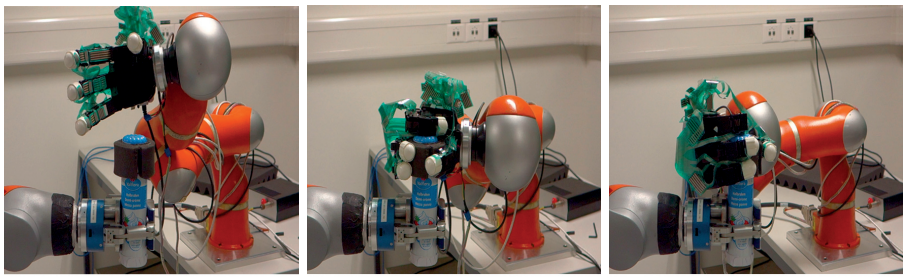


**(c)** Setup for the Open-Cap task. Another robot arm presents the bottle in the desired opening pose and also holds the bottle firmly during task execution.

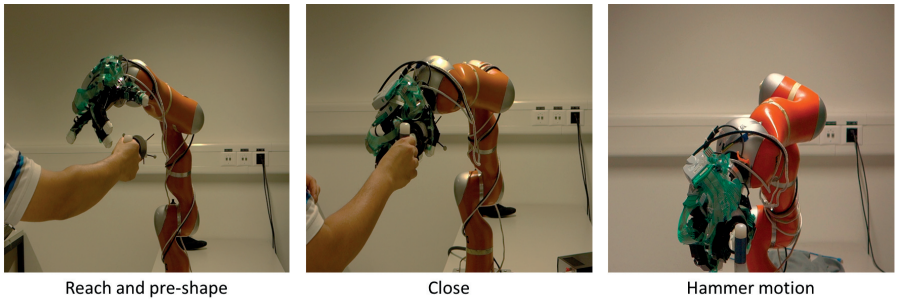


**(d)** Setup for the Hammering task. A human presents the tool according to where the hammering action is required. The tool is held in place by the human till the robot hand completes the grasp. The robot then executes the hammering motion.

**Figure 4.25:** Experiment setup for implementing task oriented configuration on a real robot hand-arm system. We consider 2 tasks: Open-Cap (c) and Hammering (d).

cap is presented to the KUKA-Allegro hand-arm system, and also held firmly during task execution, by another robot. For the Hammering task, a human hands the tool to the robot according to where the task is to be performed. The tool is held in place by the human till the robot hand completes the grasp. The graspable region of both tools is covered with padding material, firstly, to enlarge it to make it suitable for grasping by the Allegro hand and secondly, to increase compliance and friction between the object and the hand.

### Primitive basis for the Allegro hand

On the Allegro hand, using the first 2 thumb-joints, thumb orientation can be changed such that its grasping surface can oppose finger sides, the palm and the finger surfaces. Thus all 5 opposition categories identified earlier for the human

hand (see Section 4.4) can be realized with the Allegro hand. Additionally, due to the large size of the finger links, two different intentions can be identified when the thumb opposes finger surface according to whether oppositional pressure is focused towards the distal or the proximal ends. Figure 4.26 shows the primitive basis defined for the Allegro hand. As with the human hand model, each primitive is defined in terms of foci and supporting patches for the two opposing virtual fingers, the opposition vector and Primitive Reference Frame (PRF) and a preshape pose.

#### Hand closure under oppositional intention

Control of the allegro hand to realize the opposition primitives is achieved using existing work done in our lab for active compliance with tactile sensing (Sommer and Billard, 2015). In this work, the operational space framework (Khatib, 1987) is used to control contact forces on the finger links in contact coordinates. Joint torques for additional operational space goals, such as increasing the number of contacts or driving exploration of a surface, are incorporated without affecting the operational space acceleration, using the null-space of the contact Jacobian. Contact localization and force information is obtained via Tekscan sensing patches which cover the finger surfaces and thumb (Figure 4.25a).

For grasping purposes, this framework can be used to realize hand closure under known oppositional intention. The definition of an opposition primitive provides information on preshape and desired contacts along with the desired contact force distribution (corresponding to foci and supporting regions). Desired contact points for which no contact force is perceived (i.e not yet in contact) are driven towards each other using an impedance controller. The controller follows a direction determined by the line joining the centroid of the opposing foci. Once contact is detected, control for the joints influencing that contact switches to force control which allows for compliant behaviour. The net result after hand closure is that the contacts and forces which result, are oriented towards achieving a higher level oppositional intention. Figure 4.27 illustrates this for the primitive $O^{TS}_{FSH234}$. We may note here that, the position and orientation of the opposition vector in the graspable region (the grasp hypothesis), comes from higher level planning that is responsible for how oppositional intention gets applied to the object.

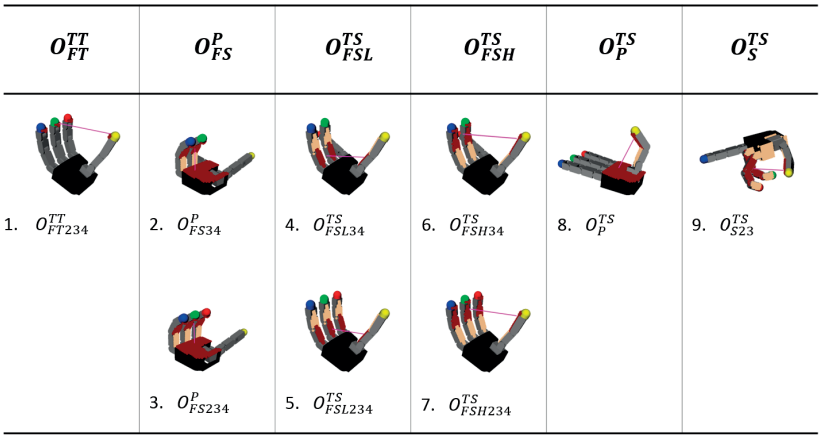


**Figure 4.26:** Primitive basis for the Allegro hand. For each primitive, the following can be observed : opposing virtual finger pair and preshape pose, focus regions (where pressure is focussed) and supporting regions in dark and light colors respectively, opposition vector. Primitive nomenclature is the same as for the human hand (Section 4.4.1). Allegro fingers are denoted by numbers 2,3,4 in the primitive labels. The thumb (finger 1) is denoted as T

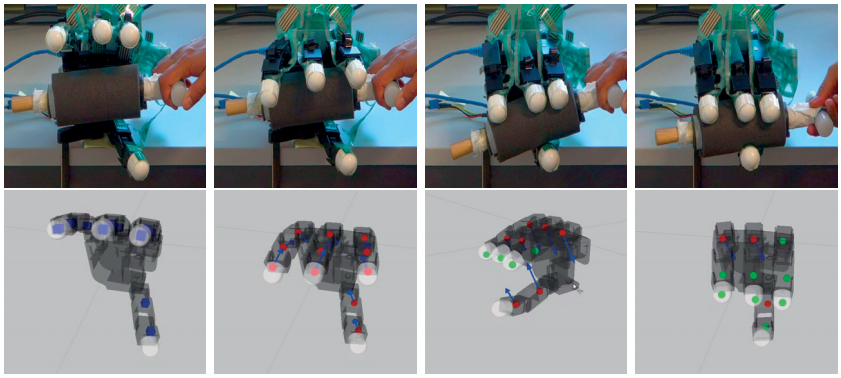

**Figure 4.27:** The figure shows different stages in hand closure for the primitive $O^{TS}_{FSH234}$ : preshape (leftmost column), closure (middle two columns), and grasping (rightmost column). The bottom row visualizes the information guiding motion of the links. Desired contacts are indicated in blue in the preshape. These change to red with arrows indicating the direction of motion during the closure phase. Color changes to green once contact is detected.

### 4.8.2 Open Cap Task

The framework for task-oriented hand-arm configuration is implemented using the OpenRave simulator (Diankov, 2010) with models for the Allegro hand and Kuka-LWR arm[7]. This is applied to the Open-Cap task using the task model defined in Section 4.5.1. After executing Phase 1 and Phase 2 of the algorithm (see Section 4.5.3) we obtain hand-arm configurations that can be examined according to task-oriented quality. Figure 4.28 shows the results, plotting hand quality against arm quality, similarly to what was done in the human model case (Section 4.7). Each point in the result plot represents a hand-arm configuration $\left[p, T^{GRF}_{PRF}, \theta_a, Q_{\Lambda_{hand}}, Q_{\Lambda_{arm}}\right]$, where $p, T^{GRF}_{PRF}$ denotes the oppositional intention and how it is applied to the graspable region, $\theta_a$ denotes the arm configuration

[7]The kinematic models correspond exactly to the real robot system so all planning decisions in OpenRave can be directly applied

and $Q_{\Lambda_{hand/arm}}$ denote the task-oriented hand and arm quality computed for a given configuration.

To identify suitable configurations which can be executed on the real robot hand-arm system, we look for the best compromise between hand and arm quality by examining the top-right quadrant of the result plot. A range of configurations in this region can be delimited using Algorithm 2. Noting that high quality grasps can yield low quality arm configurations and conversely, minimum requirements on hand/arm quality are enforced before using a linear combination of the two qualities to rank hand-arm configurations. Represented in bold are the outcome of applying this algorithm with a window size of $n = 20$. The top 5 configurations within the 20 element window are visualized in Figure 4.30. The use of Equation (4.5) in Algorithm 2 allows a trade-off to be made between hand quality with arm-quality by changing the values of $\lambda_1$ and $\lambda_2$ so that the selected configurations can be biased towards stronger arm quality (left column) or stronger hand quality (right column).

**Algorithm 2** Identify $n - best$ from $\{\mathcal{C}_{HA}\}_1^N$ hand-arm configurations

**Input:** $n, \quad Q_H \in \mathbb{R}^N, \quad Q_A \in \mathbb{R}^N, \quad \lambda_1, \quad \lambda_2, \quad \{\mathcal{C}_{HA}\}_1^N$
**Output:** $\{\Psi_{HA}\}_1^n$

$u_H \leftarrow \max\left\{Q_H(c) \,\middle|\, Q_A(c) > \frac{1}{2} \max Q_A\right\}_{\forall\, c\in[1\ldots N]}$, $l_H \leftarrow \frac{1}{2}u_H$
$l_A \leftarrow \frac{2}{3} \max Q_A$
$\Psi_{HA} = \varnothing$
**while** $|\Psi_{HA}| < n$ **do**
    $\Psi_{HA} \leftarrow \Psi_{HA} + \mathcal{S}_{HA}\left(\{\mathcal{C}_{HA}(c) \,|\, l_H \leq Q_H(c) \leq u_H,\ Q_A(c) \geq l_A\}_{\forall\, c\in[1\ldots N]}\right)$
    $\{\mathcal{S}_{HA}$ selects $n{-}best$ configurations ranked according to $\lambda_1 * Q_H + \lambda_2 * Q_A\}$
    $l_A \leftarrow l_A - 0.1$
**end while**

### Task execution

The selected configurations can then be used to execute the task on the real robot hand-arm system. Executing the task involves the following steps:

1. The hand assumes the pre-shape pose associated primitive $p$ and the arm is driven to the configuration $\theta_a$. These operations happen simultaneously and serve to position the oppositional intention in the graspable region.

2. The hand is closed using the hand-closure method outlined earlier (Section 4.8.1). Any mismatch of the opposing grasping surfaces (the foci regions in the primitive definition) with the object is manually corrected. The grasp is then tightened by increasing angles of those joints which will move the foci regions closer together.

3. To execute the task, the end-effector of the arm is rotated around the principal axis of the bottle at a speed of 5°/ second. Rotation continues till joint

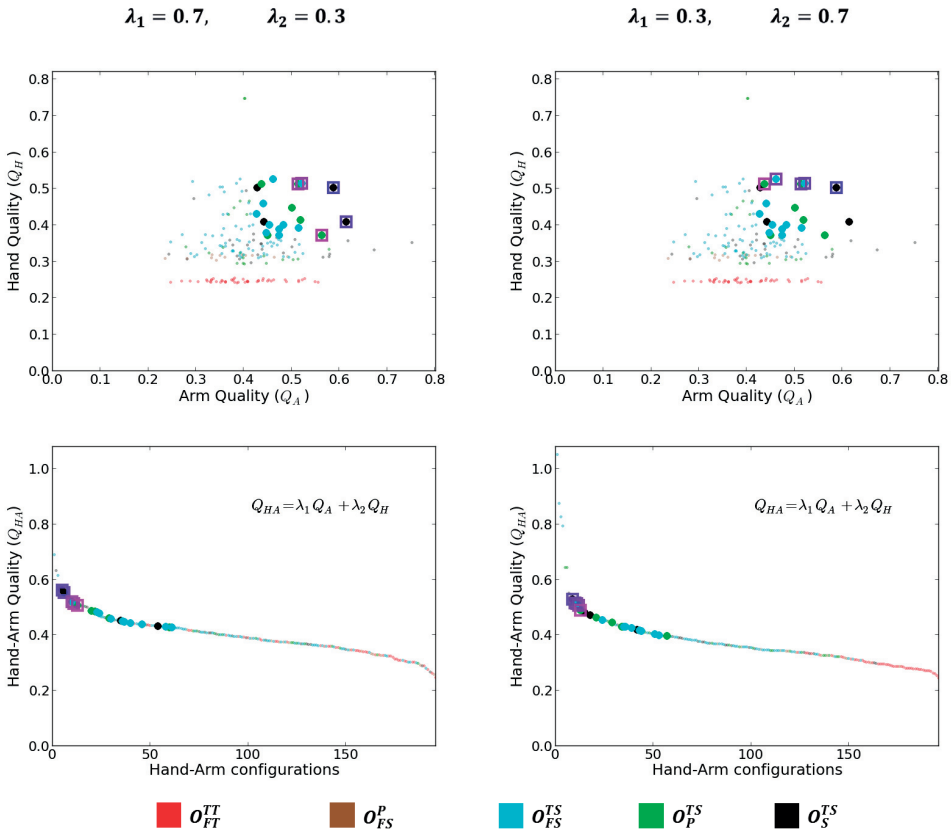


**Figure 4.28:** The plots shows Hand-Arm configurations identified for the Open-Cap task. The upper row shows hand quality ($Q_H$) plotted against increasing arm quality ($Q_A$). The bottom row shows a different view. The same configurations are plotted in decreasing order of hand-arm quality ($Q_{HA}$) computed according to $\lambda_1 Q_A + \lambda_2 Q_H$. A window of 20 configurations is selected according to Algorithm 2. These are shown in bold dots. The top 5 of these are highlighted in both views. The selection is biased towards greater arm quality in the left column and towards greater hand quality in the right column.

limits are encountered.

Figure 4.30 illustrates this for one open-cap configuration ( 4.29a). Turning of the cap was observed without slippage in the grasp. For the configurations in Figure 4.29, the arm is well positioned for opening tighter caps also. Joint torques[8] required for delivering a turning torque of 5Nm (corresponding to a very tight cap), vary between 0.4%-12% of their maximum capacity. This would be accompanied by a corresponding increase in oppositional force in the primitive. We discuss this further in Section 4.8.4.

[8]Estimated using the arm Jacobian of the identified configurations

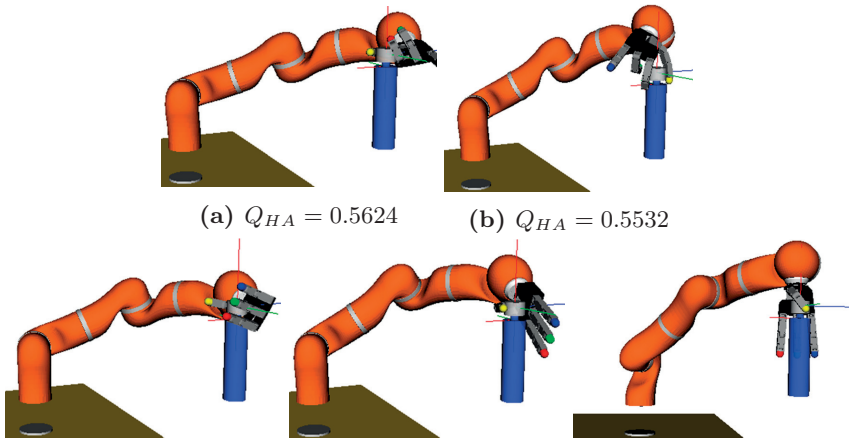

**(a)** $Q_{HA} = 0.5624$ **(b)** $Q_{HA} = 0.5532$

**(c)** $Q_{HA} = 0.5194$ **(d)** $Q_{HA} = 0.5139$ **(e)** $Q_{HA} = 0.5062$

**Figure 4.29:** (a)-(e) show the top 5 configurations selected for the Open-Cap task (see Figure 4.28), in descending order of hand-arm quality.

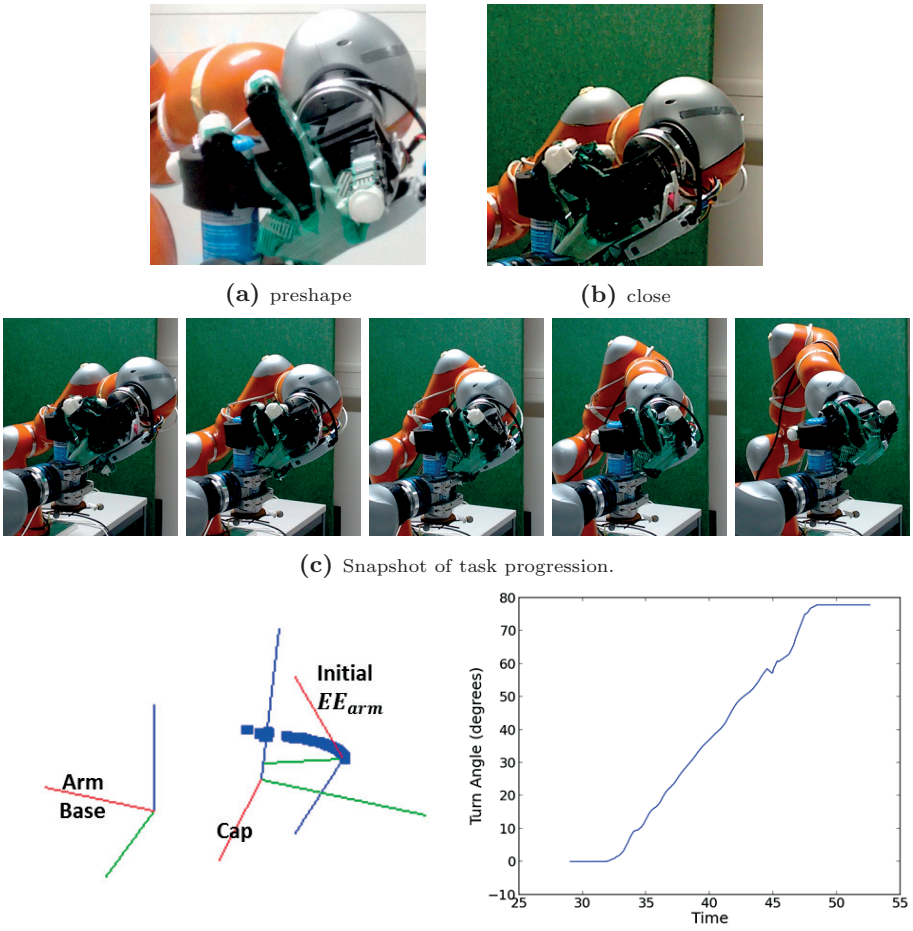


**(a)** preshape **(b)** close

**(c)** Snapshot of task progression.

**(d)** Trajectory and turning angle of the arm end-effector ($EE_{arm}$) over the task duration.

**Figure 4.30:** Implementation of (4.29a) on the real robot system.

### 4.8.3 Hammering Task

The framework is also applied to the Hammering task using the task model defined in Section 4.5.1. For the task of hammering, 3 different directions for performing the task in the environment were determined: downward, sideways (such as against a wall), and upward (such as against a ceiling). The best configurations identified are shown in Figure 4.31. Implementation on the real robot hand-arm system is shown in Figures 4.32, 4.33 and 4.34 . Task execution proceeds in a manner similar to the Open-Cap case (Section 4.8.2). To simulate the action of the hammering, the KUKA arm is controlled to move the hammer-head back and forth (i.e. $\pm\hat{z}$ of the end-effector reference frame (ERF)) with a predetermined velocity profile. For the configurations identified, expected joint torques for delivering a hammering force of 20N (along $\pm\hat{z}$ of the ERF) vary between 0.12%-8% of the maximum joint torque capacity.

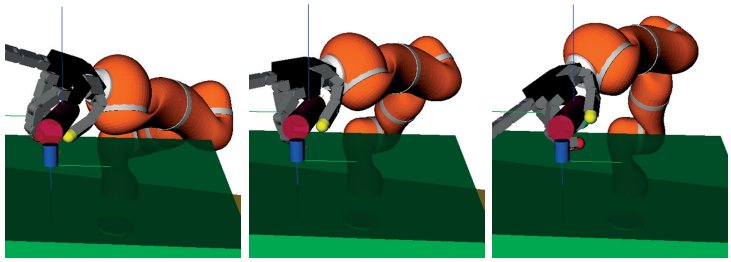

**(a) hammering downward**

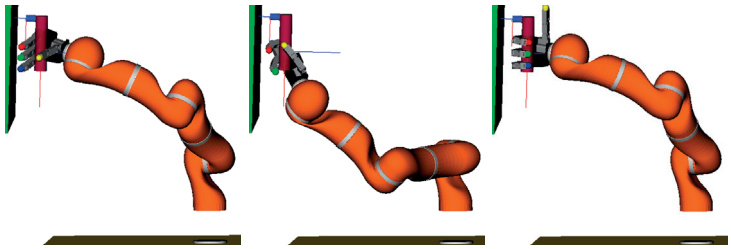

**(b) hammering sideways** (such as against a wall)

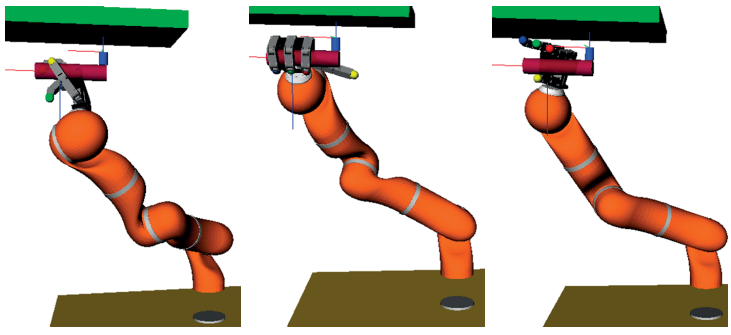

**(c) hammering upward** (such as against the ceiling)

**Figure 4.31:** Optimal hand-arm configurations identified for hammering taking $\lambda_l = 0.7$ and $\lambda_2 = 0.3$ in each case

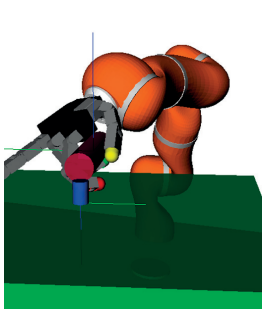

(a) hand-arm configuration

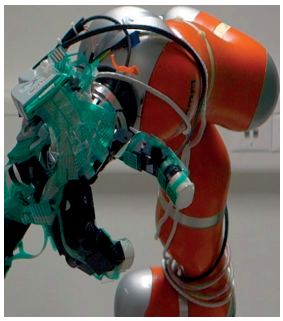

(b) preshape

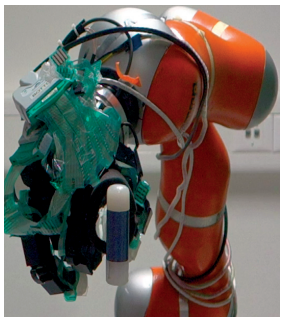

(c) close

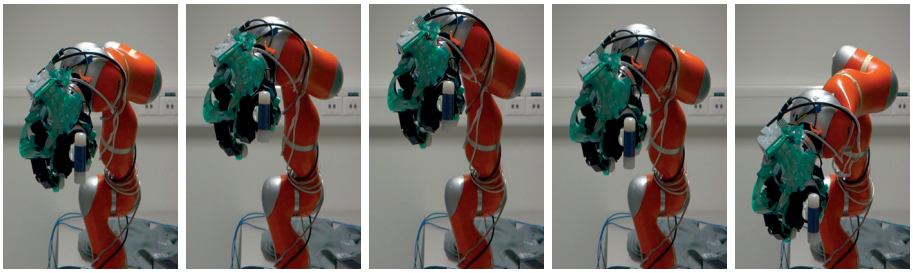

(d) Snapshot of task progression

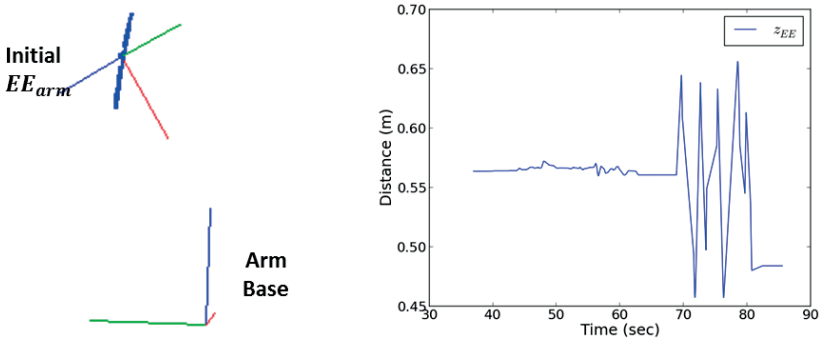


(e) Trajectory and $z$ coordinate of the arm end-effector ($EE_{arm}$) over the task duration.

**Figure 4.32:** Implementation of downward hammering on the real robot system.

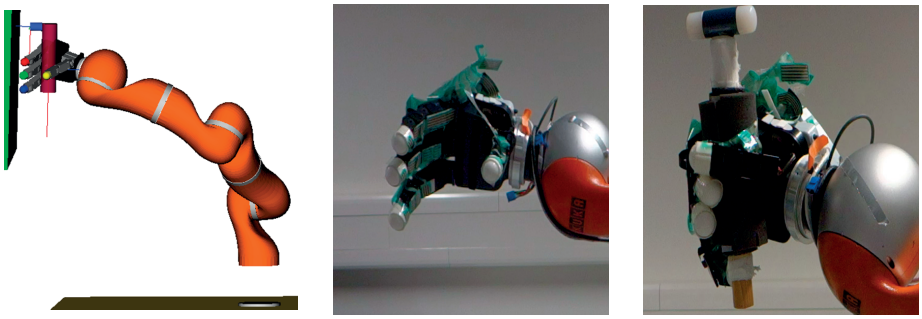

(a) hand-arm configuration (b) preshape (c) close

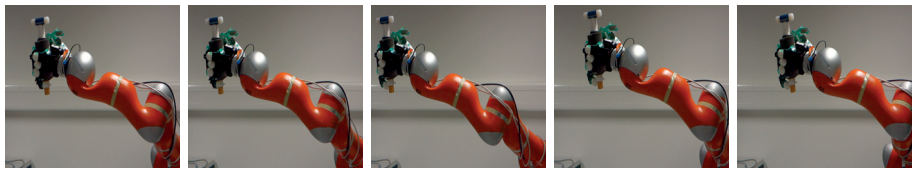

(d) Snapshot of task progression

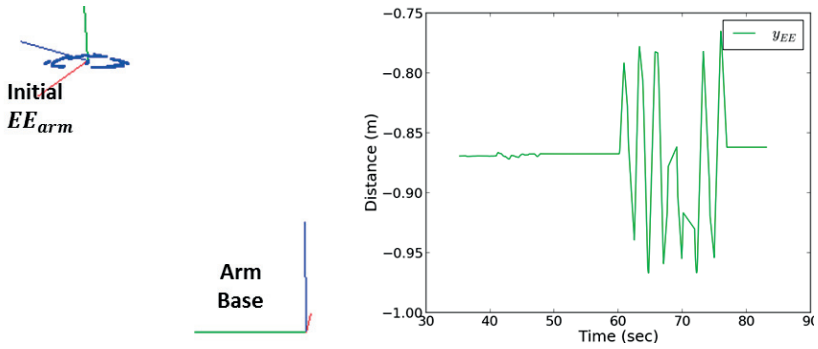


(e) Trajectory and $z$ coordinate of the arm end-effector ($EE_{arm}$) over the task duration.

**Figure 4.33:** Implementation of sideways hammering on the real robot system.

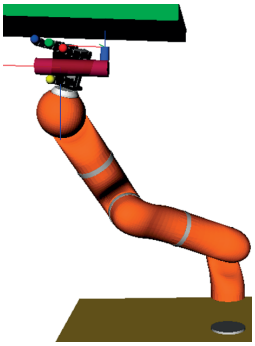

**(a)** hand-arm configuration

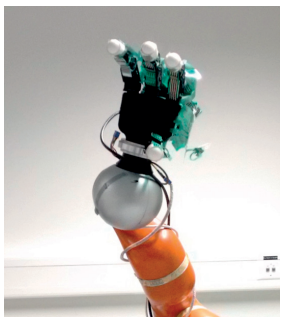

**(b)** preshape

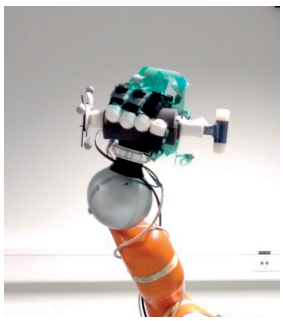

**(c)** close

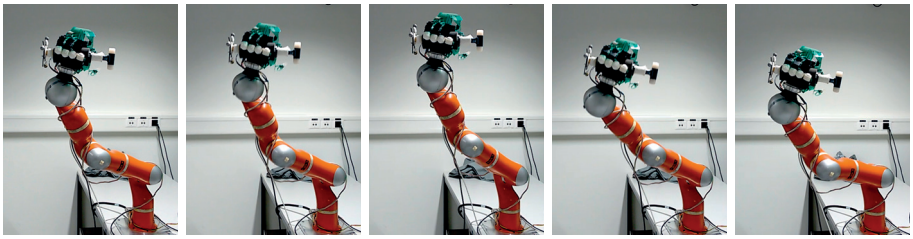

**(d)** Snapshot of task progression

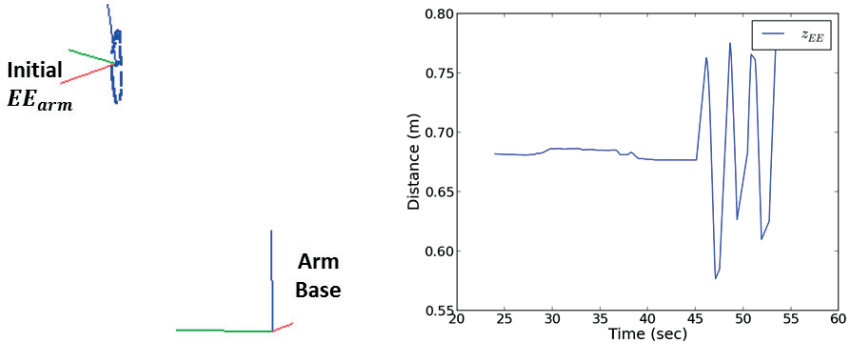


**(e)** Trajectory and $z$ coordinate of the arm end-effector ($EE_{arm}$) over the task duration.

**Figure 4.34:** Implementation of upward hammering on the real robot system.

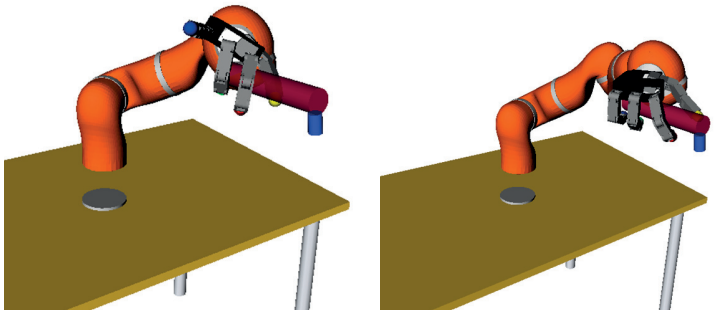

**(a)** Left image shows the good arm configuration discovered with the single primitive grasp. In the right image, the grasp is strengthed by modulating existing oppositional intention and adding a new one.

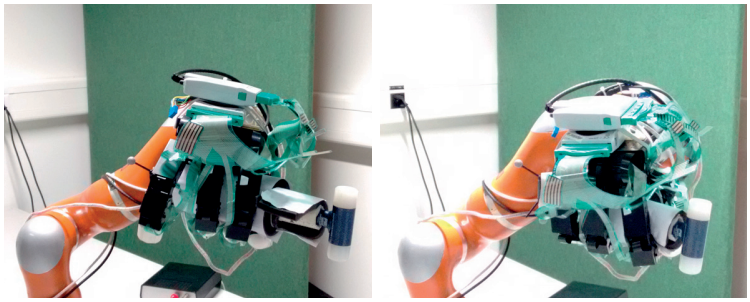

**(b)** Configurations of (a) shown on the real robot.

**Figure 4.35:** Strengthening the grasp by adapting the hand configuration with small changes to the good arm configuration discovered.

### 4.8.4 Discussion

The single primitive grasps selected may not be sufficient to keep the hammer stable or prevent slippage of the cap during turning when stronger forces (than those tested with) are involved. This requires a real-time strategy which observes and characterizes the state of the hand-object interaction and modulates the internal opposing forces or the grasp structure itself. This is an open research question which has been addressed in our lab for the case of finger-tip grasps (Li et al., 2014; Hang et al., 2014a).

It is worthwhile to note however, that the selected grasps discover good arm configurations from a manipulability perspective (i.e. ability to generate forces and motions in the task directions). They can be used as a starting points from which to build up a stronger grasp by local adaptation of the oppositional intention and adding other components to increase grasp strength. For instance, Figure 4.35 shows how a configuration of Figure 4.31a can be adapted to stabilize the hammer head so that it is always directed appropriately, while using fingers against palm to provide the overall robustness.

## 4.9 Conclusion

For accomplishing tasks such as hammering, cutting, screw-driving and opening a bottle cap, with a robotic manipulator connected to a dexterous hand, we must be able to evaluate both hand and arm capabilities in the light of task requirements. Simply optimizing the arm configuration to meet task goals is not a valid solution as there is no guarantee that the object can be stably grasped. Conversely, finding stable grasps in isolation can make it impossible or inefficient for the arm to perform the task.

In this chapter, we examined the effect of two strategies for grasp planning on the overall suitability of the hand-arm configuration for the task. The first gave importance to different oppositional intentions possible for the anthropomorphic hand whereas the second sought the $k - strongest$ grasps from a force-closure perspective. To achieve this, we modelled the task based on the essential directional forces and motion required for accomplishing task goals. Metrics were devised for the hand and arm based on their ability to provide directional force and motion. Information encoded in the primitive definition was necessary to identify and localize the different directional qualities possible for the hand and assess this against task requirements. We used both human and robotic hand-arm models to conduct the evaluation.

The results demonstrate that regardless of the grasp strategy employed, the strongest reachable grasp is not associated with good arm quality for the task. A trade-off must always be made between hand and arm capabilities to reach the best hand-arm configuration for accomplishing task goals. In light of this, a primitive-based approach explores a larger object relative wrist-pose space connected with a broader range of hand quality. This allows a larger space of arm configurations over which arm quality can be optimized and traded off with hand quality. A primitive-based approach can find relatively good grasps when the $k - strongest$ method fails, and finds comparatively good ones when the $k - strongest$ method succeeds. A component based method allows for weaker components to first discover good arm configurations and then be strengthened by locally modulating its properties or combining with other components.

Incorporating a sense of absolute values into the proposed approach for primitive-based hand-arm configuration would significantly broaden its applicability. In particular, discovering both low and high quality grasps with good arm quality is only useful for application if we know the magnitude of task disturbances expected and whether they can be countered. Additional task criteria, such as range and resolution, as well as more accurate indicators of force and motion capability for the hand and the arm, would enable us to make choices that are better adapted to the task.

Chapter 5

# Conclusion

In this chapter, we summarize the main contributions of this thesis and discuss the limitations and potential working directions for future work.

## 5.1 Main Contributions

Throughout this thesis we have emphasized the notion of encoding the functional role of fingers into the hand representation, as a means for harnessing the flexibility available to anthropomorphic hands towards task requirements. Towards this end, we leveraged different oppositional intentions possible for the hand. The main contributions of this dissertation are summarized below.

### Hand representations correlated with function

We compare hand representation schemes on how suited they are for discriminating between grasps of different functionality. We propose 2 parameterizations based on opposition and contrast them with commonly used methods, namely: joint angles, joint synergies and shape features. Opposition parameters display a strong correlation with human ranking of a grasp taxonomy based on precision and power. This was not observed for shape parameters. Projecting hand-surfaces impacting the object to their pre-shape pose, allowed to significantly reduce the number of opposition parameters required. Similar results obtained indicates that the underlying oppositional intention, as encoded by the general location of oppositional pressure and the size of the opposing grasping surfaces, is important for discriminating function.

### Interpreting human grasp behaviour

This thesis proposes a general approach to separate out and assign importance to multiple cooperating oppositional intentions in a grasp demonstration. Our method uses both interaction force and joint data as obtained from a data glove covered with tactile sensors. We propose an information template for oppositional intention which can be instantiated in the context of a grasp demonstration to obtain a measure of likelihood. Central to our method is a new way of examining tactile and joint data; by quantifying strength of pairwise interactions between the elements of a patch-decomposition imposed on the grasping

surface of hand, where all sensory elements of a single patch are assumed to act cohesively. This view better exposes the different oppositional roles of a single patch, than if tactile and joint data are taken separately or concatenated. Previous works, limited to identifying a single taxonomy category, lack instruction on how to recreate or adapt the grasp identified. To the best of our knowledge this is the first work to separate out and prioritize multiple and overlapping oppositional intentions from a grasp demonstration. The method is given thorough evaluation with humans over a wide range of grasp behaviour. Grasp scenarios combining different oppositional intentions, using both expert and naïve demonstrators, can be characterized successfully.

### Task-oriented hand-arm configuration

We provide a way of improving task performance of the overall hand-arm system by using weaker grasp components to find good arm configurations for the task. The different oppositional intentions for the hand make it possible to expose a variety of grasps to the arm for which directional qualities can be quantified and compared with task requirements. Hand-closure instructions and force-distribution encoded in an opposition primitive, aid in the characterization of directional quality without precise knowledge of contacts. The final hand-arm configuration is found by choosing the best compromise between hand quality and arm quality in the task context. Tests with tasks of cutting, hammering, screw-driving and opening a bottle cap show that our method can find better configurations for the arm when the strongest grasps constrain the arm poorly, and similar configurations when not. The proposed method is independent of hand and arm morphology and was applied to both human and robotic hand-arm systems.

### Capturing human hand response

This thesis proposes several advancements through which a more complete picture of human hand grasping response can be obtained. Noting the different oppositional roles adopted by the thumb in many commonly encountered tasks, we separate thumb action from palm action and include more comprehensive description for side-opposition. This leads to the opposition categories – $O^{TS}_{FS}$, $O^{TS}_{P}$, $O^{TS}_{S}$ – by which these oppositional roles can be recognized and reasoned with independently. To correctly detect these oppositional roles from human demonstration, we instrumented both front and sides of a data glove with tactile sensors and captured the oppositional geometry of thumb patches by modelling thumb-twist in the kinematic model and the non-linear relationships in the joint sensors of the data glove.

## 5.2 Perspectives on opposition-based grasping

This thesis pursued an opposition-based representation for grasping. This presents a different approach to the problems of task-oriented configuration of an anthropomorphic hand-arm system which parallels the current prevailing methods. Based on the results achieved in this thesis and taking inspiration from existing thinking on the topic (MacKenzie and Iberall, 1994), we may speculate on what a 'parallel universe' of opposition-based grasping looks like.

The goal of grasping would be to harness all flexibility available to the hand, towards the task, in conjunction with the task-oriented action of the entire embodiment. Task relevant capabilities offered by different sub-grasps of the hand would be encoded using an opposition-based representation. These would be available for functional reasoning against task requirements, matching with object grasping affordance and optimizing the whole embodiment during the planning stage. The chosen primitive-based representation of the desired grasp and its localization on the object would then serve as the invariant to drive reaching, pre-shaping and closing dynamics. Finally, during task execution, the goal of proprioception, vision and tactile sensing would be to monitor and control the exercise of functional abilities for which the specific opposition were chosen.

The questions of how to automatically detect and characterize properties of oppositional intention in a grasp as well as quantifying the task relevance of an opposition space and relating this to higher levels of the embodiment in a task context, assume importance for opposition-based grasping. This thesis provided strong steps forward in answer to these questions but also revealed limitations. We discuss these as well as future directions for research below.

### Grasp monitoring and adaptation

An opposition-based approach would necessarily require the means to characterize active oppositions and the extent to which hand capabilities are being manifested over the task duration. In Chapter 3 we have shown that oppositional intention can be reliably detected from the tactile and joint information present in a grasp. We considered only static grasps, but the real-time monitoring of the grasp state throughout the task duration would provide necessary control inputs by which the task relevant properties can be maintained and adapted. For grasp adaptation in a task relevant manner, opposition properties (such as grasping surface area, stiffness, opposing force, etc) would be modulated and/or grasp structure itself would be changed by transitioning to nearby opposition spaces.

### Interaction synergies

The grasp signature proposed in Chapter 3 is a distribution over 41 primitives.

Computational methods for planning always benefit from low dimensional representations. In Chapter 3 we presented the Patch Level Opposition (PLO) representation which integrates tactile and joint data into a 144-dimensional feature. This was used to assign importance to and separate out multiple cooperating oppositional intentions in a demonstrated grasp. This feature is part of an interaction space. It is possible that a low dimensional underlying representation exists in this space which is sufficient to represent variance across all types of oppositions possible for the hand. In contrast to joint-space synergies, interaction-based synergies would be more task relevant since they examine variance in how grasping surfaces will ultimately be used, and can be expected to have better correlation with hand function.

### Task relevance of opposition space

For discovering the hand-arm configurations adapted to the task, Chapter 4 identified essential directions for force and motion and measured efficiency of the hand/arm along these directions. A threshold on minimum quality was imposed to isolate the region for best compromise between hand and arm. However, without absolute force and motion levels, it is possible that the thresholds chosen may allow configurations that are not adequate for the task. Conversely, configurations that are overly strong may also be considered. Future work may incorporate additional task criteria such as range and resolution along with better indicators for force and motion ability of the hand/arm. Furthermore, several other criteria important to real world task execution such as tactile sensitivity, stiffness/compliance can be added. These would enable the discovery of opposition spaces better adapted to task goals. Future researches may consider how to quantify these requirements in the task model, represent hand capabilities along these functional dimensions and, as discussed, also monitor their realization during task execution.

### Bottom-up grasp planning involving global objectives

Chapter 4 explored a strategy for grasp planning giving importance to different oppositional intentions possible for the anthropomorphic hand. Weak components proved best for discovering the good arm configurations for the task, since they least constrain the hand and can therefore explore are wider object-relative pose space. This motivates a bottom-up approach to hand configuration where flexibility available to the hand can be matched against global objectives in the grasp planning stage. Such a strategy would first coarsely sample the graspable region with single primitives to discover the good regions of the global configuration space. This is then refined by local adaptation which may: modulate the oppositional intention, adapt the wrist-pose, add new components or transition to new components, incorporating at each stage global objectives concerning hand, arm, object and task.

# References


Aleotti, J. and Caselli, S. Grasp recognition in virtual reality for robot pregrasp planning by demonstration. In *IEEE International Conference on Robotics and Automation*, 2006. 3.2, 3.3

Aleotti, J. and Caselli, S. Interactive teaching of task-oriented robot grasps. *Robotics and Autonomous Systems*, 58(5):539–550, 2010. 1.3.4, 4.3.2

Arbib, M. A., Iberall, T., and Lyons, D. Coordinated control programs for movements of the hand. *Experimental Brain Research*, 10:111–129, 1985. 1.2, 2.2.2

Asfour, T., Regenstein, K., Azad, P., Schröder, J., Bierbaum, A., Vahrenkamp, N., and Dillmann, R. ARMAR-III: An integrated humanoid platform for sensory-motor control. *IEEE-RAS International Conference on Humanoid Robots*, pages 169–175, 2006. 1.1, 4.2

Balasubramanian, R., Xu, L., Brook, P. D., Smith, J. R., and Matsuoka, Y. Physical human interactive guidance: Identifying grasping principles from human-planned grasps. *IEEE Transactions on Robotics*, 28(4):899–910, 2012. 1.3.2

Bekey, G. A., Tomovic, R., and Karplus, W. J. Knowledge-based control of grasping in robot hands using heuristics from human motor skills. *IEEE Transactions on Robotics and Automation*, 9(6):709–722, 1993. 1.3.4, 4.3.1

Bekiroglu, Y., Song, D., Wang, L., and Kragic, D. A probabilistic framework for task-oriented grasp stability assessment. In *IEEE International Conference on Robotics and Automation*, pages 3040–3047. IEEE, 2013. 2.6

Ben Amor, H., Kroemer, O., Hillenbrand, U., Neumann, G., and Peters, J. Generalization of human grasping for multi-fingered robot hands. In *IEEE/RSJ International Conference on Intelligent Robots and Systems*, pages 2043–2050, 2012. 2.1, 3.3, 4.3.1

Berenson, D., Srinivasa, S., and Kuffner, J. Task Space Regions: A framework for pose-constrained manipulation planning. *The International Journal of Robotics Research*, 30(12):1435–1460, 2011. 1.3.4

Berenson, D. and Srinivasa, S. S. Grasp synthesis in cluttered environments for dexterous hands. In *IEEE-RAS International Conference on Humanoid Robots*, pages 189–196, 2008. 4.3.3

Berenson, D., Diankov, R., and Kuffner, J. Grasp planning in complex scenes. In *IEEE-RAS International Conference on Humanoid Robots*, pages 42–48, 2007. 4.3.3

Berenson, D., Srinivasa, S. S., Ferguson, D., Collet, A., and Kuffner, J. J. Manipulation planning with Workspace Goal Regions. *IEEE International Conference on Robotics and Automation*, pages 618–624, 2009. 1.3.4

Bernardin, K., Ogawara, K., Ikeuchi, K., and Dillmann, R. A sensor fusion approach for recognizing continuous human grasping sequences using hidden Markov models. *IEEE Transactions on Robotics*, 21(1), 2005. 3.2, 3.3

Bernardino, A., Henriques, M., Hendrich, N., and Zhang, J. Precision grasp synergies for dexterous robot hands. In *IEEE International Conference on Robotics and Biomimetics (ROBIO)*, 2013. 2.1, 4.3.1

Bicchi, A. and Kumar, V. Robotic grasping and contact: a review. In *IEEE International Conference on Robotics and Automation*, volume 1, pages 348–353. IEEE, 2000. 4.3.1

Bicchi, A. Hands for dexterous manipulation and robust grasping: A difficult road toward simplicity. *IEEE Transactions on Robotics and Automation*, 16 (6):652–662, 2000. 1.1

Bohg, J., Morales, A., Asfour, T., and Kragic, D. Data-Driven Grasp Synthesis—A Survey. *IEEE Transactions on Robotics*, pages 1–21, 2013. 4.3.1

Bonilla, M., Resasco, D., Gabiccini, M., and Bicchi, A. Grasp planning with soft hands using bounding box object decomposition. In *IEEE International Conference on Intelligent Robots and Systems*, 2015. 1.3.3

Borst, C., Fischer, M., and Hirzinger, G. Grasping the dice by dicing the grasp. *IEEE/RSJ International Conference on Intelligent Robots and Systems*, 4, 2003. 4.3.1

Borst, C., Ott, C., Wimbock, T., Brunner, B., Zacharias, F., Bauml, B., Hillenbrand, U., Haddadin, S., Albu-Schaffer, A., and Hirzinger, G. A humanoid upper body system for two-handed manipulation. In *IEEE International Conference on Robotics and Automation*, pages 2766–2767, 2007. 1.1, 4.2, 4.8.1

Borst, C., Fischer, M., and Hirzinger, G. A fast and robust grasp planner for arbitrary 3D objects. In *IEEE International Conference on Robotics and Automation*, volume 3, 1999. 1.3.1, 4.3.1, 4.3.2

Borst, C., Fischer, M., and Hirzinger, G. Calculating hand configurations for precision and pinch grasps. In *IEEE/RSJ International Conference on Intelligent Robots and Systems*, volume 2, 2002. 1.3.1

Borst, C., Fischer, M., and Hirzinger, G. Grasp planning: how to choose a suitable task wrench space. *IEEE International Conference on Robotics and Automation*, 1, 2004. 4.3.2

Borst, C., Fischer, M., and Hirzinger, G. Efficient and Precise Grasp Planning for Real World Objects. In Barbagli, F., Prattichizzo, D., and Salisbury, K., editors, *Multi-point Interaction with Real and Virtual Objects*, volume 18 of *Springer Tracts in Advanced Robotics*, chapter 6, pages 91–111. Springer Berlin / Heidelberg, 2005. 1.3.4, 4.3.2, 4.5.2, 4.6.1, 4.6.1, 4.6.1, 3)

Brown, E., Rodenberg, N., Amend, J., Mozeika, A., Steltz, E., Zakin, M. R., Lipson, H., and Jaeger, H. M. Universal robotic gripper based on the jamming of granular material. *Proceedings of the National Academy of Sciences*, 107 (44):18809–18814, 2010. 1.3.3

Bullock, I. M., Zheng, J. Z., De La Rosa, S., Guertler, C., and Dollar, A. M. Grasp frequency and usage in daily household and machine shop tasks. *IEEE Transactions on Haptics*, 6(3):296–308, 2013. 3.3

Buscher, G., Koiva, R., Schurmann, C., Haschke, R., and Ritter, H. J. Tactile dataglove with fabric-based sensors. In *IEEE-RAS International Conference on Humanoid Robots*, pages 204–209, 2012. 3.4

Catalano, M. G., Grioli, G., Farnioli, E., Serio, a., Piazza, C., and Bicchi, a. Adaptive synergies for the design and control of the Pisa/IIT SoftHand. *The International Journal of Robotics Research*, 33(5):768–782, 2014. 1.3.3

Chalon, M., Grebenstein, M., Wimböck, T., and Hirzinger, G. The thumb: Guidelines for a robotic design. In *IEEE/RSJ International Conference on Intelligent Robots and Systems*, pages 5886–5893, 2010. 3.5.2

Chiu, S. L. Task Compatibility of Manipulator Postures. *The International Journal of Robotics Research*, 7(5):13–21, 1988. 4.5.2, 4.6.2

Ciocarlie, M. T. and Allen, P. K. Hand Posture Subspaces for Dexterous Robotic Grasping. *The International Journal of Robotics Research*, 28(7):851–867, 2009. 1.3.2, 4.3.1, 4.3.2, 3)

Curtis, N. and Xiao, J. Efficient and effective grasping of novel objects through learning and adapting a knowledge base. *IEEE/RSJ International Conference on Intelligent Robots and Systems*, pages 2252–2257, 2008. 1.3.2

Cutkosky, M. R. On grasp choice, grasp models, and the design of hands for manufacturing tasks. *IEEE Transactions on Robotics and Automation*, 5(3): 269–279, 1989. 2.3, 3.2, 3.3, 4.3.1

Cutkosky, M. R. and Howe, R. D. Human Grasp Choice and Robotic Grasp Analysis. In *Dextrous Robot Hands*, pages 5–31. Springer-Verlag New York, 1990. 2.1

Cutkosky, M. R. and Kao, I. Computing and controlling the compliance of a robotic hand. *IEEE Transactions on Robotics and Automation*, 5(2):151–165, 1989. 1.3.3

Cutkosky, M. R. and Wright, K. Modeling manufacturing grips and correlations with the design of robotic hands. *IEEE International Conference on Robotics and Automation*, 3:1533–1539, 1986. 1.3.4

Cyberglove, . www.cyberglovesystems.com. 2.5, 3.4.1, 3.4.2

Dahiya, R. S., Metta, G., Valle, M., and Sandini, G. Tactile sensing-from humans to humanoids. *IEEE Transactions on Robotics*, 26(1):1–20, 2010. 3.4

Deimel, R. and Brock, O. A Novel Type of Compliant and Underactuated Robotic Hand for Dexterous Grasping. *The International Journal of Robotics Research*, 2015. 1.3.3

Diankov, R. *Automated construction of robotic manipulation programs*. PhD thesis, CMU-RI-TR-10-29. Carnegie Mellon University, 2010. 4.8.2

Ding, D., Liu, Y. H., and Wang, S. Computation of 3-D form-closure grasps. *IEEE Transactions on Robotics and Automation*, 17(4):515–522, 2001. 1.3.1, 4.3.1

Dipietro, L., Sabatini, A. M., and Dario, P. A survey of glove-based systems and their applications. *IEEE Transactions on Systems, Man and Cybernetics Part C: Applications and Reviews*, 38(4):461–482, 2008. 3.4

Dogar, M. R. and Srinivasa, S. S. Push-grasping with dexterous hands: Mechanics and a method. In *IEEE/RSJ International Conference on Intelligent Robots and Systems*, pages 2123–2130, 2010. 1.3.3

Dollar, A. M. and Howe, R. D. The Highly Adaptive SDM Hand: Design and Performance Evaluation. *The International Journal of Robotics Research*, 29 (5):585–597, 2010. 1.3.3

Dollar, A. M. and Howe, R. D. Simple, robust autonomous grasping in unstructured environments. In *IEEE International Conference on Robotics and Automation*, pages 4693–4700, 2007. 1.3.3

Doty, K., Melchiorri, C., and Bonivento, C. A critical review of the current kinematic- and dynamic- manipulability theory. In *Third International Workshop on Advances in Robot Kinematics*, 1992. 4.6.2

Doty, K. L., Melchiorri, C., Schwartz, E. M., and Bonivento, C. Robot manipulability. *IEEE Transactions on Robotics and Automation*, 11(3):462–468, 1995. 4.6.2

Ekvall, S. and Kragic, D. Grasp Recognition for Programming by Demonstration. In *IEEE International Conference on Robotics and Automation*, 2005. 2.1, 3.2, 3.3

Ekvall, S. and Kragic, D. Learning and Evaluation of the Approach Vector for Automatic Grasp Generation and Planning. *IEEE International Conference on Robotics and Automation*, (April):4715–4720, 2007. 1.3.2, 3.3

El-Khoury, S. and Sahbani, A. On computing robust n-finger force-closure grasps of 3D objects. *IEEE International Conference on Robotics and Automation*, pages 2480–2486, 2009. 1.3.1, 4.3.1

El-Khoury, S., Sahbani, A., and Perdereau, V. Learning the natural grasping component of an unknown object. *International Conference on Intelligent Robots and Systems*, pages 2957–2962, 2007. 1.3.4

El-Khoury, S., Li, M., and Billard, A. On the generation of a variety of grasps. *Robotics and Autonomous Systems*, 61(12):1335–1349, 2013. 1.3.1, 4.3.1

El-Khoury, S., De Souza, R., and Billard, A. On computing task-oriented grasps. *Robotics and Autonomous Systems*, 66:145–158, 2015. 1.3.4, 4.2, 4.3.2, 4.5.1

Eppner, C. and Brock, O. Grasping unknown objects by exploiting shape adaptability and environmental constraints. In *IEEE International Conference on Intelligent Robots and Systems*, pages 4000–4006, 2013. 1.3.3

Eppner, C., Bartels, G., and Brock, O. A compliance-centric view of grasping. Technical report, Department of Computer Engineering and Microelectronics, Technical University Berlin, 2012. 1.3.3

Eppner, C., Deimel, R., Álvarez Ruiz, J., Maertens, M., and Brock, O. Exploitation of environmental constraints in human and robotic grasping. *The International Journal of Robotics Research*, 34(7), 2015. 1.3.3

Faria, D. R., Martins, R., Lobo, J., and Dias, J. Extracting data from human manipulation of objects towards improving autonomous robotic grasping. *Robotics and Autonomous Systems*, 60(3):396–410, 2012. 3.3, 3.4, 3.6.3

Feix, T., Pawlik, R., Schmiedmayer, H., Romero, J., and Kragic, D. A comprehensive grasp taxonomy. In *Robotics, Science and Systems: Workshop on Understanding the Human Hand for Advancing Robotic Manipulation*, 2009. 2.1, 2.3, 2.3a, 3.5.2, 3.7.3, 3.1

Ferrari, C. and Canny, J. Planning optimal grasps. In *IEEE International Conference on Robotics and Automation*, pages 2290–2295, 1992. 4.2, 4.3.2, 4.6.1, 4.6.1

Finotello, R., Grasso, T., Rossi, G., and Terribile, A. Computation of kinetostatic performances of robot manipulators with polytopes. In *IEEE International Conference on Robotics and Automation*, volume 4, 1998. 4.6.2

Friedrich, H., Grossmann, V., Ehrenmann, M., Rogalla, O., Zollner, R., and Dillman, R. Towards cognitive elementary operators: grasp classification using neural network classifiers. In *International Conference on Intelligent Systems and Control*, 1999. 2.1, 3.2, 3.3

Goldfeder, C. and Allen, P. K. Data-driven grasping. *Autonomous Robots*, 31 (1):1–20, 2011. 1.3.2

Goldfeder, C., Allen, P. K., Lackner, C., and Pelossof, R. Grasp Planning via Decomposition Trees. In *IEEE International Conference on Robotics and Automation*, pages 4679–4684, 2007. 1.3.2, 4.3.1, 4.3.2

Grebenstein, M. *Approaching Human Performance The Functionality-Driven Awiwi Robot Hand*. PhD thesis, ETH Zurich, 2014. 3.5.2

Griffin, W. B., Findley, R. P., Turner, M. L., and Cutkosky, M. R. Calibration and Mapping of a Human Hand for Dexterous Telemanipulation. In *ASME IMECE Symposium on Haptic Interfaces for Virtual Environments and Teleoperator Systems*, pages 1–8, 2000. 3.4.2, 3.4.3

Hang, K., Li, M., Stork, J. A., Bekiroglu, Y., Billard, A., and Kragic, D. Hierarchical fingertip space for synthesizing adaptable fingertip grasps. In *Workshop on Autonomous Grasping and Manipulation: An Open Challenge. ICRA*, 2014a. 4.8.4

Hang, K., Stork, J. A., and Kragic, D. Hierarchical fingertip space for multifingered precision grasping. In *IEEE/RSJ International Conference on Intelligent Robots and Systems*, 2014b. 1.3.1, 4.3.1

Harada, K., Kaneko, K., and Kanehiro, F. Fast grasp planning for hand/arm systems based on convex model. In *IEEE International Conference on Robotics and Automation*, pages 1162–1168, 2008. 2.1, 4.3.1

Haschke, R., Steil, J., Steuwer, I., and Ritter, H. Task-oriented quality measures for dextrous grasping. *International Symposium on Computational Intelligence in Robotics and Automation*, 2005. 1.3.4, 4.3.2, 4.5.2

Heinemann, F., Puhlmann, S., Eppner, C., Alvarez-Ruiz, J., Maertens, M., and Brock, O. A Taxonomy of Human Grasping Behavior Suitable for Transfer to Robotic Hands. In *IEEE International Conference on Robotics and Automation*, 2015. 1.3.3

Herzog, A., Pastor, P., Kalakrishnan, M., Righetti, L., Bohg, J., Asfour, T., and Schaal, S. Learning of grasp selection based on shape-templates. *Autonomous Robots*, 36(1-2):51–65, 2014. 1.3.2

Hillenbrand, U., Brunner, B., Borst, C., and Hirzinger, G. The robutler: a vision-controlled hand-arm system for manipulating bottles and glasses. In *35th International Symposium on Robotics*, 2004. 1.3.4

Hu, H., Gao, X., Li, J., Wang, J., and Liu, H. Calibrating human hand for teleoperating the HIT/DLR hand. In *IEEE International Conference on Robotics and Automation*, volume 5, 2004. 3.3, 3.4.2, 3.4.3

Huebner, K. and Kragic, D. Selection of robot pre-grasps using box-based shape approximation. In *IEEE International Conference on Intelligent Robots and Systems*, pages 1765–1770, 2008. 1.3.2, 4.3.1, 4.3.2

Iberall, T. The nature of human prehension: three dexterous hands in one. In *IEEE Int. Conf. on Robotics and Automation*, volume 4, pages 396–401. IEEE, 1987. 1.2, 3.2, 3.5.2, 3.7

Iberall, T. Human prehension and dexterous robot hands. *The International Journal of Robotics Research*, 16(3):285–299, 1997. 1.2

Iberall, T., Bingham, G., and Arbib, M. A. Opposition space as a structuring concept for the analysis of skilled hand movements. *Experimental Brain Research*, 15:158–173, 1986. 1.2, 1.2, 1.2.1, 2.7.1

Iberall, T., Torras, C., and Mackenzie, C. Parameterizing Prehension: A mathematical model of opposition space. In *Cognitiva*, 1990. 1.2, 2.2.2, 2.3

Johansson, R. S. and Flanagan, J. R. Coding and use of tactile signals from the fingertips in object manipulation tasks. *Nature reviews. Neuroscience*, 10(5): 345–359, 2009. 3.2

Kahlesz, F., Zachmann, G., and Klein, R. 'Visual-fidelity' dataglove calibration. In *Proceedings of Computer Graphics International Conference, CGI*, pages 403–410, 2004. 3.3

Kamakura, N., Matsuo, M., Ishii, H., Mitsuboshi, F., and Miura, Y. Patterns of static prehension in normal hands. *The American journal of occupational therapy*, 34(7):437–445, 1980. 1.3.4, 3.2, 3.3, 3.6.3

Kaneko, K., Harada, K., Kanehiro, F., Miyamori, G., and Akachi, K. Humanoid robot HRP-3. In *IEEE/RSJ International Conference on Intelligent Robots and Systems*, pages 2471–2478, 2008. 1.1, 4.2

Kang, S. B. and Ikeuchi, K. Toward automatic robot instruction from perception-recognizing a grasp from observation. *IEEE Transactions on Robotics and Automation*, 9(4), 1993. 3.3

Kang, S. B. and Ikeuchi, K. Robot task programming by human demonstration: mapping human grasps to manipulator grasps. In *IEEE/RSJ International Conference on Intelligent Robots and Systems*, volume 1, 1994. 3.3

Kappler, D., Chang, L., Przybylski, M., Pollard, N., Asfour, T., and Dillmann, R. Representation of pre-grasp strategies for object manipulation. In *IEEE-RAS International Conference on Humanoid Robots, (Humanoids)*, pages 617–624, 2010. 1.3.3

Kazemi, M., Valois, J.-S., Bagnell, J. A., and Pollard, N. Robust Object Grasping Using Force Compliant Motion Primitives. In *Proceedings of Robotics: Science and Systems*, pages 1–8, 2012. 1.3.3

Khatib, O. A unified approach for motion and force control of robot manipulators: The operational space formulation. *IEEE Transactions on Robotics and Automation*, 3:43–53, 1987. 4.8.1

Kim, J., Iwamoto, K., Kuffner, J. J., Ota, Y., and Pollard, N. S. Physically based grasp quality evaluation under pose uncertainty. *IEEE Transactions on Robotics*, 29(6):1424–1439, 2013. 1.3.2

Kjellstrom, H., Romero, J., and Kragic, D. Visual recognition of grasps for human-to-robot mapping. In *IEEE/RSJ International Conference on Intelligent Robots and Systems*, 2008. 3.2, 3.3

Krug, R., Dimitrov, D., Charusta, K., and Iliev, B. On the efficient computation of independent contact regions for force closure grasps. *IEEE/RSJ International Conference on Intelligent Robots and Systems*, 2010. 1.3.1, 4.3.1

Lee, J. L. J. A study on the manipulability measures for robot manipulators. In *IEEE/RSJ International Conference on Intelligent Robot and Systems*, 1997. 4.6.2

Li, M., Bekiroglu, Y., Kragic, D., and Billard, A. Learning of Grasp Adaptation through Experience and Tactile Sensing. In *IEEE International Conference on Intelligent Robots and Systems*, pages 3339–3346, 2014. 4.8.4

Li, Y., Fu, J. L., and Pollard, N. S. Data-driven grasp synthesis using shape matching and task-based pruning. *IEEE Transactions on Visualization and Computer Graphics*, 13(4):732–747, 2007. 1.3.2, 1.3.4, 2.2.1, c), 4.2, 4.3.2

Li, Z. and Sastry, S. Task-oriented optimal grasping by multifingered robot hands. *IEEE Journal on Robotics and Automation*, 4(1), 1988. 1.3.4, 4.2, 4.3.2

Lin, Y. and Sun, Y. Robot grasp planning based on demonstrated grasp strategies. *The International Journal of Robotics Research*, 34(1):26–42, 2014. 1.3.4

Liu, J., Feng, F., Nakamura, Y. C., and Pollard, N. S. A Taxonomy of Everyday Grasps in Action. In *IEEE International Conference on Humanoid Robots*, pages 573–580, 2014. 1.3.5

MacKenzie, C. L. and Iberall, T. *The Grasping Hand*, volume 104. 1994. (document), 5.2

Michel, C., Remond, C., Perdereau, V., and Drouin, M. A robotic grasping planner based on the natural grasping axis. In *International Conference on Intelligent Manipulation and Grasping*, 2004. 1.3.2, 4.3.1, 4.4.2

Miller, A. T. and Allen, P. K. Graspit! a versatile simulator for robotic grasping. *IEEE Robotics Automation Magazine*, 11(December):110–122, 2004. 2.5

Miller, A., Knoop, S., Christensen, H., and Allen, P. Automatic grasp planning using shape primitives. In *IEEE International Conference on Robotics and Automation*, pages 1824–1829, 2003. 1.3.2, 4.3.1, 4.4.2, 4.4.2

Mirtich, B. and Canny, J. Easily computable optimum grasps in 2-D and 3-D. In *IEEE International Conference on Robotics and Automation*, pages 739–747, 1994. 1.3.1

Morales, A., Asfour, T., Azad, P., Knoop, S., and Dillmann, R. Integrated grasp planning and visual object localization for a humanoid robot with five-fingered hands. In *IEEE International Conference on Intelligent Robots and Systems*, pages 5663–5668, 2006. 1.3.4, 2.1, 4.3.1, 4.3.2

Murakami, K., Matsuo, K., Hasegawa, T., and Kurazume, R. A Decision Method for Placement of Tactile Elements on a Sensor Glove for the Recognition of Grasp Types. *IEEE/ASME Transactions on Mechatronics*, 15(1), 2010. 3.3, 3.4

Murray, R., Sastry, S., and Li, Z. *A Mathematical Introduction To Robotic Manipulation*, volume 29. CRC Press, 1994. 3.6.1

Napier, J. R. The prehensile movements of the human hand. *Journal of bone and joint surgery*, 38-B(4):902–13, 1956. 1.1

Nguyen, V.-D. Constructing stable grasps in 3D. In *IEEE International Conference on Robotics and Automation*, volume 4, pages 234–239, 1987. 1.3.1

Odhner, L. U., Jentoft, L. P., Claffee, M. R., Corson, N., Tenzer, Y., Ma, R. R., Buehler, M., Kohout, R., Howe, R. D., and Dollar, A. M. A compliant, underactuated hand for robust manipulation. *The International Journal of Robotics Research*, 33(5):736–752, 2014. 1.3.3

Patel, S. and Sobh, T. Manipulator Performance Measures-A Comprehensive Literature Survey. *Journal of Intelligent and Robotic Systems*, 77, 2014. 4.6.2

Pelossof, R., Miller, A., Allen, P., and Jebara, T. An SVM learning approach to robotic grasping. In *IEEE International Conference on Robotics and Automation*, volume 4, pages 3512–3518, 2004. 4.3.1

Pollard, N. S. Parallel methods for synthesizing whole hand grasps from generalized prototypes. Technical report, AI-TR 1464 MIT Artificial Intelligence Laboratory, 1994. 4.3.2

Prats, M., Sanz, P. J., and Pobil, A. P. A framework for compliant physical interaction. *Autonomous Robots*, 28(1):89–111, 2010. 1.3.4, 2.1, 4.3.1

Prattichizzo, D. and Trinkle, J. Grasping. In Siciliano, B. and Khatib, O., editors, *Springer Handbook of Robotics*, chapter 28, pages 671–700. Springer Science & Business Media, 2008. 4.3.1

Przybylski, M., Asfour, T., and Dillmann, R. Planning grasps for robotic hands using a novel object representation based on the medial axis transform. In *IEEE International Conference on Intelligent Robots and Systems*, pages 1781–1788, 2011. 1.3.2, 4.3.1, 4.3.2, 4.4.2

Roa, M. A. and Suárez, R. Computation of independent contact regions for grasping 3-D objects. *IEEE Transactions on Robotics*, 25(4):839–850, 2009. 1.3.1, 4.3.1

Roa, M. A., Argus, M. J., Leidner, D., Borst, C., and Hirzinger, G. Power grasp planning for anthropomorphic robot hands. In *IEEE International Conference on Robotics and Automation*, pages 563–569, 2012. 1.3.2, 4.3.1, 4.3.2

Romero, J., Kjellstrom, H., and Kragic, D. Modeling and evaluation of human-to-robot mapping of grasps. In *International Conference on Advanced Robotics*, 2009. 3.3

Rosales, C., Ros, L., Porta, J. M., and Suarez, R. Synthesizing Grasp Configurations with Specified Contact Regions. *The International Journal of Robotics Research*, 30(4):431–443, 2011. 1.3.4

Rothling, F., Haschke, R., Steil, J. J., and Ritter, H. Platform portable anthropomorphic grasping with the bielefeld 20-DOF shadow and 9-DOF TUM hand. *International Conference on Intelligent Robots and Systems*, pages 2951–2956, 2007. 1.3.4

Sahbani, A., El-Khoury, S., and Bidaud, P. An overview of 3D object grasp synthesis algorithms. *Robotics and Autonomous Systems*, 60(3):326–336, 2011. 4.3.1

Sahbani, A. and El-Khoury, S. A hybrid approach for grasping 3D objects. In *IEEE/RSJ International Conference on Intelligent Robots and Systems*, pages 1272–1277, 2009. 4.3.2

Santello, M., Flanders, M., and Soechting, J. F. Postural hand synergies for tool use. *Journal of Neuroscience*, 18(23):10105–10115, 1998. 1.3.2, b), 3.5.4, 4.3.1

Saut, J. P. and Sidobre, D. Efficient models for grasp planning with a multi-fingered hand. *Robotics and Autonomous Systems*, 60(3):347–357, 2012. 1.3.1, 4.3.1

Saxena, A., Wong, L. L. S., and Ng, A. Y. Learning Grasp Strategies with Partial Shape Information. *AAAI*, 3(2):1491–1494, 2008. 1.3.2

Shimoga, K. B. Robot Grasp Synthesis Algorithms: A Survey. *The International Journal of Robotics Research*, 15(3):230–266, 1996. 4.3.1

Sommer, N. and Billard, A. A dynamic controller for haptic exploration with redundant robots. *IEEE Transactions on Haptics, to be submitted*, 2015. 4.8.1

Song, D., Huebner, K., Kyrki, V., and Kragic, D. Learning task constraints for robot grasping using graphical models. In *IEEE/RSJ International Conference on Intelligent Robots and Systems*, pages 1579–1585, 2010. 1.3.4, 2.1, 2.6

Song, D., Ek, C. H., Huebner, K., and Kragic, D. Task-Based Robot Grasp Planning Using Probabilistic Inference. *IEEE Transactions on Robotics*, 31 (3):546–561, 2015. 2.6

Stansfield, S. Robotic Grasping of Unknown Objects: A Knowledge-based Approach. *The International Journal of Robotics Research*, 10(4):314–326, 1991. 4.3.1

Stark, M., Lies, P., Zillich, M., Wyatt, J., and Schiele, B. Functional object class detection based on learned affordance cues. In *ICVS08 Proceedings of the 6th International Conference on Computer Vision Systems*, pages 435–444. Springer, 2008. 1.3.2

Steil, J. J., RÌĹothling, F., Haschke, R., and Ritter, H. Situated robot learning for multi-modal instruction and imitation of grasping. *Robotics and Autonomous Systems*, 47(2-3):129–141, 2004. 1.3.4

Suárez, R., Roa, M., Cornella, J., and Cornell, J. Grasp quality measures. *Control*, 2006. 2.3

TekScan, . www.tekscan.com. 3.4.1

Vahrenkamp, N. and Asfour, T. Representing the robot's workspace through constrained manipulability analysis. *Autonomous Robots*, 38(1):17–30, 2015. 4.3.3, 4.6.2, 4.6.2

Vahrenkamp, N., Do, M., Asfour, T., and Dillmann, R. Integrated grasp and motion planning. In *IEEE International Conference on Robotics and Automation*, pages 2883–2888, 2010. 4.3.3

Vahrenkamp, N., Asfour, T., and Dillmann, R. Efficient Inverse Kinematics Computation Based on Reachability Analysis. *International Journal of Humanoid Robotics*, 09(04), 2012. 4.3.3

Weisz, J. and Allen, P. K. Pose error robust grasping from contact wrench space metrics. *IEEE International Conference on Robotics and Automation*, pages 557–562, 2012. 1.3.2

Yoshikawa, T. Manipulability of Robotic Mechanisms, 1985. 4.6.2

Yoshikawa, T. Translational and Rotational Manipulability of Robotic Manipulators. *American Control Conference*, 1990. 4.6.2

Zheng, Y. and Qian, W.-H. Coping with the Grasping Uncertainties in Force-closure Analysis. *The International Journal of Robotics Research*, 24(4):311–327, 2005. 1.3.1

Zhixing, X. and Dillmann, R. Efficient grasp planning with reachability analysis. *International Journal of Humanoid Robotics*, 8(4):761–775, 2011. 1.3.1

Zhou, J., Malric, F., and Shirmohammadi, S. A new hand-measurement method to simplify calibration in cyberglove-based virtual rehabilitation. *IEEE Transactions on Instrumentation and Measurement*, 59(10):2496–2504, 2010. 3.3

Zhu, X. and Wang, J. Synthesis of force-closure grasps on 3-D objects based on the Q distance. *IEEE Transactions on Robotics and Automation*, 19(4): 669–679, 2003. 1.3.1, 4.3.1

# Ravin de Souza

LASA, EPFL
ME A3 31
CH 1015, Lausanne, Switzerland

Phone: (41) 779277475
Email: ravin.desouza@epfl.ch

## Research Interests

- Robot grasping and manipulation
- Human grasp behavior
- Robot hand design, Tactile Sensing
- Human robot interaction

## Education

2010.10 – 2016.1(expected) **Ph.D. Student, IST-EPFL Joint doctoral program**
*Thesis:* Grasping for the task – Human principles for robot hands
*Supervisors:* Prof. Aude Billard, Prof. José Santos-Victor

1997 – 1999 **M.S. in Computer Science, Duke University, North Carolina, U.S.A**
*Thesis:* Visualizing memory behavior of complex data structures.
*Supervisor:* Prof. Alvin Lebeck

1994 – 1997 **B.S. in Computer Engineering, University of Mumbai, India**

## Professional & Research Experience

2011 – 2012 **Affiliated to European Union Project:**
HANDLE, http://www.handle-project.eu

2012 **iCub summer school conducted by Italian Institute of Technology**

2005 – 2010 **Larsen & Toubro Infotech, Mumbai, India**
- Centre of excellence unit. Applications for mobile robotics: tele-presence, autonomous navigation. Natural User Interface: gestures, multi-touch.
- Mobile communications unit. Mobile web browser technology.

2003 **T.J. Watson Research Laboratory, IBM, Yorktown**
Research internship. Autonomous performance tuning of AIX

1999 – 2004 **IBM, Austin, Texas, U.S.A**
Server group. AIX operating system development. Memory management for symmetric multi-processors and non-uniform memory architectures.

1998-1999 **Research Assistant, Duke University, Computer Science Dept.**
*Topic:* TUNE – Automatic tuning of applications for Memory-Friendly Programming

1997-1999 **Teaching Assistant, Duke University, Computer Science Dept.**
- Undergraduate courses: Algorithms, Programing, Artificial Intelligence
- Graduate courses: Advanced Computer Architecture

# Publications

## *Journal Articles*

1 **R. de Souza**, S. El-Khoury, J. Santos-Victor, and A. Billard. Recognizing the grasp intention from human demonstration. *Robotics and Autonomous Systems*, 2015

2 B. Huang, M. Li, **R. de Souza**, J. J. Bryson and A. Billard. A modular approach to learning manipulation strategies from human demonstration. *Autonomous Robots*, 2015

3 S. El-Khoury, **R. de Souza** and A. Billard. On Computing Task-Oriented Grasps. *Robotics and Autonomous Systems*, 2014

## *Conference Proceedings*

1 **R. de Souza**, S. El-Khoury, J. Santos-Victor, and A. Billard. Towards comprehensive capture of human grasping and manipulation skills. In *International Symposium on the 3D Analysis of Human Movement (3D-AHM)*, 2014.

2 **R. de Souza**, A. Bernardino, J. Santos-Victor, and A. Billard. On the representation of anthropomorphic robot hands: shape versus function. In *IEEE-RAS International Conference on Humanoid Robots (Humanoids)*, 2012.

## *Posters*

M. Coscia, E. Pirondini, N. Duthilleul, S. El-Khoury, **R. de Souza**, A. Billard, S. Micera. Effect of handedness on the generation and execution of upper limb planar movements. *Society for Neuroscience meeting* (*Neuroscience)*, 2015

## *Technical Design Reports (IBM-Austin)*

1 **R. de Souza**. Memory affinity considerations for the AIX virtual memory manager on Symmetric Multiprocessors machines with non-uniformity, 2003

2 **R. de Souza** and R. Swanberg. Re-organization of kernel memory layout to enable large page mapping, 2002

3 **R. de Souza** and T. Mathews. Towards a Virtual Memory Manager for NUMA machines: multiple node awareness, transparent page migration, transparent page replication, 2001

4 **R. de Souza**. Identification and lock-free resolution of contention in the AIX Virtual Memory Manager page-fault resolution mechanism, 2000

## *Patents*

Method, system, and computer program product for estimating the number of consumers that place a load on an individual resource in a pool of physically distributed resources. US Patent 6925421 issued on August 2, 2005.

# Talks

1 Tactile and force sensing to support teaching of compliant manipulation and grasp formation, *RSS Workshop on Bridging the Gap between Data-driven and Analytical Physics-based Grasping and Manipulation*, Rome, 2015

2 Concurrent Programming, *Computer Society of India (Student Chapter), NMIMS University, Mumbai*, 2008

3 AIX Internals, *T. J. Watson Research Laboratory, IBM, Yorktown*, 2003

# Academic Service

2011 – present **Reviewer:** IROS, ICRA, Humanoids

# Skills

*Robots:* iCub, KUKA LWR, Allegro Hand

*Sensing human grasp behavior:* Integrating multimodal information from Tekscan tactile sensors, OptiTrack motion capture, Dataglove joint sensors, ATI force/torque sensors.

*Robotics Software:* OpenRAVE, GraspIt!, OpenCV, ROS, YARP

*Programming:* Matlab, C, C++, C#, Java, Python, Forth, Concurrent Programming

*Platforms:* Embedded (ISOMAX, Arduino), Mobile devices (Nokia, Symbian), Windows based applications, Linux based applications

*PhD. Courses:* Estimation and Classification, Machine Learning, Computer Vision, Optimization

# Languages

English (fluent)

French (A2)

Portuguese (beginner)

# Personal

*Hobbies:* Violin, Singing – Tenor Voice, Swimming, Hiking

Indian Citizen, Born 22nd June 1975, Married to Cristina with two lovely children Mrinali and Mark